Analysis of polarity establishment during megagametogenesis and early zygotic embryogenesis in *Zea mays*

DISSERTATION

ZUR ERLANGUNG DES DOKTORGRADES
DER NATURWISSENSCHAFTEN (DR. RER. NAT.)
DER FAKULTÄT FÜR BIOLOGIE UND VORKLINISCHE MEDIZIN
DER UNIVERSITÄT REGENSBURG

vorgelegt von

Nádia Graciele Krohn

aus Marechal Cândido Rondon, Brasilien

Regensburg, im September 2010

Das Promotionsgesuch wurde eingereicht am: 04.10.2010

Die Arbeit wurde angeleitet von: Prof. Dr. T. Dresselhaus

Prüfungsausschuß: Vorsitzender: Prof. Dr. R. Sterner

                                     Erstgutachter: Prof. Dr. T. Dresselhaus

                                     Zweitgutachter: Prof. Dr. F. Sprenger

                                     Drittprüfer: Prof. Dr. H. Tschochner

Contents

Chapter 1

Introduction to asymmetric cell division in plants

Asymmetric cell division is one of the mechanisms to generate cellular diversity in multicellular organisms including flowering plants. Two major pathways have been reported by which plants perform asymmetric cell division, namely, (i) the "one mother-two different daughters" and (ii) the "coenocytes-cellularization" pathway. In the "one mother-two different daughters" pathway, a mother cell divides to generate two daughter cells which are either different in size and fate or which are initially comparable in size but subsequently get different fates (Ranganath, 2007). This pathway is exemplified by microgametogenesis, zygotic embryogenesis (zygotic asymmetric division and embryo patterning), lateral root initiation and stomata development (Ranganath, 2007; Heidstra, 2007). The first asymmetric division of the zygote in maize will be discussed in **Chapter 2**.

In contrast, the "coenocyte-cellularization" pathway is based on the formation of a coenocyte, involving nuclear migration to specific locations and cellularization. Megagametogenesis or female gametophyte development exemplifies the "coenocyte-cellularization" pathway in generating cells with different fates. In this point of view, the mother cell first undergoes several free nucleate divisions and then cellularizes to simultaneously produce several specialized daughter cells (Ranganath, 2005). Migration of nuclei to defined cellular locations associated with cellularization and concomitant fate determination are the key processes during megagametogenesis, which will be described in detail in **Chapter 3** and **Chapter 4**. However, in the present chapter discerning cases of asymmetric cell division (microgametogenesis, embryogenesis, lateral root initiation and stomata development) in plants will be emphasized to give a preface about the developmental importance of this process.

1   Microgametogenesis

A series of events occur in the anther of the stamen in *Arabidopsis* and maize resulting in the differentiation of the archesporial cell, which further differentiates to produce the microspore mother cell. The microspore mother cell goes through meiotic division to give rise to four haploid microspores (Bedinger and Fowler, 2009). Each microspore then undergoes cytoplasmic reorganization, resulting in a cell with a large

vacuole and most of the cytoplasm at one site and the nucleus at the other side in preparation for the first asymmetric mitotic division (Fig. 1). The asymmetric division gives rise to the vegetative and generative cell representing the male germline initial cell. The generative cell undergoes a second mitotic division in maize and *Arabidopsis* forming the two sperm cells. The mature pollen grain of these model plant species is, in consequence, trinucleate. The vegetative cell is responsible to form the pollen tube, a structure that conducts the two sperm cells to the female gametophyte where they participate in the double fertilization process (Heidstra, 2007).
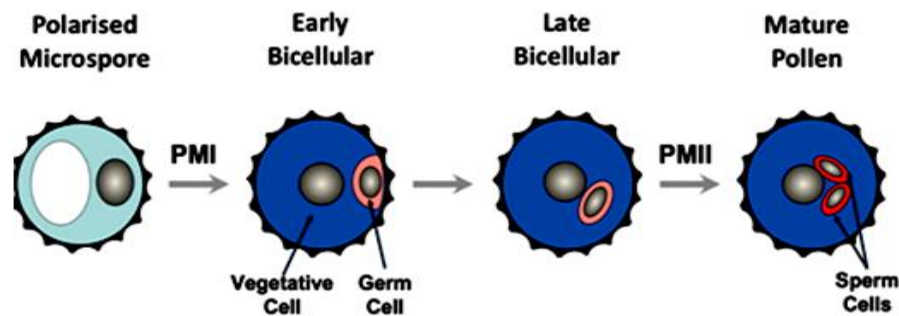
Figure 1. Microgametogenesis: the microspore undergoes a highly asymmetric division (pollen mitosis I or PMI) to produce a bicellular pollen grain with a small germ cell (generative cell) and a large vegetative cell. Whereas the vegetative cell exits the cell cycle, the germ cell undergoes a further mitotic division (PMII) to produce twin sperm cells. After Borg and Twell (2010)

Although a number of efforts have been made to identify genes involved in microgametogenis (Honys and Twell, 2004) and which are expressed exclusively in the sperm cells (Borges *et al.*, 2008), little is known about the pathway controlling asymmetric division of the microspore. Nevertheless, some proteins have been identified to play a role in microspore polarity, like the *sidecar pollen* (*scp*) mutation, which causes premature and symmetric cell division that produces two vegetative cells in *Arabidopsis* pollen grains. One of the vegetative cells then performs normal asymmetric division giving rise to the generative cell (Chen and McCormick, 1996). SCP might prevent division until polarity is fully established or direct the orientation of division such that fate determinants are polarly distributed in the microspore (Heidstra, 2007). Furthermore, MOR1 (MICROTUBULE ORGANIZATION 1)/GEM1 (GEMINI 1) is involved in cytokinesis during the asymmetric division of the microspore in *Arabidopsis*. MOR1/GEM1 is a member of the MAP215 family of microtubule-associated proteins and stimulates the growth and stability of interphase, spindle and phragmoplast microtubule arrays. *mor1/gem1* mutant microspores are either binucleate or bicellular (Park *et al.*, 1998; Whittington *et al.*, 2001; Twell *et al.*, 2002).

Arabidopsis mutants have been identified in which microspores complete asymmetric nuclear division, however fail to complete cytokinesis, resulting in binucleate pollen grains observed in *two-in-one* (*tio*) mutants. TIO is the plant homologue of the serine/threonine protein kinase FUSED from *Drosophila melanogaster* and localizes to the phragmoplast midline to play an essential role in centrifugal cell plate expansion (Oh *et al.*, 2005). Similar phenotypes were observed in *hinkel* (AtNACK1) and *tetraspore* (AtNACK2) double-mutant microspores suggesting that these proteins act together with TIO during cell plate expansion and cytokinesis. *HINKEL* and *TETRASPORE* are members of the canonical NACK-PQR MAPK (mitogen-activated protein kinase) gene family in *Arabidopsis* (Oh *et al.*, 2008).

GRSF (GERMLINE-RESTRICTIVE SILENCING FACTOR) a segregated fate determinant was first identified in lily. GRSF is present in non-germ cells, in microspores and in the vegetative cell nucleus, but is absent in the generative cell nucleus. GRSF was shown to bind silencer sequences in promoters of genes in cells other than the sperm cells (Haerizadeh *et al.*, 2006).

2   Embryogenesis

Maize and *Arabidopsis* embryos share major functional processes (Fig. 2) like the formation of a zygote, a first asymmetric zygotic division, establishment of an apical-basal polarity leading to a linear proembryo divided into suspensor and embryo proper, initial histogenesis resulting in the formation of a protoderm and organization of the shoot apical meristem (SAM) and the root apical meristem (RAM) (Vernoud *et al.*, 2005). On the other hand, morphological differences are evident when maize and *Arabidopsis* embryos are compared. The first divisions of the embryo in *Arabidopsis* are synchronized leading to easily recognizable pattern formation, while in maize embryos the divisions appear more randomly although characteristic morphological stages are formed (Sheridan, 1995; Nardmann and Werr, 2009). Moreover, the formation of leaf primordia occurs after the entrance into dormancy and seed dispersal in *Arabidopsis*, while 5 to 6 leaf primordia are elaborated in the maize embryo. Finally, the main difference, due to the fact that *Arabidopsis* is a dicot and maize a monocot, is the presence of two cotyledons in *Arabidopsis* and a scutellum (the single grass cotyledon) in the maize embryo (Vernoud *et al.*, 2005).

In *Arabidopsis* several asymmetric cell divisions occur during radial patterning to form the outer protoderm layer, the ground and provascular tissues, the precursors of

the xylem and phloem cell lineage, the epidermis/lateral root cap, the inner endodermis, the outer cortex cell layer, SAM and RAM primordia. A number of genes have been identified to be essential during radial patterning in *Arabidopsis* (for review see Nardmann and Werr, 2009).
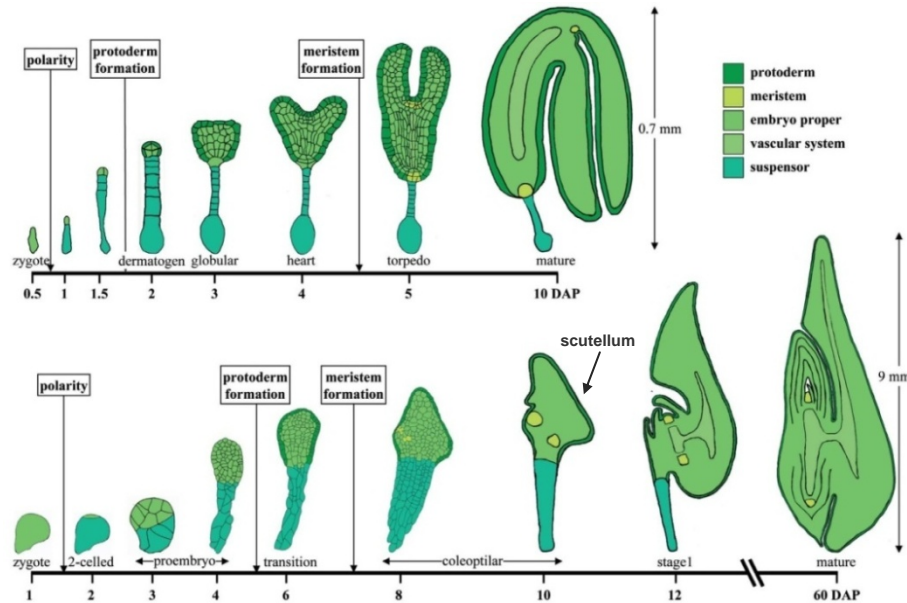
Figure 2. Comparison of embryogenesis in *Arabidopsis* and maize. Developmental stages of *Arabidopsis* (top) or maize embryos (bottom). The stages illustrated from left to right for *Arabidopsis* are zygote, two-celled proembryo, quadrant, dermatogen, globular, heart, torpedo and mature embryo. Represented stages for maize are zygote, two-celled proembryo, early proembryo, late proembryo, transition, early coleoptilar, late coleoptilar, stage 1 and mature embryo. DAP: Days after pollination. After Vernoud *et al.* (2005).

In maize only the plane of the first zygotic division is predictable, all subsequent divisions appear randomly. The apical cell descendents remain small and cytoplasm rich, whereas the basal cell descendents vacuolize and enlarge. At the transition stage, a small group of cells at the adaxial axis of the ear remains densely packed in the embryo proper while surrounding cells start to enlarge. The enlarging cells will form the scutellum. Thus the shoot/root axis is located at the opposite part of the embryo proper, namely at the adaxial axis of the ear (Fig. 2). In this domain of cytoplasmic rich cells, both SAM and RAM are initiated (Nardmann and Werr, 2009). The known molecular mechanisms that govern embryo patterning in maize were reported and comparative analysis between maize and *Arabidopsis* revealed a significant conservation of gene expression patterns (Zimmermann and Werr, 2005; Nardmann *et al.*, 2007; Chandler *et al.*, 2008; Nardmann and Werr, 2009).

3   Lateral root initiation

Root branching allows the plant to explore the environment to optimize growth and assure supply of nutrients. Lateral roots initiate from a small group of founder cells, which are located in the pericycle, the outermost layer of the vascular cylinder (Steeves and Sussex, 1989; reviewed by Heidstra, 2007). The first asymmetric founder cell division occurs, followed by an ordered set of asymmetric divisions initiating the formation of a lateral root meristem, which will subsequently grow out and form the lateral root (Malamy and Benfey, 1997; Fig. 3).
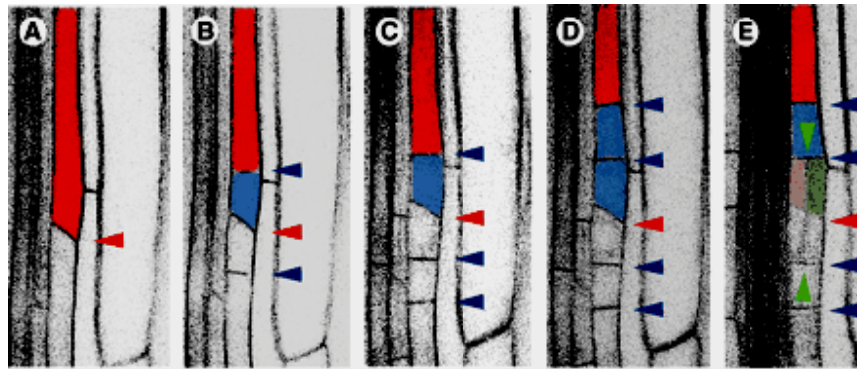
Figure 3. Asymmetric cell division during lateral root initiation. (**A-E**) Consecutive divisions in one file of xylem pole pericycle cells. Arrowheads mark the oblique cell wall between two adjacent pericycle cells (red), consecutive anticlinal asymmetric cell divisions (blue), and first periclinal divisions of the central cells (green). After De Smet *et al.* (2008).

The molecular mechanisms that initiate and control asymmetric cell division during lateral root initiation are poorly understood. The *ABERRANT LATERAL ROOT FORMATION4 (ALF4)* gene is one of the few examples identified to be involved in this pathway. The *ALF4* gene encodes a nuclear protein of unknown function required to maintain the pericycle in a mitosis-competent state (Celenza *et al.*, 1995; DiDonato *et al.*, 2004). Moreover, the receptor-like kinase ACR4 (ARABIDOPSIS CRINKLY4) was identified to promote formative cell divisions in the pericycle and to restrict the number of these divisions once organogenesis has been started. In the root tip meristem, ACR4 shows a similar action by controlling cell proliferation activity in the columella cell lineage (De Smet *et al.*, 2008).

4   Stomata development

Stomata are epidermal structures that are present in almost all shoot organs. They consist of two guard cells around a pore that acts as turgor valves to regulate gas exchange between the plant and its environment (Heidstra, 2007). The development of

stomata depends on asymmetric division. Recently, the BASL (BREAKING OF ASYMMETRY IN THE STOMATAL LINEAGE) protein was identified to play an important role in stomata formation in *Arabidopsis*. BASL is a plant-specific protein possessing no recognizable known functional domains. Polar localization of BASL results in asymmetric cell division, while localization only in the nucleus results in cell differentiation (Dong *et al.*, 2009). A model was proposed for BASL function in stomatal lineage asymmetric divisions (Fig. 4).

In summary, asymmetric cell division is a mechanism present during the whole life cycle of a flowering plant, but is poorly understood and only a few molecular players have been identified. In the present work I have made efforts to identify genes involved in the establishment of polarity during the first zygotic asymmetric division, as an example for the "one mother-two different daughters" pathway, which will be discussed in **Chapter 2**. Moreover, the function of the signaling molecule ZmEAL1 for cell fate maintenance in the female gametophyte will be described in **Chapter 3** as an example for the "coenocytes-cellularization" pathway to generate cell diversity. Additionally, the role of ZmDSUL (diSUMO-like protein) in nuclei segregation and positioning, which is a prerequisite for cell specification during female gametophyte maturation, will be clarified in **Chapter 4**.
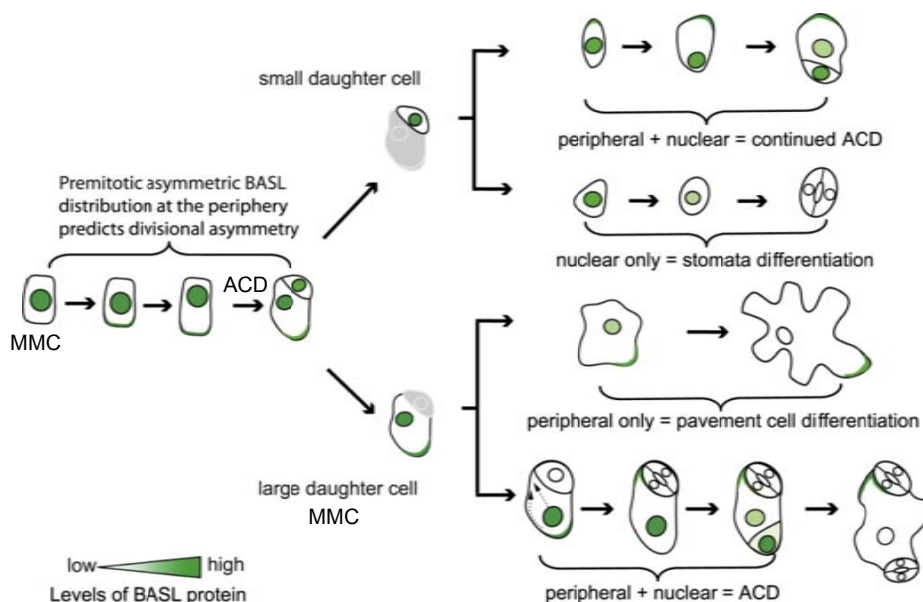
Figure 4. Model for BASL function in stomatal lineage asymmetric divisions. BASL becomes polarized in the meristemoid mother cell (MMC) with localization in the nucleus and the periphery of the cell resulting in asymmetric cell division (ACD). BASL localization in both nucleus and periphery in the small daughter cell results in the division of the cell as a MMC or meristemoid. On the other hand, BASL nuclear localization in the small daughter cell results in differentiation into a guard mother cell and eventually a pair of guard cells. In the larger daughter, BASL moves to the periphery in a region distal to the division plane. If this cell retains nuclear and peripheral BASL, it will divide asymmetrically; if it loses nuclear BASL, it will differentiate into a pavement cell. After Dong *et al.* (2009).

5 References

Bedinger PA, Fowler JE (2009) The maize male gametophyte. In: Bennetzen J, Hake S (eds) *Handbook of maize: its biology*. NY: Springer Science and Business Media, 57-77.

Bommert P, Werr W (2001) Gene expression patterns in the maize caryopsis: clues to decisions in embryo and endosperm development. *Gene* 271: 131-142.

Borg M, Twell D (2010) Life after meiosis: patterning the angiosperm male gametophyte. *Biochem. Soc. Trans.* 38, 577-582.

Borges F, Gomes G, Gardner R, Moreno N, McCormick S, Feijó JA, Becker JD (2008) Comparative transcriptomics of *Arabidopsis* sperm cells. *Plant Physiol.* 148, 1168-1181.

Celenza JL, Grisafi PL, Fink GR (1995) A pathway for lateral root formation in *Arabidopsis thaliana. Genes Dev.* 9, 2131-2142.

Chandler J, Nardmann J, Werr W (2008) Plant development revolves around axes. *Trends Plant Sci.* 13, 78-84.

Chen YC, McCormick S (1996) *Sidecar pollen*, an *Arabidopsis thaliana* male gametophytic mutant with aberrant cell divisions during pollen development. *Development* 122, 3243-3253.

De Smet I, Vassileva V, De Rybel B, Levesque MP, Grunewald W et al. (2008) Receptor-like kinase ACR4 restricts formative cell divisions in the *Arabidopsis* root. *Science* 322, 594-597.

DiDonato RJ, Arbuckle E, Buker S, Sheets J, Tobar J et al. (2004) *Arabidopsis ALF4* encodes a nuclear-localized protein required for lateral root formation. *Plant J.* 37, 340-353.

Dong J, MacAlister CA, Bergmann DC (2009) BASL controls asymmetric cell division in *Arabidopsis. Cell* 137, 1320-1330.

Haerizadeh F, Singh MB, Bhalla PL (2006) Transcriptional repression distinguishes somatic from germ cell lineages in a plant. *Science* 313, 496-499.

Heidstra R (2007) Asymmetric cell division in plant development. In: Macieira-Coelho, A (ed) *Asymmetric cell division*. Heidelberg: Springer, 1-37.

Honys D, Twell D (2004) Transcriptome analysis of haploid male gametophyte development in *Arabidopsis. Genome Biol.* 5, R85.

Malamy JE, Benfey PN (1997) Organization and cell differentiation in lateral roots of *Arabidopsis thaliana. Development* 124, 33-44.

Nardmann J, Zimmermann R, Durantini D, Kranz E, Werr W (2007) *WOX* gene phylogeny in *Poaceae*: a comparative approach addressing leaf and embryo development. *Mol. Biol. Evol.* 24, 2474-2484.

Nardmann J, Werr W (2009) Patterning of the maize embryo and the perspective of evolutionary developmental biology. In: Bennetzen J, Hake S (eds) *Handbook of maize: its biology*. NY: Springer Science and Business Media, 105-120.

Oh SA, Johnson A, Smertenko A, Rahman D, Park SK, Hussey PJ, Twell D (2005) A divergent cellular role for the FUSED kinase family in the plant-specific cytokinetic phragmoplast. *Curr. Biol.* 15, 2107-2111.

Oh SA, Bourdon V, Das 'Pal M, Dickinson H, Twell D (2008) *Arabidopsis* kinesins HINKEL and TETRASPORE act redundantly to control cell plate expansion during cytokinesis in the male gametophyte. *Mol. Plant* 1, 794-799.

Park SK, Howden R, Twell D (1998) The *Arabidopsis thaliana* gametophytic mutation *gemini pollen1* disrupts microspore polarity, division asymmetry and pollen cell fate. *Development* 125, 3789-3799.

Ranganath RM (2005) Asymmetric cell divisions in flowering plants - one mother, "two-many" daughters. *Plant Biol*. 7, 425-448.

Ranganath RM (2007) Asymmetric cell division-how flowering plants get their unique identity. In: Macieira-Coelho, A (ed) *Asymmetric cell division*. Heidelberg: Springer, 39-60.

Sheridan WF (1995) Genes and embryo morphogenesis in angiosperms. *Dev. Genet.* 16, 291-297.

Steeves TA, Sussex IM (1989) *Patterns in plant development*. Cambridge: Cambridge University Press.

Twell D, Park SK, Hawkins TJ, Schubert D, Schmidt R, Smertenko A, Hussey PJ (2002) MOR1/GEM1 plays an essential role in the plant-specific cytokinetic phragmoplast. *Nat. Cell Biol.* 4, 711-714.

Vernoud V, Hajduch M, Khaled AS, Depège N, Rogowsky PM (2005) Maize embryogenesis. *Maydica* 50, 469-483.

Whittington AT, Vugrek O, Wei KJ, Hasenbein NG, Sugimoto K, Rashbrooke MC Wasteneys GO (2001) MOR1 is essential for organizing cortical microtubules in plants. *Nature* 411, 610-613.

Zimmermann R, Werr R (2005) Pattern formation in the monocot embryo as revealed by NAM and CUC3 orthologues from *Zea mays* L. *Plant Mol. Biol.* 58, 669-685.

Chapter 2

Identification of novel genes involved in polarity establishment during the asymmetric zygotic division of maize

1   Introduction

The life cycle of a plant starts with the zygote derived from the fusion of an egg cell and a sperm cell. In maize, the asymmetric division of the zygote generates two cells with different fates. The apical cell gives rise to the embryo-proper while the basal cell forms the suspensor (Randolph, 1936). During embryo development, the apical-basal axis pattern is laid down to further specify the distinct cells types after germination of the seed. The seedling has then the ability to permanently form new tissues and organs. As a consequence asymmetric cell divisions are indispensable to generate cell diversity during embryonic and post-embryonic development. In this sense, the asymmetric zygotic division is the primary mechanism that leads to the diversity of cell types, which compose the adult plant.

The establishment of polarity is a crucial step in embryogenesis. Embryo polarity namely anterior-posterior (head-tail) in animals and apical-basal (shoot-root) in plants is originated by the breaking of symmetry in the egg cell or zygote. In *Drosophila melanogaster* eggs and in *Caenorhabditis elegans* zygotes the cytoskeleton is essential for symmetry breaking (St Johnston, 1995; Gönczy, 2008) in answer to extrinsic cues (Fig. 1A). After symmetry breaking, polarity is generated (Fig. 1B) and has to be maintained (Fig. 1C) to ensure segregation of fate determinants while the mitotic spindles are formed (Fig. 1D) resulting in two daughter cells with different fates (Fig. 1E). The conserved PAR (PARtitioning defective) proteins stabilize cell polarity via physical interaction with the cytoskeleton to control asymmetric mitotic spindle orientation, determining the division plane and localizing cell fate determinants to one side of the cell. PAR3, PAR6 are PDZ-domain proteins that form a complex with PKC-3 (atypical protein kinase C) at the anterior part of *C. elegans* zygotes. PAR2, a ring-finger protein, is located at the posterior part of the zygote together with PAR1 (protein kinase). The maintenance of distinct domains in the cell is regulated by PAR-5 (a 14-3-3 protein) and reciprocal inhibitory interactions of PAR proteins located at the anterior and posterior part of the zygote (Gönczy, 2008). Three principal mechanisms have been

identified that regulate differential distribution of fates determinants. The first mechanism is differential protein stability, exemplified in *C. elegans* embryos, where a cullin-2-based E3 ligase causes degradation in somatic cells of proteins such as the zinc-finger protein PIE-1, which is necessary for germline specification (DeRenzo *et al.*, 2003). Second, differential protein localization was as well reported during asymmetric division of neuroblasts in the *Drosophila* embryo (Gönczy, 2008). Third, polar mRNA localization was thought to be a rare phenomenon. However, genome-wide analyses of mRNA localization in early *Drosophila* embryos revealed that most mRNAs are asymmetrically distributed (Lecuyer *et al.*, 2007). Well studied examples are the localization of *bicoid* to the anterior and *oskar* and *nanos* mRNA to the posterior of the *Drosophila* oocyte. The polar localization of these mRNAs with subsequent translation and asymmetric localization of proteins is responsible for the formation of the anterior-posterior axis. Polar mRNA localization requires a large number of trans-acting factors. Among these, RNA binding proteins, like the Staufen protein, are involved in targeting the *oskar* mRNA to the posterior pole of *Drosophila* oocytes (Kugler and Lasko, 2009).
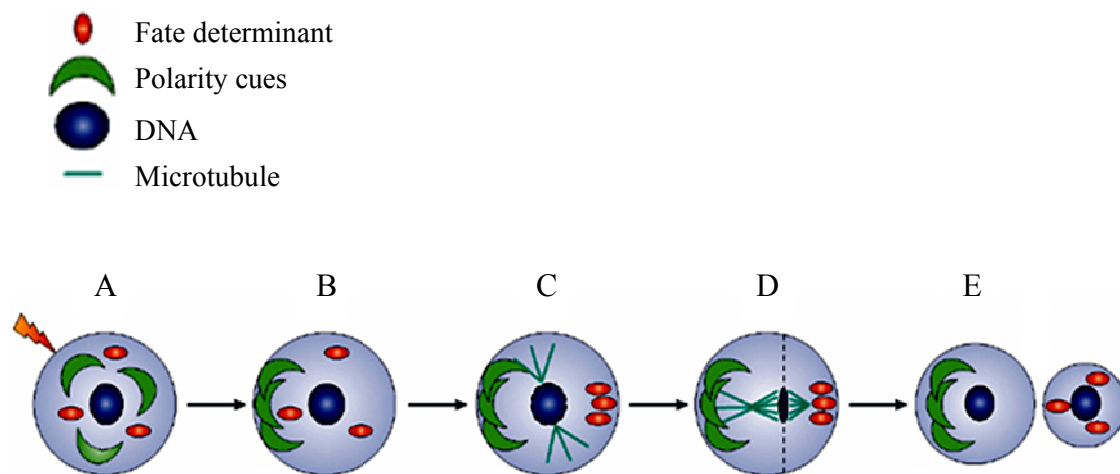
Figure 1. Asymmetric cell division. (**A**) Symmetry is disrupted by an integrated network of extrinsic positional effects, signaling and internal cues. (**B**) Cell becomes polarized. (**C**) Fate determinants are segregated towards given regions of the polarized cell. (**D**) Mitotic spindles are aligned in a way that cell division correctly distributes fate determinants to the daughter cells. (**E**) The cleavage furrow is specified to bisect the anaphase spindles. After Gönczy (2008).

Polar development is also present from the early steps on during female gametophyte development in maize. The maize embryo sac is a highly polarized structure with two synergid cells and one egg cell at the micropylar pole, antipodals cells are located at the opposite end and the central cell is located in the middle of the female gametophyte. A closer look at the egg cell reveals that it is as well highly

polarized (Fig. 2A). After fertilization, its polar organization is maintained in the maize zygote which divides asymmetrically to give rise to the small, cytoplasm-rich apical cell and to the large, vacuolated basal cell (Fig 2B). The cells of the two-celled proembryo have different fates. The apical cell gives rise to the embryo proper while the basal cell originates the suspensor (Randolph, 1936). The suspensor connects the embryo proper to the surrounding maternal and endosperm tissues. There are experimental evidences showing that the suspensor is involved in transferring nutrients and growth factors to the embryo proper (Nagl, 1990; Friml *et al.*, 2003; Stadler *et al.*, 2005). Once its functions are accomplished, the suspensor undergoes programmed cell death, which starts at 14 days after pollination in maize (Giuliani *et al.*, 2002).
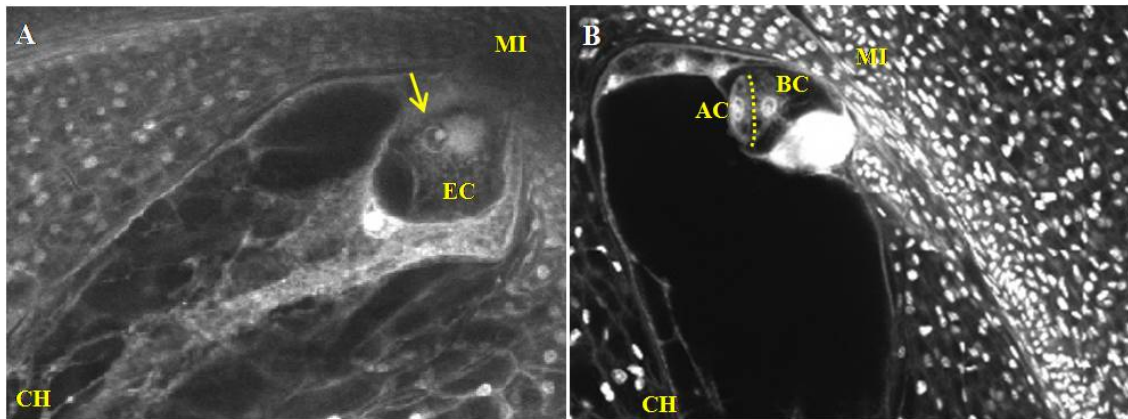
Figure 2. Polar organization of the maize egg cell and two-celled proembryo visualized with fluorescence microscopy images of sections of maize ovules stained with Kasten's fluorescent periodic acid-Schiff's reagent. (**A**) Polar organization of the egg cell through the micropylar-chalazal axis of the embryo sac; egg cell (EC), egg cell nucleus (arrow). (**B**) Asymmetric division of the zygote resulting in a small cytoplasm rich apical cell and a large vacuolated basal cell; apical cell (AC), basal cell (BC), division plane (dotted line). Micropylar (MI) and chalazal (CH) end of the embryo sac, respectively.

Two different hypotheses have been postulated about the mechanism of apical and basal cell fate establishment in the two-celled proembryo. First, a positional effect on cell fate determination was proposed. According to this theory, cell-cell signaling events derived from adjacent seed tissues or even interaction between embryo proper and suspensor trigger a cascade of events that result in the differentiation of the embryo proper and suspensor. The *YDA* (*YODA*) gene encodes a MAPKK Kinase in *Arabidopsis* and illustrates this hypothesis. In *yda* mutants, the zygote does not elongate properly, and the cells of the basal lineage are eventually incorporated into the embryo instead of differentiating into the suspensor. *YDA* gain-of-function alleles cause exaggerated growth of the suspensor and embryonic development is suppressed to a

degree where no recognizable proembryo was formed (Lukowitz *et al.*, 2004). Similarly, double mutants of mitogen-activated protein kinases *mpk3/mpk6* fail to develop a suspensor in *Arabidopsis* (Wang *et al.*, 2007). Moreover, the *suspensor* (Schwartz *et al.*, 1994) and *raspberry* (Yadegari *et al.*, 1994) mutants of *Arabidopsis* show at first place disrupted morphogenesis in the embryo proper resulting in an enlarged suspensor with features normally restricted to the embryo proper. Additionally, the suspensor has the potential to undergo embryogenic transformation, observed in *twn1* (*twin1*) and *twn2* mutants in *Arabidopsis* (Vernon and Meinke, 1994; Zhang and Somerville, 1997). Taken together, these data suggest that the embryo proper sends inhibitory signals to the suspensor that are necessary to maintain its differentiated state (Schwartz *et al.*, 1994; Yadegari *et al.*, 1994; Vernon and Meinke, 1994; Zhang and Somerville, 1997).

In addition to the cell-cell signaling events, asymmetric distribution of fate determinant mRNAs within the egg cell/zygote and subsequent segregation of these transcripts either to apical or basal cell after zygotic division was proposed in my PhD work to be responsible in determining the fates in the two-celled proembryo. The zygotic asymmetric division in maize is probably regulated by intrinsic factor (Heidstra, 2007). This conclusion was drawn from observations of *in vitro* studies where zygotes produced by *in vitro* fertilization divided asymmetrically (Kranz *et al.*, 1995; Okamoto *et al.*, 2005) and eventually developed further into fertile plants (Kranz and Lörz, 1993). Moreover, efforts have been achieved to identify genes expressed in the egg cell and/or zygote, which are up-regulated in the apical or the basal cell of the two-celled proembryo (Sprunck *et al.*, 2005; Okamoto *et al.*, 2005; Ning *et al.*, 2006). However, investigations to determine whether these up-regulated mRNAs are required for cell fate determination are still missing. The PAR proteins, which are distributed in a polar manner, are intrinsic cues for cell fate determination in animals (for review see Goldstein and Macara, 2007). Conversely, no PAR homologues have been identified in the sequenced genomes of several plant species, suggesting that fate determinants and segregation mechanisms are not generally conserved between plant and animal asymmetric divisions (Abrash and Bergmann, 2009). On the other hand, the *Hox* (homeodomain transcription factors) genes are expressed at a specific anterior-posterior position along the body axis and therefore govern body patterning after translation in *Drosophila* (Mahaffey, 2005). Similar results were obtained in the plant model system *Arabidopsis*. *WOX2* (*WUSCHEL RELATED HOMEOBOX2*) and *WOX8* are

coexpressed in the egg cell and zygote, however after zygotic division *WOX2* and *WOX8* transcripts become restricted to the apical and basal cell, respectively (Haecker *et al.*, 2004). Notably, *wox2* mutants show a range of defects in the embryo proper, whereas *wox8* single mutants do not affect embryo development. However, in *wox8wox9* double mutants neither the suspensor nor the proembryo develop normally. *WOX9* gene is not expressed in the egg cell but in the basal cell of the two-celled proembryo. The unexpectedly observed phenotype in the embryo proper in *wox8wox9* double mutants was explained due to the fact that *WOX2* expression is missing in this mutant, suggesting that WOX8/WOX9 are required for normal *WOX2* expression in the embryo proper (Breuninger *et al.*, 2008).

In summary, polar distribution of transcripts probably plays an important role during asymmetric cell division in zygotic embryogenesis of plants. However, relatively little is known about this mechanism. To change this scenario, I took the advantage of the microarray hybridization technique. The transcript profile of maize egg cell, apical and basal cell was compared. The aim of this work was the identification of mRNA fate determinants, which are present in the egg cell and after fertilization and division of the zygote segregate either to the apical or the basal cell of the two-celled proembryo.

2   Material and Methods

2.1   Plant material and isolation of cells from maize female and male gametophytes

Maize inbred line A188 was cultivated in a growth chamber at standard conditions, 16 h light at 26°C, 8 h dark at 17°C, relative air humidity varying from 50-70% and illuminance of 24000 lux. Egg cells were isolated as described before (Kranz *et al.*, 1991). Zygotes were isolated 12 and 24 hours after *in vivo* pollination as follows: the *in vivo* pollination procedure was performed using cobs with fully developed embryo sacs; the silks of those cobs were shortened in a way that 2 cm in length were left between the cutting side and the top of the last row of ovaries; zygotes were isolated from ovules dissected from the central part of the cob, using the same procedure described to microdissect of egg cells (Kranz *et al.*, 1991).

To identify the time point of the zygote division, several cobs were pollinated and analyzed at different intervals after pollination. The first zygotes were analyzed at 24 hours after pollination. Subsequent examinations were performed with 1 hour of interval and zygote division was observed at about 48 hours after pollination. Some modifications were applied to microdissect the apical and basal cell of the two-celled proembryo at about 48 h after *in vivo* pollination. The cell wall degrading enzyme solution was prepared with 1,5% driselase (Sigma), 1,5% pectinase (Fluka), 0,5% pectolyase Y23 (Karlan), 1,0% hemicellulase (Sigma), 1,0% cellulase "Onozuka R10" (Serva) and 1,5% maceroenzyme (Karlan) in mannitol solution (480 mosmol·kg^{-1} H$_2$O). This enzyme solution (100 μl) was added to 1 ml mannitol solution (480 mosmol·kg^{-1} H$_2$O) and the ovules were incubated in the diluted enzyme solution for 30 min at room temperature followed by the dissection of the two-celled proembryo. After dissection apical and basal cells were still attached. The attachment between the two protoplasts was gently touched with a very thin glass needle in order to separate both cells. Cells were then washed twice in mannitol solution (480 mosmol·kg^{-1} H$_2$O), collected in plastic reaction tubes, immediately frozen in liquid nitrogen and stored at -80°C until further usage.

2.2   DAPI staining

Isolated egg cells, zygotes, apical and basal cells were collected in mannitol droplets. DAPI (4',6-diamidino-2-phenylindole) was dissolved in a concentration of 2,5 ng·μl^{-1} in a mannitol solution (480 mosmol·kg^{-1} H$_2$0). About 0,1 μl of this DAPI

solution was added to the mannitol droplet containing the cells. The cells were incubated in this solution for 15 min at room temperature in the dark. Fluorescence was observed and documented at Eclipse TE 2000-S inverted microscope (Nikon) with UV light.

2.3   mRNA isolation and linear amplification

mRNA of dissected cells was isolated using the Dynabeads® mRNA DIRECT™ Micro Kit (Invitrogen) according to the manufacturer's protocol. Linear amplification of mRNA was performed using the TargetAmp™ 2-Round Aminoallyl-aRNA Amplification Kit 1.0 (Epicentre Biotechnologies; *Van Gelder et al.*, 1990) following the kit instructions. The procedure of mRNA amplification is illustrated in Figure 3. The quality (size of amplified fragments) and quantity of aminoallyl-anti-sense RNA (AA-aRNA) derived from the amplification procedure was assessed using the Agilent 2100 Bioanalyzer with the RNA 6000 Pico Kit (Agilent Technologies) according the manufacturer's instructions.
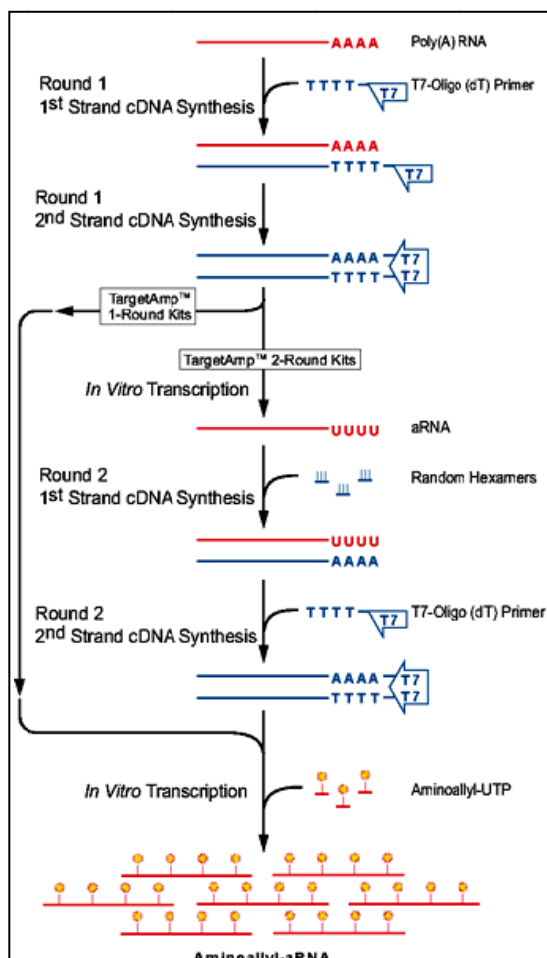
Figure 3. Procedure of linear mRNA amplification. Round 1, first-strand cDNA synthesis: isolated mRNA was reverse transcribed into first-strand cDNA. The reaction was primed from an oligo(dT) primer containing a phage T7 RNA Polymerase promoter sequence at its 5'-end. Round 1, second-strand cDNA synthesis: The RNA component of the cDNA:RNA hybrid produced in the anterior step was digested into small RNA fragments by RNase H. The RNA fragments function as primer for second-strand cDNA synthesis. The resulting product was a double-stranded cDNA containing a T7 transcription promoter in an orientation that generated anti-sense RNA (aRNA) during the subsequent *in vitro* transcription reaction. Round 1, *in vitro* transcription: high yields of anti-sense RNA (aRNA) were produced in a rapid *in vitro* transcription reaction that utilized the double-stranded cDNA. Round 2, first-strand cDNA synthesis: the aRNA produced and purified in the first round amplification process was reverse transcribed into first- strand cDNA. The reaction was primed using random sequence hexamer primers. Round 2, second-strand cDNA synthesis: the RNA component of the cDNA:aRNA hybrid produced in the anterior step was digested into small RNA fragments by RNase H. Second-strand cDNA synthesis was then primed using a T7-Oligo(dT) primer. The resulting product was a double-stranded cDNA containing a T7 transcription promoter in an orientation that generated aRNA during the second round of *in vitro* transcription reaction. *In vitro* transcription of aminoallyl-aRNA: high yields of

aminoallyl-aRNA were produced in an *in vitro* transcription reaction that utilized the double-stranded cDNA. After http://www.epibio.com/targetamp/targetamp_process.asp.

2.4 Microarray hybridization, coupling of AA-aRNA to a Cy-dye and scanning of hybridized chips

An oligo-microarray provided by the University of Arizona was used in the present study. The array consists of 46128 70-mer oligos representing about 30000 different genes of maize. The selection of oligos for this 46K array was determined by analysis of expression profiles generated for sixteen diverse maize tissues. Additional information can be obtained at www.maizearray.org/.

Prior to array hybridization, DNA was fixed on the chip by rehydrating the slides over a 55°C water bath for approximately 5 sec paying attention that spots did not over-hydrate to avoid fusion of spots. The slides were dried on a 45°C heating block for 5 sec and allowed to cool down for 1 min. The whole procedure was repeated four times. UV cross-linking was performed by exposing the slides (label side up) to 180 mJ in a cross-linker (Stratalinker-Stratagene). Slides were then washed in 1% SDS for 5 min at room temperature in wash station with a stir bar rotating at 120 rpm. SDS was removed from the slides by dipping them ten times into double-destilled water (ddH$_2$O), five times in 100% ethanol with posterior incubation in 100% ethanol for three minutes with shaking. The slides were afterwards dried by centrifugation at 200 x g for 2-4 min.

Prehybridization was performed in filter sterilized buffer (5 x SSC, 0,1% SDS, 1% BSA). 50 ml of the buffer were preheated to 42°C for 30 min. The slides were placed in a Coplin jar containing prehybridization buffer and incubated at 42°C in a water bath for 45 min. Afterwards the slides were washed twice for 5 min in a wash station filled with ddH$_2$O at room temperature. Incubation in 100% ethanol at room temperature with shaking was performed afterwards. The slides were then dried by centrifugation at 500 rpm for 5 min.

4 µg of AA-aRNA were dried in the Speed Vac Concentrator (Savant). AA-aRNA was then dissolved in 5 µl of NaHCO$_3$ (200 mM, pH 9,0) buffer by flicking the tube several times and leaving it at room temperature for at least 20 min. 5 µl of Cy3 or Cy5 monoreactive dyes (Amersham Pharmacia, dissolved in DMSO) were added to each reaction tube and mixed thoroughly by flicking the tube several times. The tubes were spun down at 1000 x g for 30 sec. AA-aRNA and dye mix was incubated at room temperature for 2 h covered in aluminum foil. Quenching of reaction was performed to inactivate any unreacted Cy dye by adding an excess of primary amines, namely 4,5 µl

of hydroxylamine (4 M) and incubating for 15 min in the dark at room temperature. Unincorporated dye was removed via the use of RNeasy MinElute Kit (Qiagen). After purification concentration of AA-aRNA coupled to Cy3 or Cy5 dye was measured using the NanoDrop ND-1000 Spectrophotometer (PeqLab). 2 µg of AA-aRNA labeled with Cy3 or Cy5 dye of each template were dried in a speed vac concentrator resuspended in 60 µl of 1 x hybridization buffer (50% formamide, 5 x SSC, 0,1% SDS, 0,4 µg·µl^{-1} of tRNA and 0,2 µg·µl^{-1} of Salmon Sperm DNA). The AA-aRNA labeled with Cy3 or Cy5 dye was then denatured at 95°C for 3 min and immediately used for hybridization.

Hybridization was performed in a loop design where samples with AA-aRNA derived from 2 or 3 egg cells, apical and basal cells, respectively, were compared (Fig. 4). The slides were inserted into the Hybridization Chamber HC4 (BioShake) and lifter slips (24 x 60I-2-4733; Erie Scientific Company) were placed over the microarray slide. The labeled and denatured AA-aRNA was slowly applied under the lifter slip to avoid the formation of air bubbles. 25 µl water were added to the lower groove inside the cassette chamber. The cassette lid was placed on top of the cassette chamber, which was incubated for 14 hours in the hybridization oven (7601; GFL) at 42°C.

After hybridization, slides were washed 5 min in each of the following solutions: (i) 2 x SSC, 0,1% SDS at 42°C; (ii) 0,1 x SSC at room temperature; (iii) 0,05 x SSC at room temperature and (iv) 0,05 x SSC at room temperature. Washing was done by immersing the slides in a glass wash station containing approximately 450 ml of wash buffer followed by placing it on a magnetic stir plate set at 120 rpm. Slides were dried by centrifugation at 1000 rpm for 4 min.

Hybridized arrays were immediately scanned with the DNA Microarray Scanner G2565CA (Agilent).
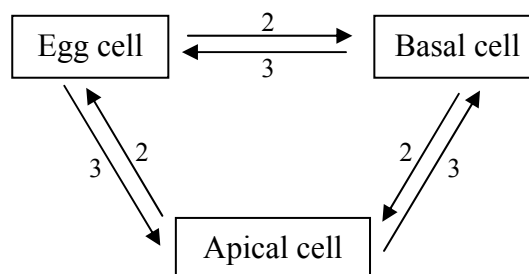
Figure 4. Microarray hybridization scheme in a loop design. 2 and 3 indicate the number of cells from which mRNA was isolated and AA-aRNA was labeled with Cy3 or Cy5 dyes. Cy3➔ Cy5 (probe at the beginning of the arrow was labeled with Cy3; probe at the arrowhead was labeled with Cy5).

2.5   Bioinformatics and candidates selection

The GenePix Pro version 7.1 software (Axon) was used to perform a spot finding, flagging and raw signal calculation of each single array. In order to focus on transcripts showing signal values well above background, the following Absent (A) / Present (P) calling procedure was applied: local background signal plus two times the standard deviation was used as a threshold for A/P calling. Lowess-Normalization and differential expression analysis (unpaired, two sided Student's t-tests) were carried out using ArrayAssist software (Stratagene).

For downstream analyses only genes called present in at least 3 replicates (total of all replicates was four) of each sample were taken into account. Genes were considered as up-regulated in one cell type when fold-change between the logarithmic expression values of the specific cell in comparison to another was above two. The same method was applied by Borges *et al.* (2008) resulting in better correlation of expression data and increased fold-change when cutoff was used and direct statistical significance was not considered.

Regulated genes were clustered into four groups: (i) up-regulated in the egg and apical cell and down-regulated in the basal cell; (ii) up-regulated in the egg and basal cell and down-regulated in the apical cell; (iii) up-regulated in the apical cell and down-regulated in the egg and basal cell and (iv) up-regulated in the basal cell and down-regulated in the egg and apical cell. BLASTX searches were performed with the regulated genes in the non-redundant protein sequences (nr) database at NCBI (http://www.ncbi.nlm.nih.gov/). Genes were functionally classified using either the DAVID gene functional classification tool (http://david.abcc.ncifcrf.gov/; Huang *et al.*, 2007) or through the analysis of published data.

3   Results

3.1   Identification of the time point of asymmetric zygotic division in maize

The fertilization process in maize was analyzed to determine the time point of zygotic division. The egg cell (Fig. 5A), before fertilization, shows less fluorescence of the nucleus after DAPI staining (Fig. 5B) in comparison with the zygote at 24 hours after pollination (hap; Fig. 5D). At 24 hap plasmogamy and karyogamy have already taken place (Fig. 5C-D). Metaphase was observed at 30 hap when chromosomes align at the metaphase plate (Fig. 5E-F). At 35 hap the paired chromosomes (sister chromatids) started to separate and move to opposite poles of the zygote, characterizing the anaphase (Fig. 5G-H). Telophase was observed at about 43 hap when two nuclei were visible (Fig. 5I-J). Cytokinesis was completed at 48 hap (Fig. 5K-L) resulting in two daughter cells with different fates. The small cytoplasm rich apical cell gives rise to the embryo proper and the large vacuolated basal cell generates the suspensor.

After determination of the time point of zygotic division, several combinations of cell wall degrading enzymes as well as duration and manner of incubation were tested. Finally, a microdissection method was established to isolate the apical and basal cell of the two-celled proembryo after *in vivo* fertilization. Figure 5M shows a two-celled proembryo after treatment with cell wall degrading enzyme solution. The apical and basal cells (Fig. 5N-P) were then separated with a thin glass needle. These cells were employed in molecular studies to identify the basis of polarity establishment during the asymmetric division of the zygote in maize. The experiments were based on the hypothesis that transcripts are distributed in a polar manner already in the egg cell with posterior segregation either to the apical or the basal cell are responsible for cell fate determinacy after asymmetric cell division.
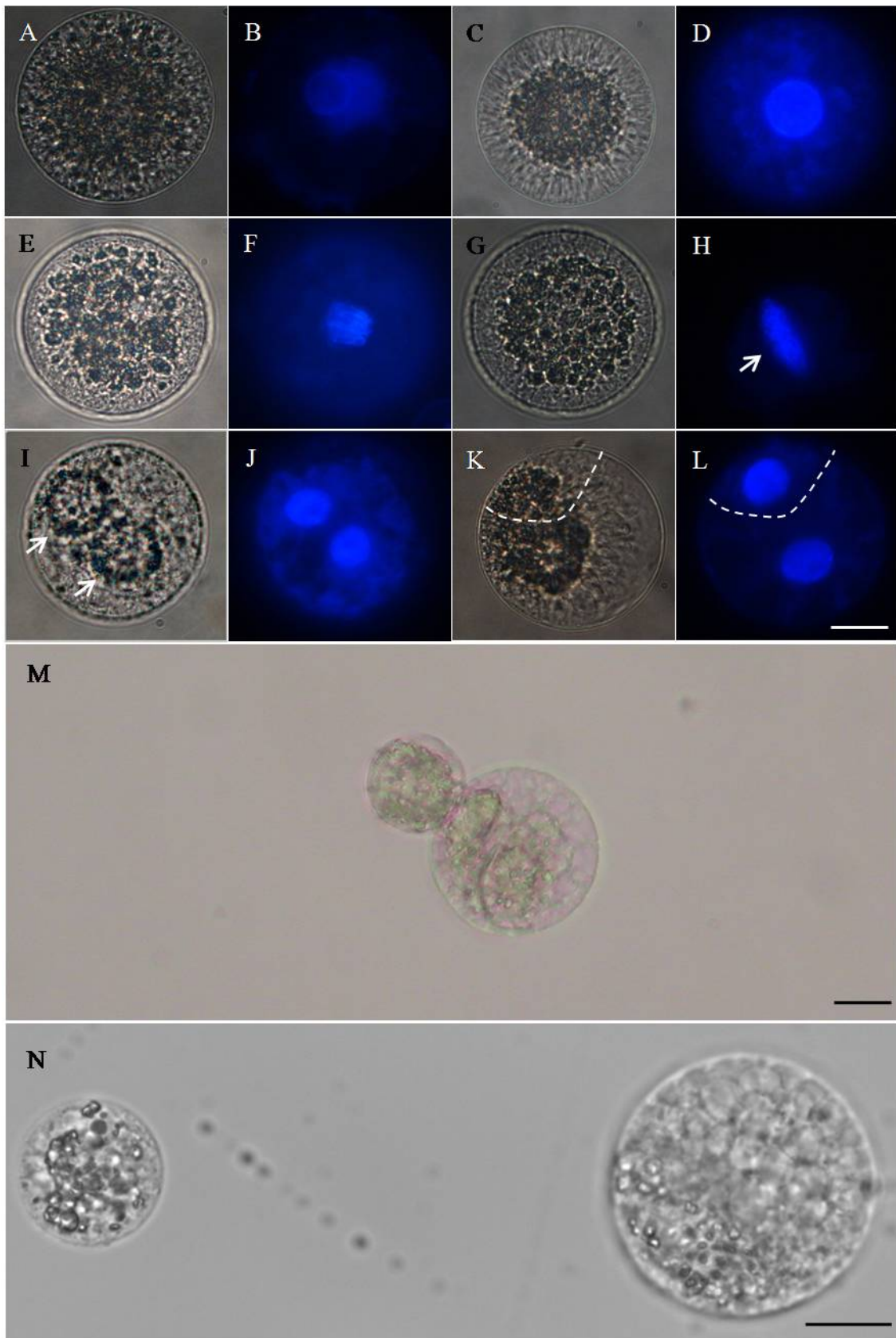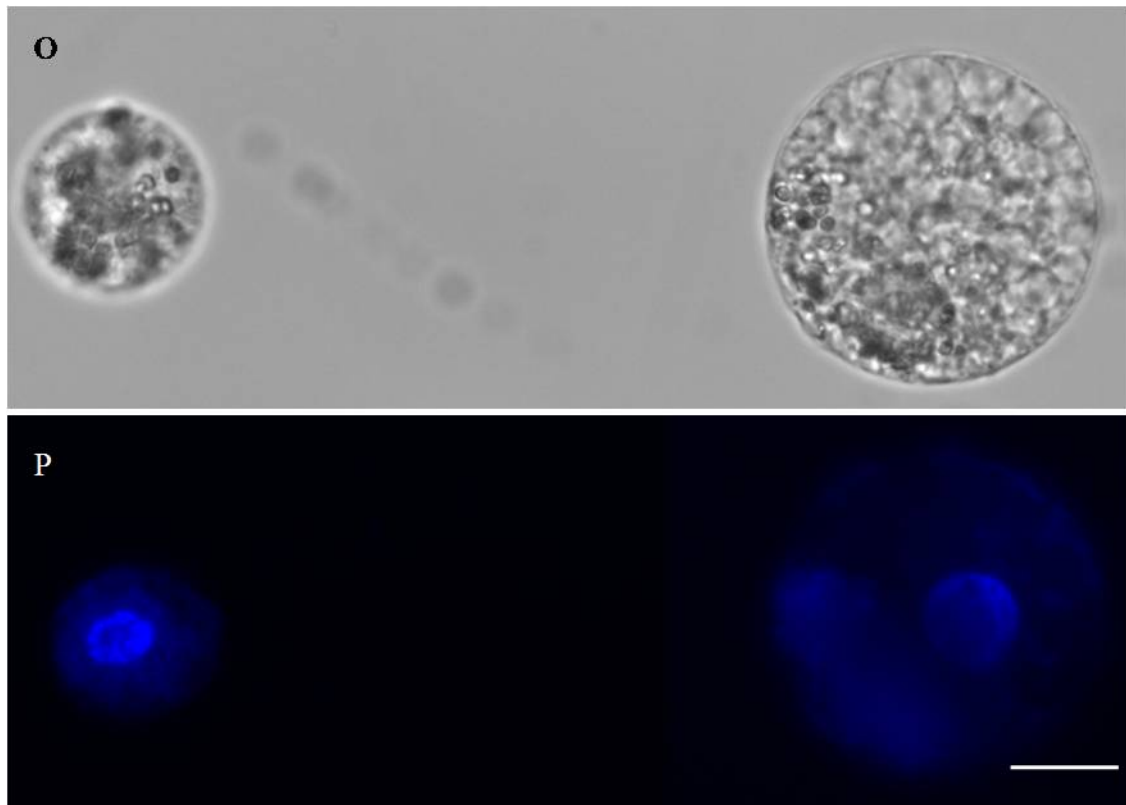
Figure 5. Development and asymmetric division of the zygote in maize. (**A**) Egg cell. (**B**) DAPI staining of the egg cell. (**C**) Zygote at 24 hours after pollination (hap). (**D**) DAPI staining of a zygote at 24 hap. (**E**) Zygote at 30 hap. (**F**) DAPI staining of a zygote at 30 hap; note the condensed and aligned chromosomes in anaphase. (**G**) Zygote at 35 hap. (**H**) DAPI staining of a zygote at 35 hap; chromosomes started to separate and move apart; arrow indicates the phragmoplast between the two nuclei. (**I**) Zygote at 43 hap; arrows indicate the two nuclei. (**J**) DAPI staining of a zygote at 43 hap; karyokinesis was completed. (**K**) Asymmetric division of the zygote occurred at 48 hap, giving rise to the two-celled proembryo; note that cell wall enzymatic treatment was not completed; dotted line indicates the division plane. (**L**) DAPI staining of a two-celled proembryo; dotted line indicates the division plane. (**M**) Two-celled proembryo after treatment with cell wall degrading enzyme solution. (**N**) Apical and basal cell after mechanical separation, closer look at the apical cell. (**O**) Closer look at the basal cell. (**P**) DAPI staning of the apical and basal cells. Bars: 20 μm.

3.2   Linear mRNA amplification of a population of few cells

Microarray hybridization experiments usually require high amounts and high quality of mRNA. The diameter of an egg cell of maize is only about 60 μm while the apical and basal cell of the two-celled proembryo are about 60 and 30 μm in diameter, respectively. The small size of these cells is a technical limitation to perform microarray hybridizations. To overcome this problem, isolated mRNA from few (2 or 3 egg cells, apical and basal cells) cells was linearly amplified using a procedure described by Van Gelder *et al.* (1990). The amplification method resulted in high yields of AA-aRNA ranging from 15 to 47 μg. The quality of the AA-aRNA was assessed using the Agilent 2100 Bioanalyzer with the RNA 6000 Pico Kit. The kit contains chips and reagents

designed for analysis of RNA fragments. The chip itself contains an interconnected set of microchannels, which is used for separation of nucleic acid fragments based on their size as they are driven through it by electrophoresis. Reproducible results were observed for the various samples after AA-aRNA generation (Fig. 6). The AA-aRNA fragments ranged from about 100 to 2000 nucleotides. A peak of AA-aRNA fragments was observed at about 500 nucleotides. The presence of degradation products was not observed. Thus the linear mRNA amplification procedure resulted in high quality AA-aRNA.
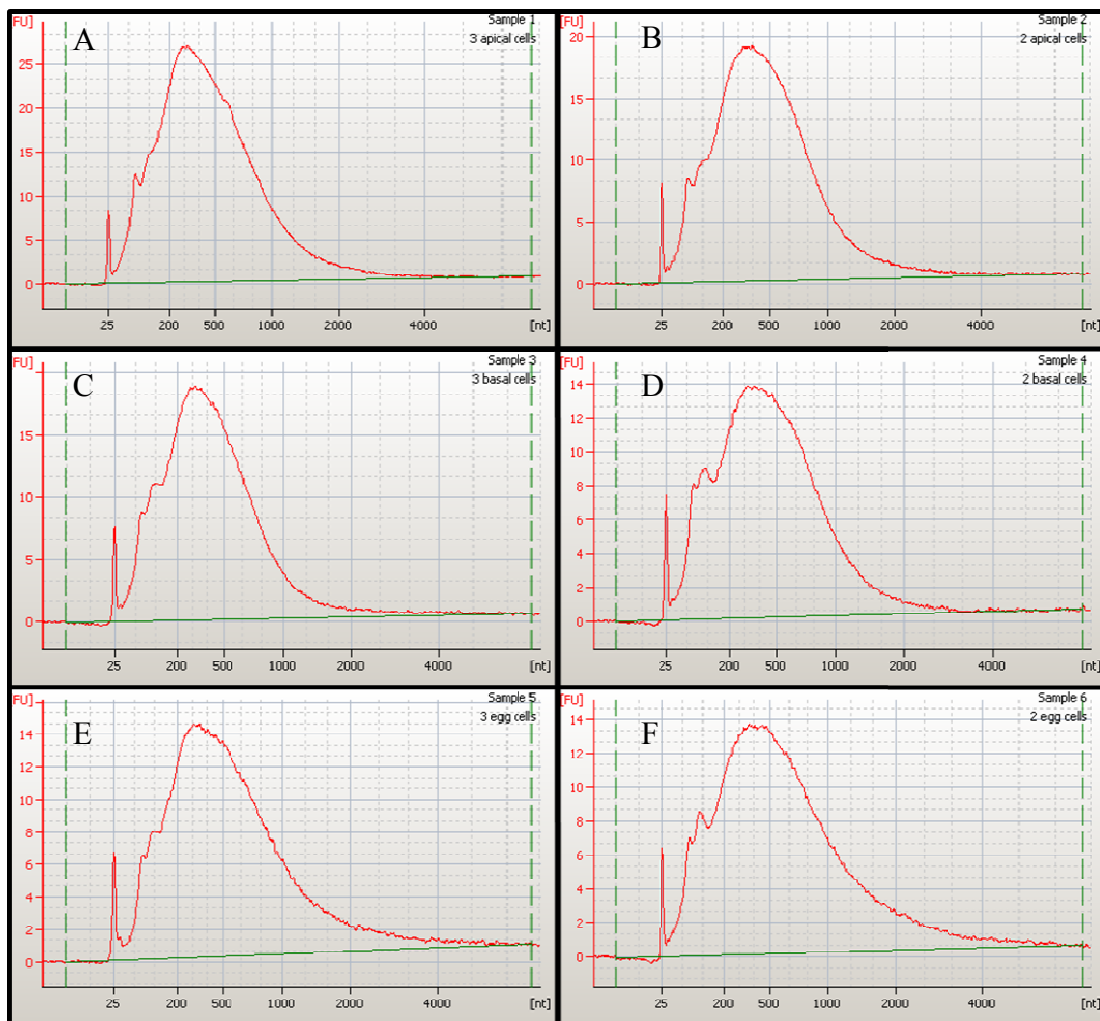
Figure 6. Quality control of linear amplified mRNA. mRNA was isolated from **(A)** and **(B)** 3 and 2 apical cells, respectively; **(C)** and **(D)** 3 and 2 basal cells, respectively; **(E)** and **(F)** 3 and 2 egg cells, respectively. Fluorescence units (FU); nucleotides (nt).

3.3 Identification of genes expressed in the egg cell and differentially expressed in the apical and basal cell of the two-celled proembryo

Microarray hybridizations were performed to compare the gene expression profile of the egg, apical and basal cell. The aim was to identify genes that are strongly

expressed in the egg cell and after zygotic division are up-regulated either in the apical or basal cell of the two-celled proembryo. The transcript segregation from the egg cell either to the apical or the basal cell could be one possible mechanism that is responsible for cell identity and fate determination. A number of genes were identified to be regulated in the cells analyzed (Table 1). The most distinct gene regulation profile was observed when the apical cell was compared with the egg cell. At FC (Fold Change) level higher than three, 363 genes were differentially expressed when the apical cell transcriptome was compared with the egg cell with a p-value ranging from 0,05 to 0,001. When gene regulation was analyzed comparing the apical and basal cell it was possible to notice that 264 genes were regulated at a FC higher than 3 with a p-value ranging from 0,05 to 0,001. Finally, 143 genes were differentially expressed when the egg and basal cells were compared at a FC higher than 3 (P<0,05-0,001).

Table 1. Differential expression analysis report of microarray experiment performed with egg cells, apical and basal cells of the two celled proembryo of maize. The numbers represent genes regulated at a given fold change (FC) and p-value (P) after the analysis of microarrays hybrized in a loop design with egg cells, apical and basal cells, with four replicates of each sample (cell type).

	P<0,05	P<0,02	P<0,01	P<0,005	P<0,001
Apical cell *versus* basal cell					
FC>1,1	455	113	38	16	1
FC>1,5	420	106	34	13	1
FC>2,0	339	81	24	10	0
FC>3,0	193	51	14	6	0
Apical cell *versus* egg cell					
FC>1,1	689	228	101	57	6
FC>1,5	641	214	93	51	6
FC>2,0	487	151	65	32	4
FC>3,0	246	69	32	15	1
Basal cell *versus* egg cell					
FC>1,1	285	84	38	19	3
FC>1,5	257	74	36	19	3
FC>2,0	189	57	28	17	3
FC>3,0	91	23	16	10	3

3.3.1 *Group 1: genes up-regulated in the egg cell and apical cell and down-regulated in the basal cell*

The apical cell gives rise to embryo-proper. Unrevealing genes involved in cell fate determination in this cell would be of great importance and interest since these genes could also be involved in patterning of the embryo structure at later stages. In total 42 genes were identified to be significantly up-regulated in the egg cell and apical cell of the two celled proembryo (Table 2). BLASTX searches were performed and

regulated genes were clustered according to the pathway they are involved. 19% of these genes are involved in gene regulation. 7,1% of genes are either involved in protein/protein interaction, vesicle trafficking or transport. 9,6% of the genes were uniformly distributed between genes involved in RNA metabolism and cytoskeleton. 14,3% of genes are either involved in signaling or cell wall biogenesis. 19% of the transcripts encode proteins involved in general and DNA metabolism and finally the largest cluster of 31% represent regulated genes encoding for proteins with unknown function.

Table 2. Group 1: genes up-regulated in the egg cell and apical cell and down-regulated in the basal cell.

Function	TIGR ID	Top BLASTX annotation (GenBank AC, specie)	Signal intensity		
			Egg cell	Apical cell	Basal cell
Gene regulation	TC213900	Zinc finger CDGSH type (NP_568764.1, *A. thaliana*)	1784	7582	94
	TC270137	Auxin response factor1 (CAC83756.1, *O. sativa*)	7019	5456	228
	TC252443	Transcription factor HBP1 (Q41558.2, *T. aestivum*)	7113	2345	483
	TC273875	PHD zinc finger-containing protein (XP_002444141.1, *S. bicolor*)	1403	1238	180
	AW191070	AP2/EREBP transcription factor-like protein (BAD19450.1, *O. sativa*)	13272	1719	762
	AZM4_125444	Putative HIRA (repressor) (BAD46207.1, *O. sativa*)	1248	709	93
	TC262294	Zinc finger HIT-type domain containing protein (BAF07393.1, *O. sativa*)	2291	6455	86
	TC271463	ARID/BRIGHT DNA-binding domain-containing protein (BAH20138.1, *A. thaliana*)	6494	3985	421
RNA metabolism	TC262841	Putative RNA binding protein (AAG59664.1, *O. sativa*)	714	1335	62
	OGYBR86TH	Putative splicing factor (NP_201232.1, *A. thaliana*)	2601	1207	59
Protein/ protein interaction	CF017581	14-3-3-like protein (CP65-357, *Saccharum cultivar*)	2349	2141	101
Cytoskeleton	TC271477	Profilin5 (NP_001105622.1, *Z. mays*)	5492	4896	104
	TC252670	Actin bundling protein135 (AAD54660.1, *L. longiflorum*)	2449	8541	725
Vesicle trafficking	TC260574	Ras-related protein Rab-2-A (AAA63901.1, *Z. mays*)	1138	686	71
Signaling	TC261326	Putative LRR receptor-like protein kinase (BAB39873.1, *O. sativa*)	1345	1612	436
	AW400228	CPK34 calcium- dependent protein kinase (NP_197437.1, *A. thaliana*)	1361	987	42
	TC251622	BRI1 supressor1 (BSU1)-like1 (NP_192217.2, *A. thaliana*)	1301	1725	270
Cell wall biogenesis/ structure	TC270190	Adhesive/proline-rich protein (EU952432.1, *Z. mays*)	36494	29952	778

Cell wall biogenesis/ structure	AZM4_124484	Phi-1-like phosphate-induced protein (ACG26284.1, *Z. mays*)	2449	948	172
	TC262581	Putative beta-N-acetylhexosaminidase (AAB60911.1, *A. thaliana*)	8471	1347	148
General and DNA metabolism	TC258503	Metallothionein-like protein type2 (ACG46107.1, *Z. mays*)	32100	15951	411
	TC272430	Alpha-amylase/subtilisin inhibitor (AAN86549.1, *O. sativa*)	1109	1197	162
	TC263087	Glycosyl hydrolase (BAD45807.1, *O. sativa*)	4352	5855	116
	CF023928	Putative trehalose-6-phosphate synthase (CBH32509.1, *T. aestivum*)	4099	3073	97
	TC262083	Putative trehalose-6-phosphate phosphatase (NP_192980.1, *A. thaliana*)	2041	2735	195
	TC254030	Delta-8 sphingolipid desaturase, putative (NP_182144.1, *A. thaliana*)	11713	3252	781
	TC249210	DNA topoisomerase II (AAN85207.1, *N. tabacum*)	23927	5058	86
	TC260284	Putative replication factor-C (AAO37979.1, *O. sativa*)	7457	4104	529
Transport	TC271162	SPX (SYG1/Pho81/XPR1) domain-containing protein (NP_001077763.1, *A. thaliana*)	2517	6469	372
Unknown function	CD974206	Hypothetical protein (XP_002452078.1, *S. bicolor*)	1696	3169	121
	TC273889	Unknown protein (BAD81619.1, *O. sativa*)	2253	3195	291
	TC256902	hypothetical protein (AAO39858.1, *O. sativa*)	2920	1630	135
	CD438095	Unknown protein (BAB39974.1, *O.sativa*)	2579	3237	384
	CD441285	Hypothetical protein (ACG44331.1, *Z. mays*)	2597	2852	262
	TC260920	Hypothetical protein (NP_001144187.1, *Z. mays*)	1654	1388	250
	TC278226	Expressed protein (AAT76412.1, *O. sativa*)	945	1244	219
	TC272321	Putative DegP2 protease (BAD15737.1, *O. sativa*)	9398	5842	249
	BE123301	Putative pectate lyase (AAK54283.1, *O. sativa*)	14333	7116	131
	AZM4_1101	Putative glycosyl hydrolase of unknown function DUF1680 (NP_569013.1, *A. thaliana*)	1546	1460	54
	TC250222	Membrane protein COV-like (BAB89792.1, *O. sativa*)	3317	1929	246
	AZM4_14282	hypothetical protein (XP_002462883.1, *S. bicolor*)	1074	2637	347
	BM080817	No match	1336	1629	127

3.3.2 *Group 2: genes up-regulated in the egg cell and basal cell and down-regulated in the apical cell*

The basal cell originates the suspensor. The suspensor is an important structure for the normal development of the embryo-proper since it is thought to transfer nutrients from the maternal tissue to the developing embryo (Yeung and Meinke, 1993). Surprisingly, only seven genes were identified to be up-regulated in the egg cell and

basal cell of the two-celled proembryo (Table 3). Up-regulated genes may play a role in basal cell specification and are involved in gene regulation, signaling, cell wall remodeling, vesicle trafficking, general metabolism and are associated with cytoskeleton.

Table 3. Group 2: genes up-regulated in the egg cell and basal cell and down-regulated in the apical cell.

Function	TIGR ID	Top BLASTX annotation (GenBank AC, specie)	Signal intensity		
			Egg cell	Apical cell	Basal cell
Gene regulation	TC276644	Homeobox-like resistance transcription factor (ABY85265.1, *T. aestivum*)	1268	103	1278
Cytoskeleton	CF007156	Spiral1-like1 (NP_001117356.1, *A. thaliana*)	8105	215	8396
Signaling	AZM4_13308	Harpin-induced protein 1 containing protein (ABF95102.1, *O. sativa*)	1371	205	1592
Cell wall remodeling	AZM4_114498	Xyloglucan endotransglucosylase/ hydrolase protein 23 (ACG35105.1, *Z. mays*)	5690	189	12656
Vesicle trafficking	CD996811	Putative vacuolar sorting receptor 1 precursor (XP_002528694.1, *R. communis*)	1327	208	1326
General metabolism	AI444705	Protease inhibitor/seed storage/lipid transfer protein (LTP) family protein (NP_565348.1, *A. thaliana*)	2114	124	2133
	NP672200	Phosphoserine phosphatase (NP_001151556.1, *Z. mays*)	914	74	1035

3.4   Fertilization induced genes in the apical and basal cell of the two-celled proembryo

3.4.1   *Group 3: genes up-regulated in the apical cell and down-regulated in the egg cell and basal cell*

The identification of fertilization induced genes can provide new information about the process regulating zygotic embryogenesis. 39 genes were indentified to be up-regulated in the apical cell and down-regulated in the egg cell and basal cell (Table 4). Genes clustered into the gene regulation and signaling pathway represented each 7,7% of up-regulated genes in the apical cell. Similarly, genes encoding for proteins involved in vesicle trafficking, protein folding and protein degradation enclosed each 5,1% of the total of genes with increased expression in the apical cell. Moreover, a high proportion of up-regulated genes (25,6%) in the apical cell act in regulating general metabolism. Genes encoding for proteins involved with transport, RNA metabolism, ion uptake and cytoskeleton represented each about 2,6% of the overall genes up-regulated in the apical cell. Finally, 33,3% of the genes encode for proteins with unknown function.

Table 4. Group 3: genes up-regulated in the apical cell and down-regulated in the egg cell and basal cell.

Function	TIGR ID	Top BLASTX annotation (GenBank AC, specie)	Signal intensity		
			Egg cell	Apical cell	Basal cell
Gene regulation	TC262991	Putative transcription factor II H (XP_002519045.1, *R. communis*)	764	1970	495
	BM660004	Transcription factor/ zinc ion binding (NP_680116.2, *A. thaliana*)	380	1741	577
Protein/ protein interaction	TC259989	14-3-3 protein 7 (AAL04425.1, *L. esculentum*)	702	1175	509
Vesicle trafficking	TC250999	Putative ADP-ribosylation factor (AAG46163.1, *O. sativa*)	809	2059	898
	TC248330	Putative Ras-GTPase activating protein SH3 domain-binding protein 2 (BAC84474.1, *O. sativa*)	553	1247	644
Signaling	TC250774	Tyrosine-specific protein phosphatase (AAT74541.1, *O. sativa*)	677	3455	871
	TC266591	Putative serine/threonine-protein kinase (NP_912073.1, *O. sativa*)	592	1827	586
	TC253925	Protein kinase-like (BAD27770.1, *O. sativa*)	306	1480	208
General metabolism	BF727942	Putative allyl alcohol dehydrogenase (BAB90185.1, *O. sativa*)	991	3294	607
	BG517703	Pantoate-beta-alanine ligase (ACG42174.1, *Z. mays*)	481	1965	85
	BG319647	Multiple inositol polyphosphate phosphatase PhyIIc (ABJ98334.1, *T. aestivum*)	399	1247	190
	TC262314	Pyridoxamine 5-phosphate oxidase family protein (NP_001149182.1, *Z. mays*)	399	1273	529
	TC257498	Putative methionyl-tRNA synthetase/methionine tRNAligase (BAD61657.1, *O. sativa*)	581	2105	854
	TC263844	Digalactosyldiacylglycerol synthase 1 (AAT67420.1, *G. max*)	481	1914	189
	AW216347	Putative 12-oxophytodienoate reductase (NP_001061975.1, *O. sativa*)	396	1859	450
	TC261329	Oxidoreductase, 2OG-Fe(II) oxygenase family protein (NP_192203.1, *A. thaliana*)	641	3055	212
	BG268420	Carbonic anhydrase (NP_001150123.1, *Z. mays*)	453	3858	700
	CD974060	Pantoate-beta-alanine ligase (NP_199695.1, *A. thaliana*)	470	2112	80
Transport	BG320728	Auxin transporter PIN1 (AAS19858.1, *T. aestivum*)	309	1884	383
RNA metabolism	BM499989	YLS8 DMI splicing factor (AAG40036.1, *A. thaliana*)	580	1005	357
Targeting proteins for degradation	AZM4_50869	Ubiquitin fusion degradation UFD1 family protein (NP_565504.1, *A. thaliana*)	378	1345	437
	TC265976	F-box domain containing protein (NP_001151411.1, *Z. mays*)	601	2215	353
Ion uptake	TC253416	Putative shaker-like potassium channel (BAD45736.1, *O. sativa*)	506	1256	386
Cytoskeleton	TC277169	AR791 actin binding (NP_564600.1, *A. thaliana*)	240	1345	127
Protein folding	TC250116	Chaperonin heat shock protein 60-3A (AAU95459.1, *A. thaliana*)	784	2155	565
	TC254703	ATPase/chaperone (AAN72234.1, *A. thaliana*)	125	2071	496
Unknown function	TC252469	Reticulon protein (ACG27675.1, *Z. mays*)	328	2741	431

	TC210061	Hypothetical protein (XP_002438863.1, *S. bicolor*)	710	4338	595
	TC275920	Hypothetical protein (XP_002448154.1, *S. bicolor*)	412	2544	440
	AZM4_25066	Hypothetical protein (XP_002457003.1, *S. bicolor*)	615	3424	548
	BG517703	No match	481	1965	85
	TC264925	Hypothetical protein (XP_002441985.1, *S. bicolor*)	778	2602	363
Unknown function	BE051165	Hypothetical protein (XP_002439406.1, *S. bicolor*)	152	977	80
	CD957537	Hypothetical protein (XP_002461801.1, *S. bicolor*)	292	1077	204
	AW267421	Hypothetical protein (XP_002467979.1, *S. bicolor*)	259	1716	462
	CD974060	Hypothetical protein (XP_002448154.1, *S. bicolor*)	470	2112	80
	AZM4_92287	LAP4 leucine-rich repeat protein (NP_001148341.1, *Z. mays*)	375	1072	161
	TC278141	Expressed protein (AAT77082.1, *O. sativa*)	377	1841	245
	TC277336	Hypothetical protein (EEC71321.1, *O. sativa*)	367	1314	550

3.4.2   *Group 4: genes up-regulated in the basal cell and down-regulated in the egg cell and basal cell*

In the same way, 13 genes were up-regulated in the basal cell and down-regulated in the egg cell and apical cell (Table 5). Genes responsible for gene regulation, cell wall biogenesis and senescence contributed equally to 23,1% of the up-regulated genes in the basal cell. On the other hand, genes classified into signaling and general metabolism pathways enclosed each 23% of genes with increased expression in the basal cell. The largest portion of 30,9% of the genes encode proteins with unknown function.

Table 5. Group 4: genes up-regulated in the basal cell and down-regulated in the egg cell and basal cell.

Function	TIGR ID	Top BLASTX annotation (GenBank AC, specie)	Signal intensity		
			Egg cell	Apical cell	Basal cell
Cell wall biogenesis	TC265649	Cellulose-synthase like C12 (AAP68209.1, *A. thaliana*)	477	673	1396
Gene regulation	TC277899	CBS domain containing protein (NP_001148069.1, *Z. mays*)	559	642	1271
Senescence	BE129876	Putative senescence-associated protein (BAB33421.1, *P. sativum*)	492	902	2109
Signaling	TC272919	Gibberellin receptor GID1L2 (NP_001150146.1, *Z. mays*)	547	663	1179
	TC275908	Putative somatic embryogenesis receptor kinase (NP_001061919.1, *O. sativa*)	556	711	1676
	TC248938	MFS18 protein precursor (NP_001105446.1, *Z. mays*)	657	379	1216
General metabolism	TC265568	Putative triacylglycerol lipase (XP_002515304.1, *R. communis*)	566	396	2354
	AI461557	Phosphatidylcholine-sterol O-acyltransferase (NP_196868.1, *A. thaliana*)	607	171	1216
	CF031024	Succinyl-CoA ligase alpha-chain 2 (NP_001149702.1, *Z. mays*)	653	177	1145
Unknown function	TC255063	No match	247	466	1035
	TC263129	No match	494	405	1051
	TC265197	Unknown protein (NP_567597.2, *A. thaliana*)	557	316	1614
	AW165636	Expressed protein (AAR89874.1, *O. sativa*)	562	469	1020

4   Discussion

The asymmetric zygotic division in maize generates the apical and basal cells, which have different fates. The apical cell gives rise to the embryo proper, while the basal cell generates the suspensor. Although several histological analyses have been performed (Randolph, 1936; Abbe and Stein, 1954; Diboll, 1968; Van Lammeren, 1986; reviewed by Vernoud *et al*., 2005) little is known about the molecular mechanism controlling cell fate determination during zygotic embryogenesis. Probably, one mechanism involved in cell fate specification is the asymmetric distribution of fate determinant mRNAs in the egg cell/zygote, which would be inherited by either the apical or basal cell. Comparative transcriptome analyses were performed with maize egg cells, apical and basal cells to investigate this hypothesis. The results will be now discussed and genes that were identified as differentially expressed are listed (the most homologous genes are given in brackets).

4.1   Cytoskeleton and polar distribution of mRNAs and proteins

Regulation of expression of genes encoding for proteins involved in the organization of the cytoskeleton seems to play an important role during the asymmetric division of the zygote in maize. The zygote is highly asymmetricaly organized at the end of telophase with one nucleus located closer to the periphery of the zygote with higher concentration of cytoplasm in this area. This part of the zygote gives rise to the apical cell while the region where the other nucleus is more distant from the cell periphery, the cytoplasm is not so dense and is rich in vacuoles, generates the basal cell. The cytoskeleton is not only important in correctly placing the nuclei during asymmetric division but also in allocating cell fate determinants in a polar manner. For example, the RNA binding protein STAUFEN is required for the microtubule-dependent localization of *oskar* mRNAs to the posterior of the *Drosophila* oocyte (Ephrussi *et al*., 1991; Kim-Ha *et al*., 1991; St Johnston *et al*., 1991; Irion *et al*., 2006). The polar localization of these mRNAs with subsequent translation and asymmetric localization of proteins is responsible for the formation of the anterior-posterior axis (Irion *et al*., 2006). Interestingly, a gene encoding for a putative RNA binding protein (AAG59664.1, *O. sativa*) is up-regulated in the egg cell and apical cell.

Another mechanism to generate polar distribution of fate determinants is differential protein localization, exemplified during asymmetric division of neuroblast cells in *Drosophila* (Gönczy, 2008). In the present study several genes encoding for

proteins involved in vesicle trafficking showed differential expression between the egg cell, apical and basal cells. Proteins involved with vesicle trafficking could be responsible for polar localization of proteins in charge for cell fate determination.

Moreover, genes encoding for proteins (actin bundling protein135, AAD54660.1, *L. longiflorum*; profilin5, NP_001105622.1, *Z. mays*) involved in cytoskeleton organization are up-regulated in the egg cell and apical cell. The gene encoding for Spiral1-like1 (NP_001117356.1, *A. thaliana*) protein is up-regulated in the egg cell and basal cell. *SPIRAL1* encodes for a plant-specific microtubule-localized protein (Nakajima *et al.*, 2004). Finally, a gene encoding for the AR791 actin binding protein (NP_564600.1, *A. thaliana*) is up-regulated in the apical cell. These data suggest that cytoskeleton (re)organization occurs during asymmetric division of the zygote.

4.2   Transcription profile of the basal cell

During my PhD study efforts were made to identify transcripts encoding for fate determinants that are differentially expressed in the apical and basal cell of the two-celled proembryo in maize. The transcripts were classified into four different groups (see results) of which a large number encode for proteins with yet unknown function. A reduced number of genes were categorized into the group 2 [genes up-regulated in the egg and basal cell (generates the suspensor) and down-regulated in the apical cell (gives rise to the embryo proper)] and group 4 (genes up-regulated in the basal cell and down-regulated in the egg and apical cell). Recently, it was discussed that the suspensor evolved independently from the embryo proper. A significant proportion (~20%) of transcripts identified in soybean and *Arabidopsis* suspensors encode for proteins with unknown function. This situation might be due to the fact that the suspensor is a highly specialized structure, which has no role in subsequent plant development, meaning that a large number of the genes required for suspensor development are involved in yet undiscovered biological processes. Moreover, suspensor cells are probably direct clonal descendants of the basal cell. In this sense, molecular mechanisms, which control suspensor-specific gene expression might be directly linked to the pathways that establish basal cell fate (Kawashima and Goldberg, 2009).

The selection of oligo(s) nucleotides for the microarray chip employed in the present study was determined by analysis of expression profiles generated for sixteen diverse maize tissues (www.maizearray.org/). Probably, some genes that are specifically

expressed in the egg cell and/or zygote and are responsible for cell fate determination in the basal cell, are not represented on this microarray.

To overcome this problem, a microarray chip was designed with genes that are expressed in the egg cell and zygote of maize (Kliwer *et al.*, unpublished data). This microarray was hybridized with labeled samples of AA-aRNA from egg cells, apical and basal cells. The microarray data is currently being analyzed in the frame of the PhD work of Irina Kliwer.

4.3   Gene regulation

Gene regulation seems to be a mechanism of great importance during cell fate determination in the apical and basal cell of the two-celled proembryo in maize. A classical example from the model system *Arabidopsis* is the segregation of transcripts encoding WOX homeobox transcription factor proteins in the apical and basal cells. *WOX2* and *WOX8* transcripts become restricted to the apical and basal cell, respectively (Haecker *et al.*, 2004). *wox2* mutants showed abnormal development of the embryo, and *wox8wox9* double mutants showed defects in embryo proper and suspensor development. The phenotypes observed in the embryo proper in *wox8wox9* mutants might be due to the regulation that these proteins display on *WOX2* expression in the embryo proper (Breuninger *et al.*, 2008).

In maize I have also identified eight transcription factors that are up-regulated in the egg cell and apical cell but down-regulated in the basal cell. On the other hand, only two transcription factors are up-regulated in the egg cell and basal cell but down-regulated in the apical cell. Recently, several *cis*-regulatory sequences have been identified to be required for transcriptional activation in the suspensor of *Phaseolus coccineus*, *Arabidopsis* and *Nicotiana tabacum* (Kawashima *et al.*, 2009) reinforcing the importance of gene regulation during cell fate determination. Such efforts to identify *cis*-regulatory sequences responsible to active transcription in the apical cell in maize or other plants species were not achieved until now.

Transcriptional repression has been showed to be present in cells with different fates generated by asymmetric cell division. For example, the GERMLINE RESTRICTIVE SILENCING FACTOR (GRSF) is expressed in non-male gamete lineage cells and represses the expression of several sperm cell specific transcripts in these cells (Haerizadeh *et al.*, 2006). The putative transcriptional repressor HIRA (BAD46207.1, *O. sativa*), which is up-regulated in the egg and apical cells, but down-

regulated in the basal cell could have a similar function in repressing basal cell specific transcripts in the apical cell.

4.4 The splicing machinery and cell fate determination

Alternative splicing of messenger RNA precursors also plays an important role in generating sources of protein diversity (Blaustein *et al.*, 2007). Splicing factors have been shown to participate in the pathway where cell fate decisions are determined. The *Arabidopsis clo/gfa1*, *ato* and *lis* mutants, for example, show defects in cell fate determination in the female gametophyte. *CLO/GFA1* encodes the *Arabidopsis* homologue of Snu114 of yeast and *LIS* is homologous to the yeast splicing factor PRP4. Both proteins are essential components of the spliceosome. *ATO* encodes the *Arabidopsis* homologue of SF3a60, which is involved in pre-spliceosome formation in yeast (Groß-Hardt *et al.*, 2007; Moll *et al.*, 2008). The mechanisms by which splicing factors act in cell specification could be the involvement in correct splicing of signals responsible for fate determination or even the correct splicing of some regulators (Groß-Hardt *et al.*, 2007). The polar localization of the *Stardust* mRNA in the apical region of *Drosophila* epithelial cells, for example also involves the splicing machinery. The mRNA localization signal is enclosed in an alternatively spliced coding exon of *Stardust*, which enables the transcript to be transported in a dynein-dependent manner to the apical region (Horne-Badovinac and Bilder, 2008)

Taken together, the putative splicing factor (NP_201232.1, *A. thaliana*) that is up-regulated in the egg cell and apical cell could be an interesting candidate playing a role in cell fate determination in the apical cell of the two-celled proembryo in maize.

4.5 Signaling

There are indications that after the asymmetric zygotic division, when the embryo proper starts to develop from the apical cell and the suspensor from the basal cell, the embryo itself represses embryonic development in the suspensor. Mutations in several genes resulted in the formation of a secondary embryo from the suspensor cells after the primary embryo arrested development or even if it continued to develop resulting in polyembryony (Schwartz *et al.*, 1994; Vernon and Meinke, 1994; Zhang and Somerville, 1997). Thus, signaling molecules sent by the embryo proper might play an important role in inhibiting embryonic development in the suspensor.

Auxin signaling is, most likely, the best characterized signaling event in embryo patterning. Many examples demonstrate an important role for cellular auxin response in

different parts of the embryo and at different stages (Fischer-Iglesias *et al.*, 2001; Friml *et al.*, 2003; Forestan *et al.*, 2010). Moreover, high concentration of auxin was detected, by the activity of the DR5 promoter (Ulmasov *et al.*, 1997), already in the apical cell of the two-celled proembryo in *Arabidopsis*. The auxin efflux carrier PIN1 (PIN-FORMED) protein was detected in *Arabidopsis* when the embryo proper consisted of two cells (Friml *et al.*, 2003). Similar results were observed in the present study. The *PIN1* transcript (AAS19858.1, *T. aestivum*) was detected to be up-regulated in the apical cell in comparison with the egg cell and basal cell. Another indication that auxin plays an important role early in embryogenesis is the fact that *ARF1* (Auxin response factor1; CAC83756.1, *O. sativa*) is up-regulated in both the egg cell and apical cell and down-regulated in the basal cell.

Moreover, several genes encoding for proteins involved in signaling are differentially expressed in the egg cell, apical and basal cells indicating that this pathway plays an important role in fate determination during early steps of zygotic embryogenesis.

4.6   Outlook

The asymmetric division of the zygote in maize generates the apical and basal cell, which are distinct in size and fate. The small apical cell gives rise to the embryo proper while the large basal cell forms the suspensor. Polar distribution of fate determinants probably plays an important role during asymmetric cell division, like it is well documented for the animal model systems *C. elegans* and *D. melanogaster*. However, in plants only indirect evidence suggests segregation of molecules during asymmetric cell division, and polar localization of fate determinants before cell separation still has to be demonstrated. Thus, the λN (Daigle and Ellenberg, 2007) and the MS2 (Bertrand *et al.*, 1998) systems could be used for *in vivo* imaging of asymmetrically localized mRNAs identified in this work, which appear differentially expressed in the apical and basal cell after zygotic division. The two systems were shown to be applicable in plants (Hamada *et al.*, 2003; Hammes *et al.*, 2010). Both systems are based on the capacity of virus RNA binding proteins to bind complementary RNA-hairpins. In this sense, the RNA binding protein could be fused with a fluorescent protein and a nuclear localization signal (NLS) and used to generate transgenic plants. A second line of transgenic plants is required where the candidate gene contains the RNA hairpin sequence in its 5' or 3' UTR. These transgenic lines can then be crossed to follow the localization of candidate mRNA. Furthermore, knockdown mutants could be generated

for genes, of which mRNAs were identified to be polarly localized to get more insights into the function of these genes. Another alternative would be the ectopically expression of mRNA that are found to be localized in a polar manner. Finally, yeast three-hybrid screens (Hook *et al*., 2005) could be performed with candidate mRNAs to identify the interacting proteins to elucidate, for example the pathway of mRNA polar localization during asymmetric zygotic division in maize.

5   Summary

Asymmetric cell division is an important process in animal and plants to generate cell diversity. This pathway is notable even at the first step of the plant life cycle, namely after fertilization of the egg cell by a sperm cell during asymmetric division of the zygote. The molecular mechanisms controlling cell fate determination in the two-celled proembryo are poorly understood. Comparative transcriptome analyses were performed with maize egg cells, apical and basal cells. The aim of my work therefore was to identify candidate transcripts that are polarly localized in the egg cell and which segregated either to the apical or basal cell of the two-celled proembryo after zygotic division. I have therefore first analyzed the fertilization process in maize to determine the time point of zygotic division, which occurs at about 48 hours after pollination. Afterwards, a procedure was established to microdissect the apical and basal cell from ovules after *in vivo* pollination. A linear amplification procedure was carried out with mRNA derived from these cells to increase the yield and to make microarray hybridizations possible. Microarray hybridizations and bioinformatics analysis were performed. Several interesting candidate genes were identified to be expressed in the maize egg cell and differentially expressed in the apical or basal cell. The majority of differentially expressed genes encode for proteins involved in gene regulation, metabolism and proteins with unknown function. Furthermore, other classes of transcripts encode for proteins involved in signaling, vesicle trafficking, cytoskeleton, RNA metabolism, protein/protein interaction, cell wall biogenesis/structure, transport, targeting proteins for degradation and protein folding. Some of these processes were previously shown to be associated with asymmetric cell division and cell fate determination.

6   References

Abbe EC, Stein OL (1954) The growth of the shoot apex in maize: embryogeny. *Am. J. Bot.* 41, 285-293.

Abrash EB, Bergmann DC (2009) Asymmetric cell divisions: a view from plant development. *Dev. Cell* 16, 783-796.

Bertrand E, Chartrand P, Schaefer M, Shenoy S, Singer R, Long R (1998) Localization of *ASH1* mRNA particles in living yeast. *Mol. Cell* 2, 437-445.

Blaustein M, Pelisch F, Srebrow A (2007) Signals, pathways and splicing regulation. *Int. J. of Biochem. and Cell Bio.* 39, 2031-2048.

Borges F, Gomes G, Gardner R, Moreno N, McCormick S, Feijo JA, Becker JD (2008) Comparative transcriptomics of *Arabidopsis thaliana* sperm cells. *Plant Physiol.* 148, 1168-1181.

Breuninger H, Rikirsch E, Hermann M, Ueda M, Thomas L (2008) Differential expression of *WOX* genes mediates apical-basal axis formation in the *Arabidopsis* embryo. *Developmental Cell* 14, 867-876.

Daigle N, Ellenberg J (2007) LambdaN-GFP: an RNA reporter system for live-cell imaging. *Nat. Methods* 4, 633-636.

DeRenzo C, Reese KJ, Seydoux G (2003) Exclusion of germ plasm proteins from somatic lineages by cullin-dependent degradation. *Nature* 424, 685-689.

Diboll AG (1968) Fine structural development of the megagametophyte of *Zea mays* following fertilization. *Am. J. Bot.* 55, 787-806.

Ephrussi A, Dickinson LK, Lehmann R (1991) *oskar* organizes the germplasm and directs localization of the posterior determinant *nanos*. *Cell* 66, 37-50.

Fischer-Iglesias C, Sundberg B, Neuhaus G, Jones AM (2001) Auxin distribution and transport during embryonic pattern formation in wheat. *Plant J.* 26, 115-129.

Forestan C, Meda S, Varotto S (2010) ZmPIN1-mediated auxin transport is related to cellular differentiation during maize embryogenesis and endosperm development. *Plant Physiol.* 152, 1373-1390.

Friml J, Vieten A, Sauer M, Weijers D, Schwarz H, Hamann T (2003) Efflux-dependent auxin gradients establish the apical-basal axis of *Arabidopsis*. *Nature* 426, 147-153.

Giuliani C, Consonni G, Gavazzi G, Colombo M, S Dolfini (2002) Programmed cell death during embryogenesis in maize. *Ann. Bot.* 90, 287-292.

Goldstein B, Macara IG (2007) The PAR proteins: fundamental players in animal cell polarization. *Dev. Cell* 13, 609-622.

Gönczy P (2008) Mechanisms of asymmetric cell division: flies and worms pave the way. *Nature Rev. Mol. Cell Biol.* 9, 355-366.

Groß-Hardt R, Kägi C, Baumann N, Moore JM, Baskar R et al. (2007) *LACHESIS* restricts gametic cell fate in the female gametophyte of *Arabidopsis*. *PLoS Biol.* 5, 494-500.

Haecker A, Groß-Hardt R, Geiges B, Sarkar A, Breuninger H, Herrmann M, Laux T (2004) Expression dynamics of *WOX* genes mark cell fate decisions during early embryonic patterning in *Arabidopsis thaliana. Development* 131, 657-668.

Haerizadeh F, Singh MB, Bhalla PL (2006) Transcriptional repression distinguishes somatic from germ cell lineages in a plant. *Science* 313, 496-499.

Hamada S, Ishiyama K, Sakulsingharoj C, Choi S-B, Wu Y et al. (2003) Dual regulated RNA transport pathways to the cortical region in developing rice endosperm. *Plant Cell* 15, 2265-2272.

Hammes U, Schönberger JK, Dresselhaus T (2010) Visualisierung von mRNA und mRNP-Komplexen in Pflanzenzellen. *BIOspektrum* 16, 169-171.

Heidstra R (2007) Asymmetric cell division in plant development. In: Coelho AM (ed) *Asymmetric cell division*. Heidelberg: Springer, 1-37.

Hook B, Bernstein D, Zhang B, Wickens M (2005) RNA–protein interactions in the yeast three-hybrid system: affinity, sensitivity, and enhanced library screening. *RNA* 11, 227-233.

Horne-Badovinac S, Bilder D (2008) Dynein regulates epithelial polarity and the apical localization of *stardust A* mRNA. *PLoS Genet.* 4, e8.

Huang DW, Sherman BT, Tan Q, Collins JR, Alvord WG et al. (2007) The DAVID gene functional classification tool: a novel biological module-centric algorithm to functionally analyze large gene lists. *Genome Biol.* 8, R183.

Irion U, Adams J, Chang C-W, St Johnston D (2006) Miranda couples *oskar* mRNA/Staufen complexes to the *bicoid* mRNA localization pathway. *Dev. Biol.* 297, 522-533.

Kawashima T, Goldberg RB (2009) The suspensor: not just suspending the embryo. *Trends in Plant Sci.* 15, 23-30.

Kawashima T, Wang X, Henry KF, Bi Y, Weterings K, Goldberg RB (2009) Identification of *cis*-regulatory sequences that activate transcription in the suspensor of plant embryos. *PNAS* 106, 3627-3632.

Kim-Ha J, Smith JL, Macdonald PM (1991) *oskar* mRNA is localized to the posterior pole of the *Drosophila* oocyte. *Cell* 66, 23-35.

Kranz E, Bautor J, Lörz H (1991) In vitro fertilization of single, isolated gametes of maize mediated by electrofusion. *Sex. Plant Reprod.* 4, 12-16.

Kranz E, Lörz H (1993) *In vitro* fertilization with isolated, single gametes results in zygotic embryogenesis and fertile maize plants. *Plant Cell* 5, 739-746.

Kranz E, Wiegen P, Lörz H (1995) Early cytological events after induction of cell division in egg cells and zygote development following *in vitro* fertilization with angiosperm gametes. *Plant J.* 8, 9-23.

Kugler JM, Lasko P (2009) Localization, anchoring and translational control of *oskar*, *gurken*, *bicoid* and *nanos* mRNA during *Drosophila* oogenesis. *Fly* 3, 15-28.

Lecuyer E, Yoshida H, Parthasarathy N, Alm C, Babak T et al. (2007) Global analysis of mRNA localization reveals a prominent role in organizing cellular architecture and function. *Cell* 131, 174-187.

Lukowitz W, Roeder A, Parmenter D, Somerville C (2004) A *MAPKK kinase* gene regulates extraembryonic cell fate in *Arabidopsis*. *Cell* 116, 109-119.

Mahaffey JW (2005) Assisting Hox proteins in controlling body form: are there new lessons from flies (and mammals)? *Curr. Opin. in Gen. & Dev.* 15, 422-429.

Moll C, von Lyncker L, Zimmermann S, Kägi C, Baumann N et al. (2008) CLO/GFA1 and ATO are novel regulators of gametic cell fate in plants. *Plant J.* 56, 913-921.

Nagl W (1990) Translocation of putrescine in the ovule, suspensor and embryo of *Phaseolus coccineus*. *J. Plant Physiol.* 136, 587-591.

Nakajima K, Furutani I, Tachimoto H, Matsubara H, Hashimoto T (2004) *SPIRAL1* encodes a plant-specific microtubule-localized protein required for directional control of rapidly expanding *Arabidopsis* cells. *Plant Cell* 16, 1178-1190.

Ning J, Peng XB, Qu LH, Xin HP, Yan TT, Sun M (2006) Differential gene expression in egg cells and zygotes suggests that the transcriptome is restructed before the first zygotic division in tobacco. *FEBS Letters* 580, 1747-1752.

Okamoto T, Scholten S, Lörz H, Kranz E (2005) Identification of genes that are up- or down-regulated in the apical or basal cell of maize two-celled proembryos and

monitoring their expression during zygote development by a cell manipulation- and PCR-based approach. *Plant Cell Physiol.* 46, 332-338.

Randolph LF (1936) Developmental morphology of the caryopsis in maize. *J. of Ag. Res.* 53, 881-916.

Schwartz BW, Yeung EC, Meinke DW (1994) Disruption of morphogenesis and transformation of the suspensor in abnormal *suspensor* mutants of *Arabidopsis*. *Development* 120, 3235-3245.

Sprunck S, Baumann U, Edwards K, Langridge P, Dresselhaus T (2005) The transcript composition of egg cells changes significantly following fertilization in wheat (*Triticum aestivum* L.). *Plant J.* 41, 660-672.

Stadler R, Lauterbach C, Sauer N (2005) Cell-to-cell movement of green fluorescent protein reveals post-phloem transport in the outer integument and identifies symplastic domains in *Arabidopsis* seeds and embryos. *Plant Physiol.* 139, 701-712.

St Johnston D, Beuchle D, Nüsslein-Volhard C (1991) *staufen*, a gene required to localize maternal RNAs in the *Drosophila* egg. *Cell* 66, 51-63.

St Johnston D (1995) The intracellular localization of messenger RNAs. *Cell* 81, 161-170.

Ulmasov T, Murfett J, Hagen G, Guilfoyle TJ (1997) Aux/IAA proteins repress expression of reporter genes containing natural and highly active synthetic auxin response elements. *Plant Cell* 9, 1963-1971.

Van Gelder RN, Zastrow ME von, Yool A, Dement WC, Barchas JD, Eberwine JH (1990) Amplified RNA synthesized from limited quantities of heterogeneous cDNA. *PNAS* 87, 1663-1667.

Van Lammeren AAM (1986) Developmental morphology and cytology of the young maize embryo (*Zea mays* L.). *Acta Bot. Neerl.* 35, 169-188.

Vernon DM, Meinke DW (1994) Embryogenic transformation of the suspensor in twin, a polyembryonic mutant of *Arabidopsis*. *Dev. Biol.* 165, 566-573.

Wang H, Ngwenyama N, Liu Y, Walker JC, Zhang S (2007) Stomatal development and patterning are regulated by environmentally responsive mitogen-activated protein kinases in *Arabidopsis*. *Plant Cell* 19, 63-73.

Yeung EC, Meinke DW (1993) Embryogenesis in angiosperms: development of the suspensor. *Plant Cell* 5, 1371-1381.

Yadegari R, Paiva GR, Laux T, Koltunow AM, Apuya N et al. (1994) Cell differentiation and morphogenesis are uncoupled in *Arabidopsis raspberry* embryos. *Plant Cell* 6, 1713-1729.

Zhang JZ, Somerville CR (1997) Suspensor-derived polyembryony caused by altered expression of valyl-tRNA synthetase in the *twn2* mutant of *Arabidopsis*. *PNAS* 94, 7349-7355.

Chapter 3

The egg cell secreted peptide ZmEAL1 is a cell fate maintenance factor in the female gametophyte

1   Introduction

Typically for a flowering plant (angiosperm) the life cycle of maize (Fig. 1) alternates between a diploid sporophytic and a haploid gametophytic generation. The sexually dimorphic, multicellular gametophytes produce the gametes and are thus in the center of reproductive biology research. The male gametophytes (pollen grain) develop within the anthers, which grow at the tassel. The female gametophytes (megagametophytes or embryo sacs) develop within the ovules, which compose the female inflorescence (ear) in maize. The male spore undergoes asymmetric mitotic division to produce a small generative cell and a large vegetative cell. In maize the mature male gametophyte contains the vegetative cell and two sperm cells derived from a mitotic division of the generative cell (Bedinger and Fowler, 2009). Maize megagametogenesis is of the *Polygonum* type, containing seven cells of four distinct types (Randolph, 1936), which occurs in more than 70% of angiosperm species examined (Huang and Russel, 1992). These four cell types are the egg cell and two accessory synergid cells together forming the egg apparatus at the micropylar pole (opening of the integuments), of the embryo sac. The large and vacuolated central cell is diploid and located in the middle of the embryo sac and finally three antipodal cells, which in some species including all grasses proliferate to form a cluster of cells at the chalazal end of the embryo sac (Evans and Grossniklaus, 2009). When maize pollen lands on the stigma, it forms a structure called pollen tube that penetrates the transmitting tissues of the silk to grow towards the inner integument, penetrates the embryo sac through the micropyle and releases two sperm cells in the receptive synergid where they participate in double fertilization (Nawaschin, 1898; Guignard, 1899). The egg cell is fertilized by one of the sperm cells and gives rise to the diploid embryo. The central cell develops into the triploid endosperm after being fertilized by the second sperm cell. The synergid cells are important for pollen tube attraction (Higashiyama *et al*., 2001; Márton *et al*., 2005; Okuda *et al*., 2009), to stop the growth of the pollen tube to achieve fertilization (Escobar-Restrepo *et al*., 2007; Capron *et al*.,

2008), to mediate pollen tube burst (Amien *et al.*, 2010) and to promote sperm cell migration, due to the formation of actin 'coronas' that extend from the middle of the synergid cell, to fertilization targets, egg and central cell (Huang *et al.*, 1999). The antipodals cells are believed to function as transfer cells for the embryo sac (Diboll and Larson, 1966; Maeda and Miyake, 1997) and to serve as a backup for gametic cells (Groß-Hardt *et al.*, 2007). The entire female gametophyte is enclosed within diploid tissues called nucellus.
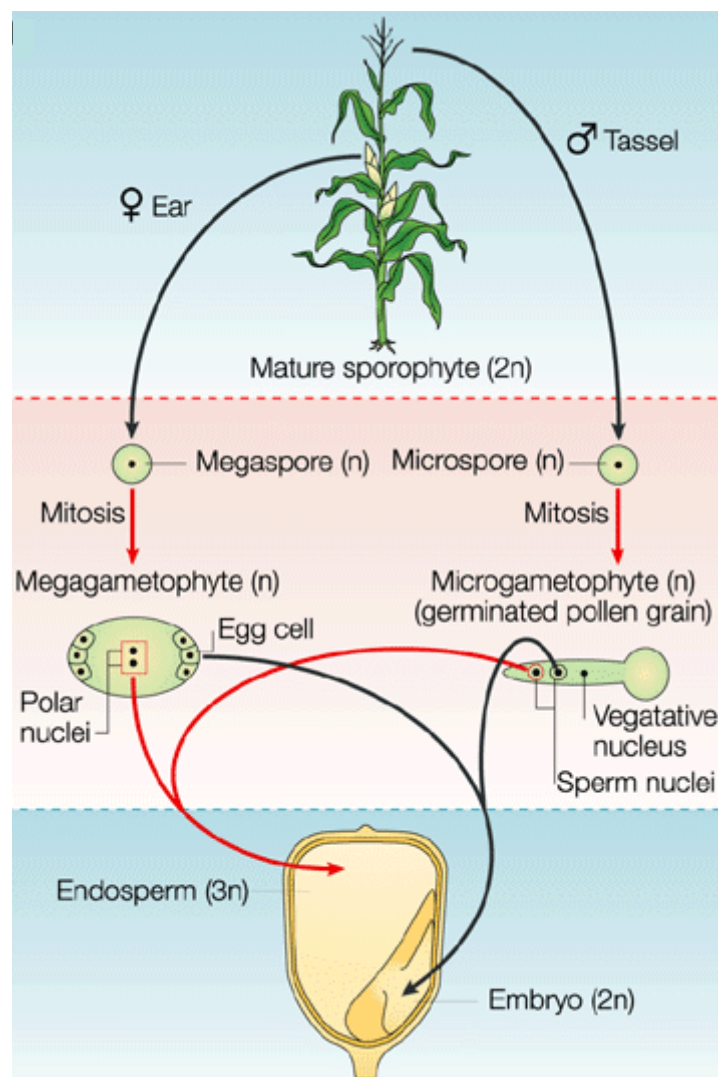
Figure 1. Maize life cycle represented by the diploid sporophytic stage and the haploid gametophytic stage. In the gametophytic stage, meiosis followed by mitotic divisions, produces the female megagametophyte and the male microgametophyte (pollen grain). In the pollen grain, two mitotic divisions give rise to a three-celled gametophyte. The two sperm cells are enclosed within the vegetative cell. The vegetative cell is responsible to form the pollen tube which delivers the two sperm cells to the female gametophyte to participate in the double fertilization process. Within the megagametophyte, one sperm cell fertilizes the haploid differentiated egg cell to produce an embryo and the second sperm cell fuses with the diploid central cell giving rise to the triploid endosperm. After Walbot and Evans (2003).

The development of the embryo sac in maize is outlined in Figure 2. In the developing ovule, a single cell from the nucellus tissue is specified as an "archesporial" cell, which enlarges and differentiates into the megaspore mother cell (MMC). The MMC undergoes two rounds of meiotic divisions to generate four spores, three of which undergo programmed cell death (Evans and Grossniklaus, 2009). The only functional megaspore is the largest, chalazal-most located, and lower in callose than the non-functional megaspores, particularly at its chalazal pole (Russel, 1979). The MMC then undergoes three sequential mitotic nuclear divisions designated as stages FG2 to FG5 (Christensen *et al.*, 1997) to generate eight nuclei, four at each pole, which will contribute to the differentiated embryo sac. The features of each female gametophyte developmental stage in maize were described in detail (Vollbrecht and Hake, 1995). Stage FG1 is characterized by the formation of a vacuole. The first nuclear division, which is parallel to the micropylar-chalazal axis, occurs and the two nuclei are separated by a vacuole. Eventually, a second vacuole is formed at the chalazal end of the embryo sac at stage FG2/3. At developmental stage FG4 the chalazal nucleus divides along the micropylar-chalazal axis, while the division of the micropylar nucleus is perpendicular to the same axis, resulting in T-arrangement of nuclei. The third round of division generates the eight-nucleate coenocytic embryo sac, at early stage FG5. Subsequent cellularization results in the formation of seven cells. After cellularization (late stage FG5) the two polar nuclei, which were located at distinct poles (micropylar and chalazal end of the embryo sac), migrate to the center of the female gametophyte. At stage FG6 the polar nuclei partially fuse, and then migrate to the micropylar end of the embryo sac adjacent to the egg cell. During female gametophyte maturation (stage FG7) the antipodal cells continue to divide reaching a final number of 20 to 100 cells (Evans and Grossniklaus, 2009).
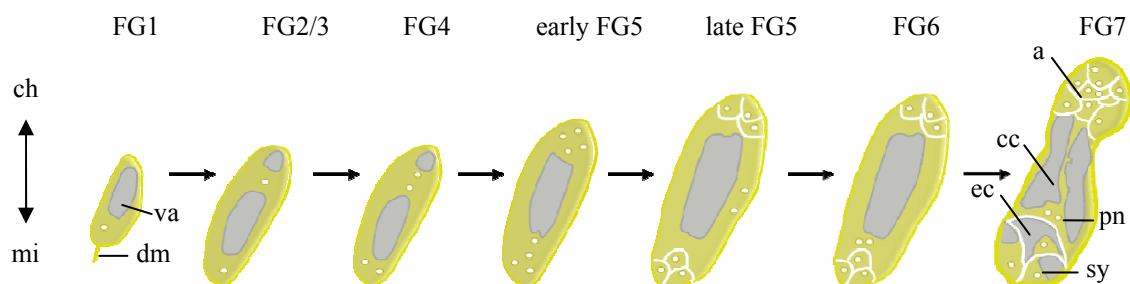

Figure 2. Megagametogenesis in maize. Development of the female gametophyte from stage FG1 to FG7. micropyle (mi); chalaza (ch); degenerated megaspores (dm); vacuole (va), always represented in gray in all developmental stages; synergid cell (sy); egg cell (ec); central cell (cc); polar nuclei (pn); antipodal cells (a). Adapted from Evans and Grossniklaus (2009).

Vollbrecht and Hake (1995) described a collection of mutants with phenotypes due to specific deletion of essential, embryo sac expressed genes suggesting autonomy of the female gametophyte in respect to cell-cycle control and cytoskeletal elements. Moreover, plasmodesmata connect the cells of the female gametophyte to one another, but there are no plasmodesmata connecting the embryo sac to nucellar tissue (Diboll and Larson, 1966; Maeda and Miyake, 1997; Han *et al.*, 2000). These findings can be interpreted to be important for establishing the environment for female gametophyte development and to be related to the gametophyte belonging to a distinct generation from the surrounding sporophyte (Diboll and Larson, 1966). At the transition from somatic to germline fate, sporophytic tissues are able to regulate archesporial cell fate (Sheridan *et al.*, 1996; Nonomura *et al.*, 2003). However, as soon as the archesporial cell is specified, the switch from mitotic to meiotic division is under the control of genes specifically expressed in the megaspore mother cell (Ravi *et al.*, 2008; Pawlowskia *et al.*, 2009). Interestingly, when the megaspore mother cell fails to enter meiosis, resulting in the formation of two unreduced megaspores, only the chalazal most spore expresses functional megaspore specific markers, suggesting that this specification is a position-dependent mechanism (Ravi *et al.*, 2008). Simultaneously, the progression in meiosis is a crucial point for normal development of the megaspores (Nonomura *et al.*, 2007).

A number of gametophytic mutations have been identified as early as the one nucleate stage (stage FG1) starts to develop. Mutation in *AtAGL23* (*AGAMOUS-LIKE23*) gene, which encodes a type I MADS-box protein expressed in the functional megaspore and throughout embryo sac development is blocked at the first nuclear division, namely the transition from stage FG1 to FG2 (Colombo *et al.*, 2008). In the same way, the knockdown of *AtAGP18* (*ARABINOGALACTAN PROTEIN18*) results in the failure of the functional megaspore to enlarge and divide (Acosta-García and Vielle Calzada, 2004). Further on, regulation of free nuclear mitotic divisions is critical for the formation of a functional gametophyte. The APC/C (ANAPHASE PROMOTING COMPLEX/CYCLOSOME) is a multiple-subunit E3 ubiquitin-protein ligase involved in transitions during mitotic progression and exit by sequentially targeting many cell cycle regulators, such as cyclins, for degradation (Perez-Perez *et al.*, 2008). Mutations of APC/C components, like *APC6/CDC16* (Capron *et al.*, 2003) or *APC2* (Kwee and Sundaresan, 2003) result in female gametophyte development arrest at stage FG2. Similarly, *rpt5a-4rpt5b-1* double mutants show arrest at stage FG1 and FG2 (Gallois *et*

al., 2009). *RPT*s (*REGULATORY PARTICLE TRIPLE A ATPase*) are part of a sub-complex of 19S RP, which itself is part of the 26S proteasome, responsible to interact with targets for subsequent degradation (for review see Gallois *et al.*, 2009).

Besides cell cycle regulation, the cytoskeleton plays an important role during nuclei division and cytokinesis in the female gametophyte development. In *tubg1-1 tubg2-1* double mutant phragmoplast failed to form resulting in uncellularized female gametophytes with abnormal number, position and morphology of nuclei. *AtTUBG1* and *AtTUBG2* (*TUBULIN GAMMA1* and 2) encode for γ-tubulin, which is known as one of the key molecular players for microtubule nucleation in animal and fungal cells (Pastuglia *et al.*, 2006). Recently, a similar phenotype was described for knockdown of *ZmDSUL*. The functional characterization of ZmDSUL will be described in more detail in **Chapter 4**.

The female gametophyte is a highly polarized structure containing gametophytic cells that are polarized themselves. The synergid and egg cell are located at the micropylar pole, forming the egg apparatus. The synergid cells and central cell nuclei are located toward the micropylar pole, while the egg cell nucleus is located toward the chalazal pole. The opposite polarity of egg and central cell leads to closer location of their nuclei, which favors the double fertilization process (Yang *et al*., 2010). The polarity observed in the female gametophyte is due to coordination in nuclear division and positioning, expansion of vacuoles, cellularization, establishment and maintenance of cell identity. Some genes have been identified to play important role in establishing and maintaining cell identity in the embryo sac. A tight regulation of the cell cycle is indispensable, before and after cellularization, to ensure the correct specification and cell fate maintenance for the normal course of the double fertilization process. Extra rounds of free nuclear division during megagametogenesis can result in extra egg cells, central cells and polar nuclei. This phenotype was observed in *ig1* (*indeterminate gametophyte1*) mutant in maize (Evans, 2007). *ZmIG1* encodes a LATERAL ORGAN BOUNDARIES domain protein with high similarity to ASYMMETRIC LEAVES2 of *Arabidopsis*. *ZmIG1* is expressed from stage FG1 onwards and is most strongly expressed in the antipodals at stage FG7 (Evans, 2007). The stages at which the gene is expressed correlates with the proliferative process, explaining the expression in antipodals, which proliferate during embryo sac maturation in maize. A set of additional phenotypes were observed ranging from prefertilization failure, miniature and aborted seeds, as well as kernels with more than one embryo, depending on the genetic

background in which the *ig1* mutant was backcrossed. The miniature and aborted seed can be explained due to the fact that maize endosperm development is very sensitive to deviations from the normal 2 maternal:1 paternal genome ratio in the endosperm (Lin, 1984), since the *ig1* mutant has extra polar nuclei. Cell cycle regulation after cellularization is important for cell fate maintenance according to phenotypes observed in *rbr1-1* mutants in *Arabidopsis*. *AtRBR1* encodes a retinoblastoma-related protein (Ebel *et al.*, 2004). Embryo sacs of *rbr1-1* mutant develop normally until stage FG5 before cellularization. After cellularization, at stage FG7, megagametophytes have supernumerary nuclei at the micropylar region. The nuclei have irregular size and were partially enclosed by membranes or cell-wall-like structures. Nuclei proliferation occurred either in all cell types or was restricted to the egg apparatus or the central cell region only. Moreover, most proliferating *rbr* mutant female gametophytes failed to express cell-specific markers that are detected in a fully differentiated wild-type mature embryo sac. The arrest of the cell cycle was confirmed due to the absence of expression of mitotic *cyclin B* in the female gametophyte of the *rbr1-1* mutant, suggesting that those nuclei are arrested either in G1 or G2 phase just prior to the expression of the B1;1 cyclin (Johnston *et al.*, 2008). Furthermore, autonomous endosperm development was observed in ovules of *rbr1-1* mutants resembling the phenotype observed in *fis2* (*fertilization-independent seed2*) mutant ovules (Ebel *et al.*, 2004). *AtFIS2* is an imprinted gene encoding for a C2H2 zinc finger-containing polycomb group protein, involved in central cell differentiation and suppression of premature endosperm development (Luo *et al.*, 1999). AtRBR1 controls its expression (Johnston *et al.*, 2008).

Additionally, a few mutants have been identified to form an aberrant number of gametic cells. In *eostre* mutants, a second egg cell is formed in detriment of one synergid. The misspecification is due to the ectopic expression of a *BEL1-like homeodomain 1* (*AtBLH1*) gene in the female gametophyte, which does not occur in wild type. AtBEL1 protein interaction with KNOX proteins, such as AtKNAT3, is necessary for the *eostre* phenotype. Ectopic expression of AtBEL1 could interfere with a functional BEL1-KNOX interaction in the female gametophyte of the *eostre* mutant. Additionally, mutations in AtOFP5, which interacts with AtKNAT3, results in embryo sac with supernumerary egg cells (Pagnussat *et al.*, 2007). Analysis of the *clo* (*clotho*) mutant in *Arabidopsis* revealed that synergid and central cell can be misspecified into egg cell, and antipodal cells can adopt central-cell fate. Additionally, AtCLO, a plant homologue of yeast Snu114p (a component of the U5 snRNP of the spliceosome), is

necessary for the gamete specific expression of AtLIS (Moll *et al*., 2008). In *lis* (*lachesis*) mutant embryo sacs, the expression of egg-specific markers is extended to the synergid and central cells. Moreover, *lis* synergid cells display egg cell morphology and synergid cell specific gene expression is down-regulated, compromising pollen tube attraction. AtLIS is homologous to the yeast splicing factor PRP4 and shows high expression in gametic cells but is down-regulated in synergid cells shortly after cellularization (Groß-Hardt *et al*., 2007). Taken together, these data led to the formulation of the "lateral inhibition model". According to this model all gametophytic cells are competent to adopt gametic cell fate. Additionally, two levels of cell fate regulation were proposed, one between the gametic cell and accessory cells, and the other between egg cell and central cell (Groß-Hardt *et al*., 2007; Yang *et al*., 2010).

Recently, Pagnussat and co-workers reported that patterning of the *Arabidopsis* female gametophyte depends on an asymmetric distribution of auxin in the eight-nucleate coenocytic embryo sac (early stage FG5). The use of *DR5:GFP* reporter (Ulmasov *et al*., 1997), which is responsive to auxin, allowed the tracing of auxin response by monitoring reporter gene expression. Figure 3 shows a representation of auxin distribution during megagametogenesis. At stage FG1 GFP expression was detected in the nucellus tissue outside the embryo sac (Fig. 3A). At stage FG3, the signal was detected inside the female gametophyte at the micropylar end, with increased signal intensity at the same region at stage FG4 (Fig. 3B). At early stage FG5 a maximum of *DR5:GFP* activity was observed at the micropylar end of embryo sac, with decreasing expression from the middle to the chalazal end of the female gametophyte (Fig. 3C). The distribution of *DR5:GFP* signal became less polarized after cellularization had taken place. The influence of auxin in patterning the female gametophyte was shown by down-regulation of *ARF* (*AUXIN RESPONSE FACTOR*) gene expression resulting in synergid cells that adopt egg cell fate. Moreover, PIN proteins, which are responsible for auxin polar transport, are not expressed in the embryo sac, suggesting that the auxin gradient is due to location of auxin biosynthesis and diffusion. The expression of *YUC1* and *YUC2* (*YUCCA*) genes encoding key enzymes in auxin biosynthesis overlap with the auxin response signal in the ovules during megagametogenesis. Furthermore, homogeneous ectopic expression of *YUC1* in the embryo sac led to disruption of the auxin gradient during megagametogenesis. A final consequence of homogeneous distribution of auxin in the embryo sac was that egg and synergid cells showed altered polarity, polar nuclei failed to fuse, antipodals did not

degenerate and embryo sacs collapsed. Moreover, expression of synergid specific marker was detected in egg cell, central cell and antipodal cells. Similarly, an egg cell specific marker showed expression in antipodal cells (Pagnussat *et al.*, 2009).
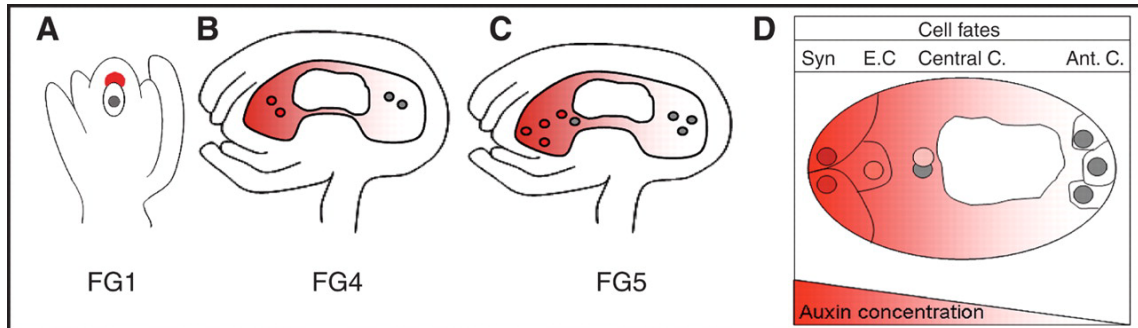
Figure 3. Model for cell specification in the female gametophyte of *Arabidopsis* as a consequence of an auxin gradient. (**A**) At stage FG1, the auxin source is derived from the nucellus tissue. (**B**) Further on, the auxin source is specified within the gametophyte at the micropylar pole. (**C**) At stage FG5, in the eight-nucleate coenocytic embryo sac, auxin gradient with a maximum at the micropylar pole of the embryo sac. (**D**) Auxin concentration determines cell fates, a maximum of auxin concentration at the micropylar end of embryo sac, specifying synergid cells (Syn), followed by egg cells (E.C), with decreasing concentration from the middle to the chalazal end of the female gametophyte resulting in central cell (Central C.) and antipodal cells (Ant. C.). After Pagnussat *et al.* (2009).

The activity of the *DR5* promoter (*DR5:RFP*; http://maize.jcvi.org/cgi-bin/maize/cellgenomics/geneDB_report.pl?search=1009) was analyzed during megasporogenesis and megagametogenesis in maize (Fig. 4). *DR5:RFP* signals were observed in the nucellus tissue, at the micropylar end of the embryo sac, from the megaspore mother cell stage until early stage FG7 (Fig. 4A-E). *DR5:RFP* signals at the micropylar end of the embryo sac were no longer observed at late stage FG7 (Fig. 4F). However, at the same stage signals were now observed at the chalazal end of the female gametophyte, in antipodal cells (Fig. 4G). Probably auxin difuses from the nucellus tissue in the female gametophyte of maize generating a morphogenic gradient responsible for cell specification and induction of antipodals proliferation.
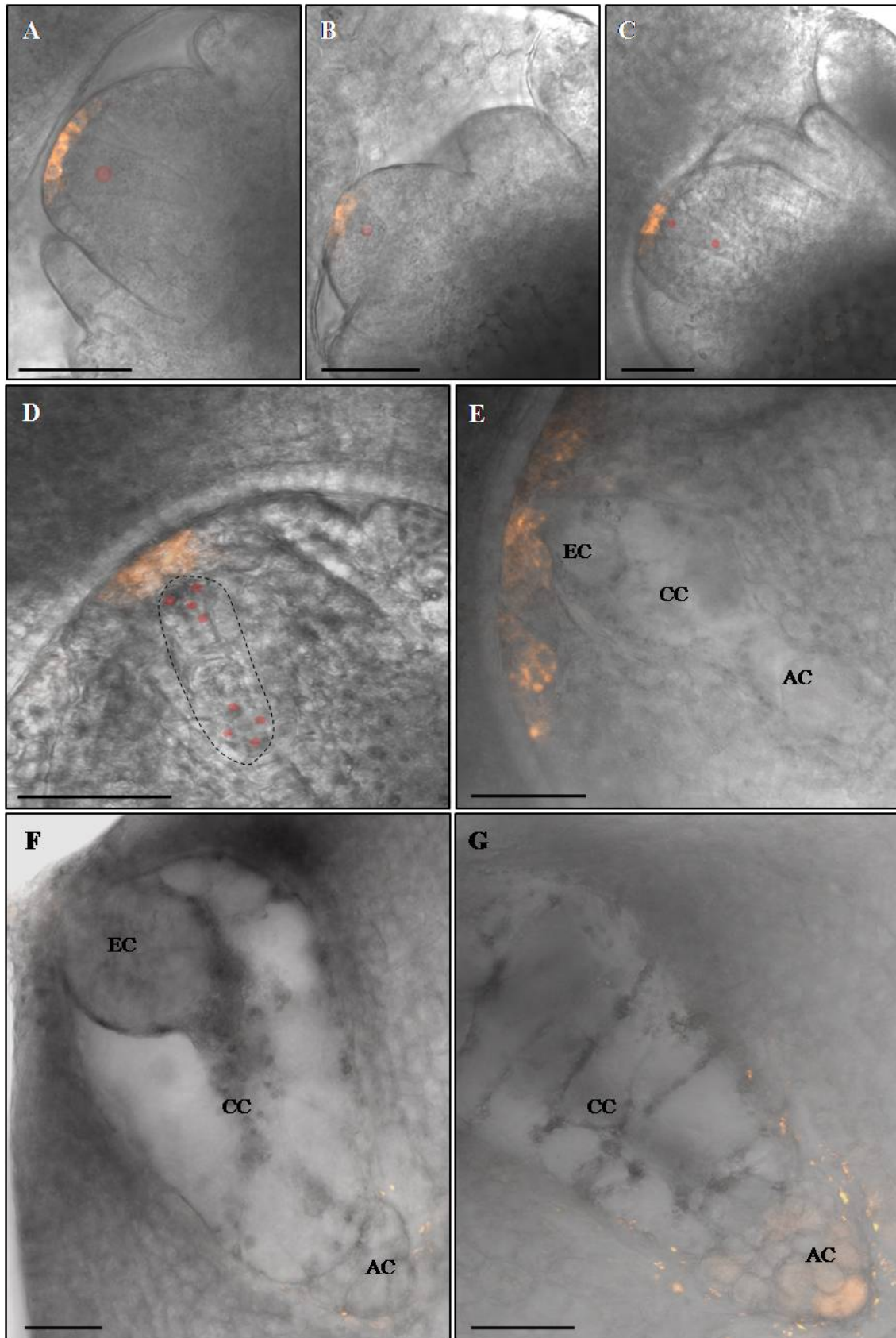
Figure 4. Expression of the reporter *DR5:RFP* during megasporogenesis and megagametogenesis in maize. (**A**) Megaspore mother cell stage. (**B**) Stage FG1 after completion of meiosis and degeneration of the micropylar most megaspores. (**C**) Stage FG2. (**D**) Stage FG5, immature embryo sac contains eight nuclei; dotted line marks the embryo sac. (**E**) Early stage FG7; egg cell (EC), central cell (CC) and antipodal cells (AC) are cellularized. (**F**) Late stage FG7; egg cell (EC), central cell (CC) and antipodal cells (AC) are fully

differentiated. (**G**) Same as (F), but with closer look at antipodal cells. Nuclei in (A-D) are colored to show their position. Bars: 50 μm.

Some genes have been identified to play an important role in differentiation of specific cells in the embryo sac. In the *dia, agl61* (*diana*) mutant, the morphology of the central cell is abnormal, with unfused polar nuclei impairing central cell fertilization. *AtDIA*, a TypeI MADS-box gene, is expressed exclusively in the mature central cell, and the protein is localized in polar nuclei. AtDIA and AtAGL80 form a heterodimer, and most likely are required for fusion of polar nuclei and central cell differentiation (Bemer *et al*., 2008; Portereiko *et al*., 2006). As polar nuclei fuse, central cell specification occurs (Yang *et al*., 2010). This final step of central cell specification is missing in *maa1* and *maa3* (*magatama1* and *magatama3*) mutants in *Arabidopsis* and fertilization cannot take place (Shimizu and Okada, 2000; Shimizu *et al*., 2008). *AtMAA3* encodes a homolog of yeast SPLICING ENDONUCLEASE1 (SEN1) helicase implicated in processing of a variety of RNA species in yeast (Shimizu *et al*., 2008; Yang *et al*., 2010). The molecular mechanism underlying the fusion of polar nuclei is poorly understood. However, electron microcopy analysis revealed that it begins with contact of the endoplasmic reticulum membranes that are continuous with the outer nuclear membranes of the two nuclei. Fusion of the endoplasmic reticulum membranes results in outer nuclear membranes that are continuous. Finally, the inner nuclear membranes come into contact and merge (Jensen, 1964). Interestingly, mitochondrial proteins have been reported to be involved in polar nuclei fusion, like GPT1 (GLUCOSE 6-PHOSPHATE/PHOSPHATE TRANSLOCATOR) and GFA2 (GAMETOPHYTIC FACTOR2) (Niewiadomski *et al*., 2005; Christensen *et al*., 2002).

GFA2 encodes a J-domain-containing protein, which functions as a chaperone in the mitochondrial matrix. Besides the unfused polar nuclei, the synergid cell fails to degenerate upon pollen tube arrival in the *gfa2* mutant, resulting in impairment of fertilization (Christensen *et al*., 2002). At the micropylar pole, the synergid cell wall is extensively thickened and elaborated, forming the filiform apparatus. The filiform apparatus has numerous finger-like projections into the synergid cytoplasm and may function in pollen tube reception, import of metabolites, and export of the pollen tube attractant (for review see Higashiyama, 2002). Mutations in the *AtMYB98* synergid specifically expressed gene, which encodes a R2R3-type MYB transcription factor, abolishes the formation of the filiform apparatus (Kasahara *et al*., 2005). Recently, it was shown that a large number of small defensin-like cystein rich proteins (CRPs) were

down-regulated in *myb98* mutant in *Arabidopsis*. CRPs are secreted into the filiform apparatus suggesting that they play a role in either the formation or function of this structure (Punwani *et al*., 2007).

Taken together, progresses have been achieved to uncover the factors controlling pattern formation, establishment of polarity across the whole embryo sac and within the individual cells. However, the contribution of cell-cell communication on cell fate determination and maintenance is poorly understood. Maize egg cells were mechanically isolated and a cDNA library was generated (Dresselhaus *et al*., 1994) with the aim to identify signaling molecules involved in megagametogenesis. One candidate identified through the analysis of the cDNA library was the *ZmEAL1* (*Zea mays EA1 Like1*) gene. According to the results, *ZmEAL1* gene encodes a small secreted protein involved in cell fate maintenance in female gametophyte of maize. Here I report the expression pattern through the analysis of promoter activity and protein localization with green fluorescent marker gene. Moreover, I describe the functional analysis of *ZmEAL1* involving the generation and analysis of *ZmEAL1*-RNAi plants.

2   Material and Methods

2.1   Plant material and isolation of cells from maize female and male gametophyte

Maize inbred lines A188 and H99 as well as transgenic lines were grown under standard greenhouse conditions at 26°C with 16 h light and a relative air humidity of about 60%. Cells of unfertilized female and male gametophyte were isolated as described before (Kranz *et al.*, 1991). Zygotes were isolated 24 h after *in vivo* pollination. The *in vivo* pollination procedure was performed using cobs with fully developed embryo sacs. The silks of those cobs were shortened in a way that 2 cm in length were left between the cutting side and the top of the last row of ovaries. Zygotes were isolated from ovules dissected from the central part of the cob, using the same procedure described to microdissect egg cells (Kranz *et al.*, 1991).

2.2   EST and bioinformatic analyses

The analysis of putative novel expressed sequence tags (ESTs) from a maize egg cell cDNA library (Dresselhaus *et al.*, 1994) revealed the presence of a transcript encoding a putative secreted protein as one of the most abundant transcript in the maize egg cell. The cDNA sequence and the corresponding coding sequence (CDS) of the maize clone *ZmEC222* was used to run TBLASTN 2.2.17 homology searches in the non-redundant   nucleotide   collection   (nr/nt)   database   at   NCBI (http://www.ncbi.nlm.nih.gov/). The putative open reading frame (ORF) was identified and translated into protein using the Vector NTI software (Invitrogen[TM]). The predicted protein was named ZmEAL1 (Zea mays EA1 Like1) and used as query to perform BLASTP searches using the Plant Genome Database (http://www.plantgdb.org/) to identify homologous proteins (Evalue < $8e^{-05}$). ZmEAL1 and homologous proteins were aligned using MCoffee webserver (http://www.tcoffee.org/; Moretti *et al.*, 2007). GeneDoc version 2.7.000 (Nicholas *et al.*, 1997) was used for manual editing of alignments. Further, *ZmEAL1* cDNA sequence was used for searches using the *Zea mays* BAC (*Zmbac)* Plant Genome Database (http://www.plantgdb.org/) to identify the promoter region, taking 700 bp upstream of the transcription initiation site as the putative promoter. Promoter motifs were analyzed using PlantCARE to identify *cis*-acting regulatory elements (http://bioinformatics.psb.ugent.be/webtools/plantcare/html/; Lescot *et al.*, 2002). Analysis of conserved motifs in maize egg cell expressed genes was performed using the MEME - Motif discovery tool (Bailey and Elkan, 1994) and

Vector NTI software to identify *cis*-regulatory sequences homologous in various promoters of genes expressed in the egg cell.

All transgenic constructs were planned *in silico* with Clone Manager version 6 (Scientific & Educational Software) and Vector NTI. Visualization of gene and protein sequences, analysis of sequencing data and design of primers were performed using Vector NTI.

2.3   DNA and RNA extraction, Southern and Northern blot analysis, RT-PCR and semi-quantitative Single Cell RT-PCR

Genomic DNA (gDNA) extraction from leaves was performed according to Pallotta *et al*. (2000). For southern blot analysis (Southern, 1975) restriction endonuclease digestion of gDNA of P_{ZmEAL1}*:eGFP* and P_{ZmEAL1}*:ZmEAL1-eGFP* plants was performed with *Bgl*II and *Swa*I and of *ZmEAL1*-RNAi plants with *Not*I and *Afl*I. Those enzyme combinations cut out the whole cassette from P_{ZmEAL1}*:eGFP*, P_{ZmEAL1}*:ZmEAL1-eGFP* and *ZmEAL1*-RNAi vectors, respectively. 30 μg of restricted gDNA was separated on 0,8% agarose gel. The agarose gel was then treated with denaturing and neutralizing solution with posterior transfer of gDNA onto Hybond-XL membranes (GE Healthcare) by capillary transfer with 20xSSC. gDNA was fixed to the membrane by using UV crosslinking (UV Stratalinker TM 1800; Stratagene, USA) procedure, with 70 000 μjoules/cm^2. Pre-hybridization was performed in Church buffer (0,34 M Na_2HPO_4; 0,16 M NaH_2PO_4; 7% SDS; 1 mM EDTA; pH 7,2), during 3 h, with denatured salmon sperm DNA (100 μg of salmon sperm DNA/ml of buffer). The probe for hybridization of southern blots of transgenic plants transformed with P_{ZmEAL1}*:eGFP* and P_{ZmEAL1}*:ZmEAL1-eGFP* constructs was generated by PCR using the primer pair Neu GFP-for (5'-ACAAGCTTGACGAAGTGGTC-3') and Neu GFP-rev (5'-TCACTTGTAGAGTTCATC-3') to amplify a fragment from the eGFP coding sequence, using the vector P_{ZmEAL1}*:eGFP:NOSt* as template. For southern blots of transgenic plants transformed with *ZmEAL1*-RNAi vector the primer pair UbiR1 (5'-GAGCATCGACAAAAGAAACAG-3')   and   ZmEC222-1   fwd   (5'-GTAGATAATGCCAGCCTGTTA-3') was used to amplify a fragment of the *ZmEAL1*-RNAi construct. The probes were then purified and labelled with ^{32}P-α-dCTP according to specifications of the Primer-it II Random Primer Labeling Kit (Stratagene). The following hybridization was done during 12 h. Afterwards, the membrane was washed in solutions with decreasing concentration of SSC from 2xSSC/0,1%SDS to 0,1xSSC/0,1%SDS and exposed to an X-ray film from one to three days at -70°C using

intensifier screens. Pre-hybridization, hybridization and washing steps were performed at 65°C.

For northern blot analysis different tissues were collected from greenhouse grown plants of the inbred line A188 and from embryogenic and non-embryogenic maize suspension lines (Krantwig and Lörz, 1995). The isolation of total RNA was performed according to Logemann *et al.* (1987) with an additional overnight precipitation step at 4°C in 2,5 M LiCl. Total RNA extraction from suspension cultures was carried out as described before (Stirn *et al.*, 1995). 15 µg total RNA was separated on 1,5% agarose gel containing 15% formaldehyde. The total RNA was then transferred to Hybond N+ membrane with 10xSSC. RNA was fixed to the membrane by using UV crosslinking as described above. The probe was generated according to Cordts (2000). Pre-hybridization, hybridization, washing step and X-ray film exposure were performed in the same way as described for southern blot analysis.

For the expression analysis of a *ZmEAL1*-RNAi construct in maize transgenic lines total RNA was isolated with TRIzol® (Invitrogen). Afterwards 1 µg of total RNA was used for first-strand cDNA synthesis using Oligo (dT)$_{18}$ (MBI Fermentas) and Reverse Transcriptase (RevertAid™ MMuLV Reverse Transcriptase, MBI Fermentas) following the manufacturer's protocol. The quality of generated cDNAs was analyzed by PCR using maize *GAPDH* (Glyceraldehyde 3-phosphate dehydrogenase)-specific primers ZmGap1 (5'-AGGGTGGTGCCAAGAAGGTTG-3') and ZmGap2 (5'-GTAGCCCCACTCGTTGTCGTA-3'). To verify the expression of the *ZmEAL1*-RNAi construct PCRs were performed with the primer pair UbiD fwd (5'-CACACACACAACCAGATCTC-3') and ZmEC222-1 fwd (5'-CACTCTCCTTCAAGATCATGG-3').

Single cell RT-PCR was performed as described before (Richert *et al.*, 1996) with minor modifications. First-strand cDNA synthesis was performed using 100 units of RevertAid™ H Minus Reverse Transcriptase (MBI Fermentas) with addition of buffer supplied with the enzyme, 20 units of RiboLock™ RNase Inhibitor (MBI Fermentas), 2,5 µM of primers ZmGap2 and ZmEC222 500 rev (5'-ATAGGCATTATATTGCAAGCGACG-3'). The RT reaction was performed at 50°C for 70 min and the RT enzyme was subsequently inactivated at 70°C for 10 min. After RT, each reaction was split into two reaction tubes and two PCR reactions were carried out. The first reaction was performed with ZmGap1 and ZmGap2 primer pairs as a control to visualize gDNA contaminations. For the second reaction the primer pair

ZmEC222 RT fwd (5'-CGCGGTGTCTATCAATAGTACC-3') and ZmEC222 500 rev was used. Both PCR reactions were conducted with 40 cycles and PCR products were separated on agarose gel, blotted on membranes hybridized with probes labeled with ^{32}P-α-dCTP as described above. gDNA served as template for probe generation by PCR using the same primer combinations as for SC RT-PCR reactions. After hybridization, membranes were exposed to Cyclone^{TM} Storage Phosphor Screen RS (PerkinElmer). Signals were scanned with the Cyclone Storage Phosphor System (PerkinElmer) and signal quantification was performed by using the OptiQuant^{TM} Image Analysis Software (PerkinElmer). Expression levels of *ZmEAL1* were normalized with *GAPDH* signals.

2.4 Generation of constructs, biolistic transformation and regeneration of transgenic maize plants

ZmEAL1-RNAi construct (*P$_{UBI}$:ZmEAL1-AS:iF2intron:ZmEAL1:OCSt*): the RNAi construct directed against *ZmEAL1* under the control of the maize ubiquitin promoter (*Ubi1*) was cloned by DNA Cloning Service (Hamburg) using the plasmid P$_{UBI}$-iF2 (DNA Cloning Service). In a first step, a 368 bp fragment starting at 20 bp upstream of the start codon to 125 bp downstream of the stop codon of the *ZmEAL1* gene was amplified from gDNA using the primers 222-BSR (5'-CGGCTGTACATCACTCTCCTTCAAG-3') and 222-Mlu (5'-CAGTACGCGTCCACGTGCA-3') introducing *BsrGI* and *MluI* restriction sites allowing the cloning of the *ZmEAL1* fragment in sense orientation into the *P$_{Ubi}$-iF2-222* vector. Further, the *ZmEAL1* fragment was PCR amplified from vector *P$_{Ubi}$-iF2-222* using primers 222-Eco (5'-CCGGGAATTCATCACTCTCCTTC-3') and 222-Bam (5'-CTGAGGATCCACGTGCACC-3') and cloned in anti-sense orientation into the *Bam*HI and *Eco*RI restriction sites of the vector *P$_{Ubi}$-iF2-222* vector generating the *ZmEAL1*-RNAi construct (DNA Cloning Service).

P$_{ZmEAL1}$:eGFP:NOSt: the *pLNU-eGFP* vector (DNA Cloning Service) was digested with *Not*I and *Bam*HI, to cut out the *Ubi* promoter. Afterwards, the digestion reaction was separated on 1% agarose gel and the vector fragment without the *Ubi* promoter was purified. The promoter of *ZmEAL1* was amplified from gDNA using the primers A188 EC222 GFP fwd (5'-TCGAGCGGCCGCCCGGGCAGGTATCGCGTACGGG-3') and EC222GFPcontrol rev (5'-TGTGTCGGATCCGATCTTGAAGGAGAGTGATGAA-3') introducing *Not*I and *Bam*HI restriction sites to clone the *ZmEAL1* promoter into the pLNU-eGFP vector generating the *P$_{ZmEAL1}$:eGFP* vector.

P_{ZmEAL1}:ZmEAL1-eGFP:NOSt: for cloning ZmEAL1-eGFP-fusion protein under control of the *ZmEAL1* promoter, e*GFP* was C-terminally fused to the coding sequences of *ZmEAL1*. Again the *pLNU-eGFP* vector (DNA Cloning Service) was used and digested with *Not*I and *Spe*I with a final purification step of the fragment of interest. The *ZmEAL1* gene (promoter, 5'UTR and ORF) was amplified from gDNA using the primers B73 EC222 GFP fwd (5'-GACACAGCGGCCGCAATGAACAAGCTCAAGCGTAG-3') and B73 EC222 GFP rev (5'- TGTGTCACTAGTGCCAGCAAACATACGAACAGC-3') introducing the *Not*I and *Spe*I restriction sites to clone the *ZmEAL1* gene into the *pLNU-eGFP* vector generating the *P_{ZmEAL1}:ZmEAL1-eGFP* vector.

Immature hybrid embryos of the maize inbred lines A188 and H99 were isolated 11 to 13 days after pollination for subsequent stable transformation using biolistic particle bombardment with a particle gun (BioRad) using the parameters described by Becker *et al.* (1994). The constructs *ZmEAL1*-RNAi, *P_{ZmEAL1}:eGFP* and *P_{ZmEAL1}:ZmEAL1-eGFP* were each co-transformed with the vector *P_{35S}:PAT* carrying the selectable marker PAT for glufosinate ammonium resistance (Becker *et al.*, 1994). Immature embryos were transformed after mixing gold particles with 60 µm in diameter, 2 µg DNA of the *P_{35S}:PAT* vector for selection plus 3 µg DNA of *ZmEAL1*-RNAi, *P_{ZmEAL1}:eGFP* and *P_{ZmEAL1}:ZmEAL1-eGFP* vectors, respectively. DNA was precipitated on 2 mg of gold particles, using CaCl$_2$ and spermidine. After DNA precipitation, washing procedures were performed with absolute ethanol and gold particles then resuspended with 150 µl ethanol. 3,5 µl of the solution containing DNA precipitated on gold particles was each applied on the macrocarriers. Each plate, with immature embryos on the surface exposing the scutellum, was bombarded twice, using 1350 psi rupture discs for transformation. Particle bombardment, tissue culture and selection of transgenic maize plants were performed using modified N$_6$ medium (D'Halluin *et al.*, 1992) according to Brettschneider *et al.* (1997).

2.5 Transient transformation of maize BMS cells and plasmolysis experiments

Transient transformation of embryo derived "Black Mexican Sweet" (BMS) suspension cells (Quayle *et al.*, 1991) via biolistic procedure was carried out as follows: BMS cells growing on solid MS medium (Murashige and Skoog, 1962) for BMS cells (30g·l^{-1} of sucrose, 4,4 g·l^{-1} of MS-salts from Duchefa, 2 mg·l^{-1} of 2,4-

Dichlorophenoxyacetic acid, pH 5,8), were first sterile filtrated through a 500 μm metal net, passed through a 100 μm pore sized nylon mesh, transferred to liquid MS medium for BMS cells and cultivated for 1 week at 26°C in a dark chamber shaking at 110 rpm. After growing one week 25 ml of cell culture was transferred to a clean and sterile flask and 35 ml fresh MS medium for BMS cells was added. Culture was cultivated again for one week. Before biolistic transformation, a small volume of the cell culture was uniformly distributed in a thin layer of cells on solid MS medium for BMS cells. Cells were incubated at 26°C for 1 to 2 h. BMS cells were transformed using gold particles with 60 μm in diameter. 10 μg of DNA was each precipitated on 2 mg of gold particles using $CaCl_2$ and spermidine. After DNA precipitating and washing procedures with absolute ethanol, gold particles were resuspended with 150 μl of ethanol. 7,5 μl of the solution containing DNA precipitated on gold particles was applied on the macrocarriers. Each plate, with BMS cells on the surface, was bombarded three times using the 1100 psi rupture discs for transformation. After transformation, plates were incubated overnight in the dark at 26°C. Cells were transferred to fresh liquid medium and cultivated in darkness using a shaker at 110 rpm for at least 4 h before microscopic observations.

To study plasmolysis, first the osmolarity of the MS medium for BMS cells was measured, which was 550 mosmol·kg^{-1}. Hepes buffer (10 mM) pH 7,2 was prepared and mannitol was added as osmotic agent to adjust the osmolarity to 950 mosmol·kg^{-1}. The BMS suspension cells were transformed with P_{ZmEAL1}:ZmEAL1-eGFP, P_{ZmEAL1}:eGFP and PMON30049 (Pang et al., 1996; used as a positive control) and cultivated as described above. Before microscopic observations, medium was sucked up from the suspension cells and 1 ml of Hepes buffer with osmotic agent was added to suspension cells followed by incubation at room temperature for 30 min and shaking at 110 rpm.

2.6   Histological studies and eGFP imaging

Transgenic plants with glufosinate ammonium resistance lacking integration of the RNAi construct were used as wild type control for phenotypical analysis of ZmEAL1-RNAi embryo sacs. Immature and mature cobs were harvested from green-house grown maize plants. Whole cobs were treated according to a fixing/clearing method using Kasten's fluorescent periodic acid-Schiff's reagent (Kasten, 1981) described by Vollbrecht and Hake (1995). The phases of hydration and dehydration of ears were performed for 30 minutes in each step and ears were dissected with two

longitudinal sections to the silk axis after they were cleared with methyl salicylate (Young *et al.*, 1979). Samples were mounted in methyl salicylate on glass slides under a cover slip and analyzed with a LSM 510-META confocal laser scanning microscopy (CLSM, Zeiss) with 488 nm excitation and a LP 505 filter.

For the analyses of P_{ZmEAL1}:*eGFP* and P_{ZmEAL1}:*ZmEAL1-eGFP* embryo sacs, ovaries were dissected with two longitudinal sections to the silk axis to remove nucellar tissue. eGFP fluorescence from embryo sacs of maize as well as from transiently transformed BMS suspension cells were monitored by CLSM with 488 nm excitation and a BP 505-550 filter for selective GFP visualization. Image capture and processing were done using the Zeiss LSM 510 META software and the Zeiss LSM image browser version 3.5.0.359.

3   Results

3.1   ZmEAL1 is an EA1-box protein

A transcriptomics based approach was used to identify cell-type specific transcripts present in a cDNA library generated from isolated maize egg cells (Dresselhaus *et al.*, 1994). The *ZmEAL1* was identified as one of the most abundant transcript in egg cells. The Zm*EAL1* transcript encodes a predicted protein precursor of 74 amino acids. Protein blast searches showed significant similarities of ZmEAL1 with ZmEA1 (Márton *et al.*, 2005), one predicted proteins in maize, which was named ZmEAL2 (AC194599.2_FGP002; http://www.maizesequence.org), six hypothetical proteins in *Oryza sativa*, one hypothetical protein in *Sorghum bicolor*. Multiple sequences alignment revealed that the EA1-box is the most conserved domain between the ZmEAL1 homologous proteins (Fig. 5).

According to *in silico* analysis ZmEAL1 is predicted to represent a secreted protein. The predicted cleavage site for the signal peptide is shown in Figure 5. According to this prediction, the mature ZmEAL1 has 48 amino acids.
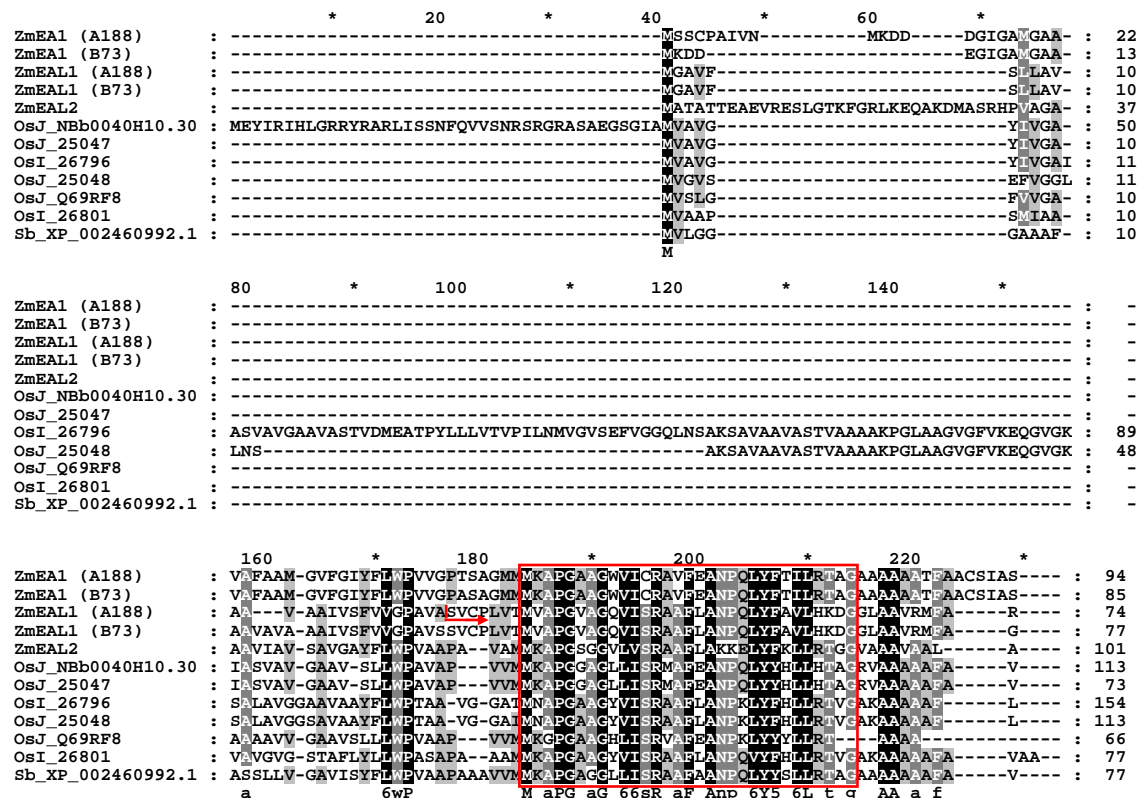

Figure 5. ZmEAL1 is a predicted secreted protein with high homology to EA1-box proteins. Red arrow shows the predicted cleavage site of the ZmEAL1 signal peptide; red box indicates the conserved EA1-box. Note that ZmEA1 and ZmEAL1 of inbred maize lines A188 and B73 were aligned.

3.2 Genomic location of *ZmEAL1* and analysis of *cis*-acting elements in the *ZmEAL1* promoter

The genomic location of *ZmEAL1* was determined using the Plant Genome Database (*Zea mays* BAC) with subsequent BLAST searches on NCBI database to identify possible genes located in the vicinity of *ZmEAL1*. Interestingly the *ZmEA1* gene is located only at about 1000 bp upstream of *ZmEAL1* start codon (Fig. 6). *ZmEA1* ORF is transcribed in opposite direction of *ZmEAL1* ORF. Moreover, a putative *SAUR* gene was identified to be located 500 bp upstream of *ZmEAL1* start codon, being as well transcribed in opposite direction of *ZmEAL1* ORF, thus separating both EA1-box protein encoding genes. The ORF of putative the *ZmSAUR* gene shared 71% identity with the ORF of *ZmSAUR1* (Yang and Poovaiah, 2000). Analysis of 3 kb upstream of *ZmEA1* and 3 kb downstream of *ZmEAL1* did not reveal regions with homology to any transcribed sequence identified so far.

Further on, *ZmEAL1* gene sequences of inbred maize lines A188 and B73 were compared showing 92% of identity. Besides that, the *ZmEAL1* and *ZmEA1* genes were aligned, since ZmEAL1 and ZmEA1 proteins have significant similarity. The alignment of the promoters revealed 42,9% of identity compared with 46,5% of the corresponding ORFs. Predicted CAAT and TATA (TA(C)AAATA) boxes are identical as well as the auxin responsive element (TGTCTC) found on the (-) and (+) strand of the *ZmEAL1* and *ZmEA1* promoters, respectively. Three conserved motifs were identified CGTTCTCACT, CTTCTGCATT and TGATCG (Fig. 7; motif 1-3). Motifs 1 and 2 have a quite similar sequence, namely TTCTCA for motif 1 and TTCT(G)CA for motif 2. The sequences TTCT(G)CA and TTCTCA are also present in the egg cell expressed *ZmMAB1* promoter (Leljak-Levanić, unpublished data). Moreover, the *ZmDSUL* promoter (Srilunchang *et al*., 2010), which is also expressed in the maize egg cell, contains the element TTCTCA. Additionally, a fourth motif (Table 1) was identified with significant similarity.
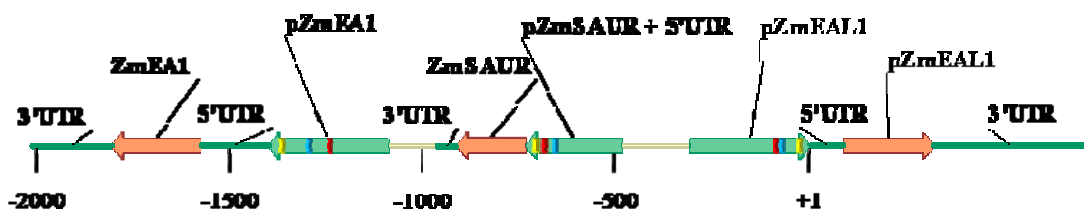
Figure 6. Genomic location of *ZmEA1*, a *ZmSAUR* gene and *ZmEAL1* on chromosome 7. +1 indicates the start codon of *ZmEAL1*. Please note that none of the genes contain introns. Yellow, blue and red bars indicate the TATA box, CAAT box and auxin responsive element, respectively.
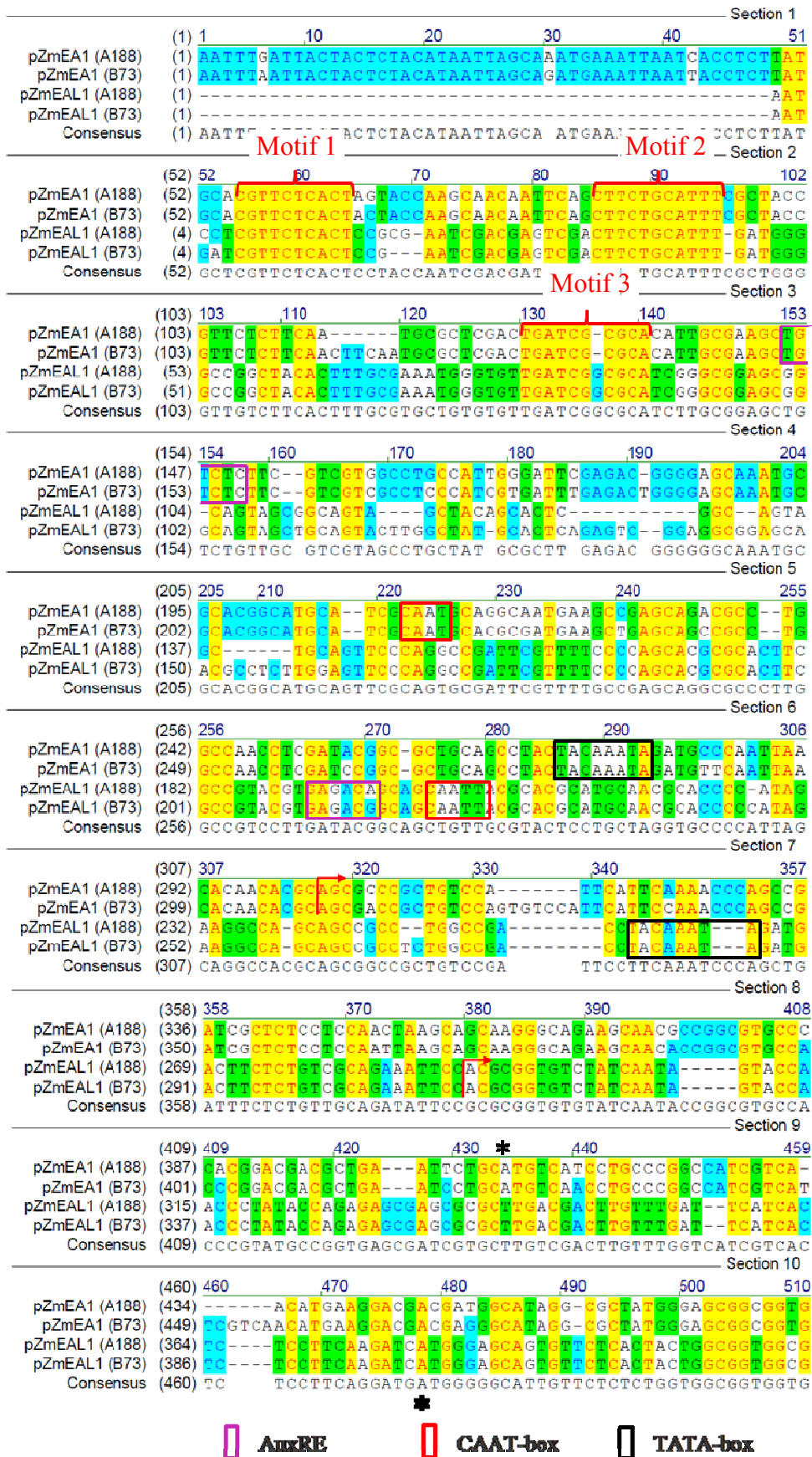
Figure 7. Alignment of *ZmEA1* and *ZmEAL1* promoters from inbred lines A188 and B73.
Auxin response element (AuxRE), CAAT-box, TATA-box and conserved motifs (motif 1-3) within the promoters are indicated. Red arrows and asterisks mark the transcription initiation site and the start codon, respectively.

Table 1. Motif 4 identified within promoters of genes expressed in the maize egg cell.

	Upstream of TIS (bp)	Sequence
pZmEAL1	232	CATGCAACGCACCCC
pZmEA1	208	CATGCATCGCAATGC
pZmMAB1	84	CATCCAACGCAACGC
pZmDSUL	1763	CATGCAACTCAACCG

The *ZmEAL1* promoter region used for promoter-eGFP studies was analyzed *in silico* (Fig. 8) using the database PlantCARE (Lescot *et al*., 2002). The transcription initiation site (TIS) of the *ZmEAL1* mRNA was predicted through the analysis of the 5' ends of sequenced ESTs, and is located 86 bp upstream of the start codon. The classical TATA box (TATA(T/A)AT; Joshi, 1987) could not be identified at 30 bp upstream from the TIS, which is the typical distance in most eukaryotic genes. However, a TA(C)AAATA box was localized at 29 to 36 bp upstream of the *ZmEAL1* TIS. This motif was also identified as a putative TATA-core promoter element in a stamen-specific promoter from rice (Patent number W09213956-A/8). Besides this general promoter motif, a CAAT(T)-box was found 52 bp upstream of the TATA-box. Both basic *cis*-acting elements were located at typical distances from the transcription initiation site within plant promoters. Several additional specific regulatory elements were identified (Fig. 8) such as ABRE (involved in abscisic acid responsiveness), CGTA-motif (involved in methyl jasmonate responsiveness), GCC (ethylene-responsive element), TGACG-motif (involved in methyl jasmonate responsiveness) and AuxRE (auxin responsive element, Ulmasov *et al*., 1997). A second type of regulatory elements includes those for abiotic factors such as an ARE element (essential for anaerobic induction), C-repeat/DRE (cold- and dehydration-responsive element), G-box and Sp1 (both responsible for light responsiveness). Additionally, the Skn-1-motif was identified, which is required for endosperm expression (*cis*-elements according to PlantCARE).

```
+ CGGCCGCCCG GGCAGGTATC GCGTACGGGT CCGATCCGAT GGTGGGTATT GATGGCGGAG ATCCTTGGTA
- GCCGGCGGGC CCGTCCATAG CGCATGCCCA GGCTAGGCTA CCACCCATAA CTACCGCCTC TAGGAACCAT

+ AAACCGTGCA CCAAAAGCTT CTGTGGACGC CTACATTAGC TTCTTAAGTA GTAGTAGAGA TTGGTGAGCA
- TTTGGCACGT GGTTTTCGAA GACACCTGCG GATGTAATCG AAGAATTCAT CATCATCTCT AACCACTCGT

+ GGAGCAGGAC TGCCGTCTTT GATAAAATAG TTTGTCGGCC TCTAAAAATC TAAATCATAT TAGAGTGTTA
- CCTCGTCCTG ACGGCAGAAA CTATTTTATC AAACAGGCGG AGATTTTTAG ATTTAGTATA ATCTCACAAT

+ ATTATTTATT CAAATTATTG GTTTTGCACC ACATCAAACC AGCAGATCAA TAATAAATCA AGAGATATGC
- TAATAAATAA GTTTAATAAC CAAAACGTGG TGTAGTTTGG TCGTCTAGTT ATTATTTAGT TCTCTATACG

+ CAAAAATAAT ACGTTCAAAT AATATAAAGG ATCAAATTTT CCGGTAAACT ACCGGCAGAA TCCATTAGTT
- GTTTTTATTA TGCAAGTTTA TTATATTTCC TAGTTTAAAA GGCCATTTGA TGGCCGTCTT AGGTAATCAA

+ ACGAACTCGT AAAACAAAGT CATTTTATGA ATCCTCGTTC TCACTCCGCG AATCGACGAG TCGACTTCTG
- TGCTTGAGCA TTTTGTTTCA GTAAAATACT TAGGAGCAAG AGTGAGGCGC TTAGCTGCTC AGCTGAAGAC

+ CATTTGATGG GGCCGGCTAC ACTTTGCGAA ATGGGTGTTG ATCGGCGCAT CGGGCGGAGC GGCAGTAGCG
- GTAAACTACC CCGGCCGATG TGAAACGCTT TACCCACAAC TAGCCGCGTA GCCCGCCTCG CCGTCATCGC

+ GCAGTAGCTA CAGCACTCGG CAGTAGCTGC AGTTCCCAGG CCGATTCGTT TTCCCCAGCA CGCGCACTTC
- CGTCATCGAT GTCGTGAGCC GTCATCGACG TCAAGGGTCC GGCTAAGCAA AAGGGGTCGT GCGCGTGAAG

+ GCCGTACGTG AGACAGCAGC AATTACGCAC GCATGCAACG CACCCCATAG AAGGCCAGCA GCCGCCTGGC
- CGGCATGCAC TCTGTCGTCG TTAATGCGTG CGTACGTTGC GTGGGGTATC TTCCGGTCGT CGGCGGACCG

                                        TIS

+ CGACCTACAA ATAGATGACT TCTCTGTCGC AGAAATTCCA CGCGGTGTCT ATCAATAGTA CCAACCCTAT
- GCTGGATGTT TATCTACTGA AGAGACAGCG TCTTTAAGGT GCGCCACAGA TAGTTATCAT GGTTGGGATA

+ ACCAGAGAGC GAGCGCGCTT GACGACTTGT TTGATTCATC ACTCTCCTTC AAGAT
- TGGTCTCTCG CTCGCGCGAA CTGCTGAACA AACTAAGTAG TGAGAGGAAG TTCTA
```

Legend:
- ABRE
- ARE
- C-repeat/DRE
- CGTCA-motif
- G-Box
- G-box
- GCC box
- Skn-1_motif
- Sp1
- TGACG-motif
- AuxRE
- CAAT-box
- TATA-box

Figure 8. Predicted *cis*-acting elements within the *ZmEAL1* promoter sequence. ABRE (involved in abscisic acid responsiveness); ARE (essential for anaerobic induction); C-repeat/DRE (cold- and dehydration-responsive element); G-box (responsible for light responsiveness); GCC (ethylene-responsive element); Skn-1-motif (required for endosperm expression); Sp1 (responsible for light responsiveness); TGACG-motif (involved in methyl jasmonate responsiveness); AuxRE (auxin responsive element); TIS (transcription initiation site).

3.3 *ZmEAL1* expression and protein localization during female gametophyte development and zygotic embryogenesis in maize

Northern blot analysis was performed using a *ZmEAL1* probe. The expression of two transcripts was observed, one with 500 and another with 700 nt. All tissues examined showed a low expression pattern besides embryogenic cell suspension, in which the expression was higher (Fig. 9A), which signal was taken for the calculation of relative signal intensities. The signal of the 700 nt transcript was slightly stronger compared to the 500 nt transcript that occurred in seedlings 5 and 10 days after germination, shoot apical meristem, immature and mature leaf, internode, root tip, root without tip, immature (1 cm length) and mature (20 cm length) male inflorescence, immature female inflorescence (1 cm length), immature and mature embryos and non-embryogenic cell suspension. However, the 500 nt showed about 100% higher expression in embryogenic cell suspension compared to the 700 nt transcript. Expression analysis of *ZmEAL1* by semi-quantitative single cell RT-PCR revealed high expression in egg cells, which signal was taken for the calculation of relative signal

intensities, with down-regulation of about 50% after fertilization in zygotes 24 hours after pollination (Fig. 9B). The gene is also slightly expressed in central cells (detected only after blotting PCR products) and sperm cells, for which 50 cells were used to perform the experiment.
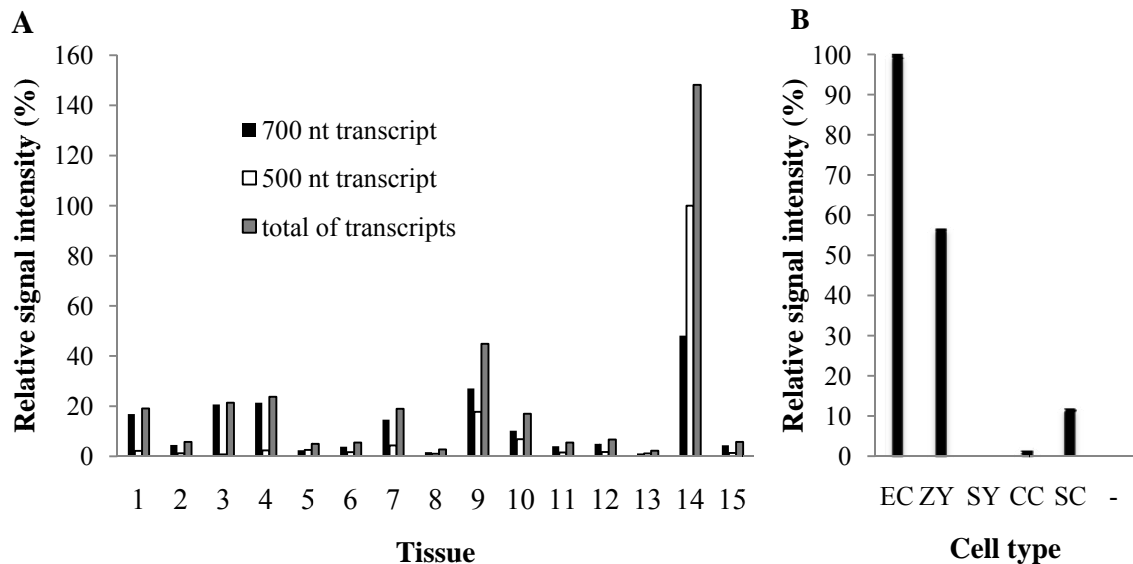

Figure 9. Expression of *ZmEAL1* in various tissues and microdissected cells of the female and male gametophyte. (**A**) Northern blot analysis with a specific probe against *ZmEAL1*. Tissues are as follow: 1. seedling 5 days after germination; 2. seedling 10 days after germination; 3. shoot apical meristem; 4. immature leaf; 5. mature leaf; 6. internode; 7. root tip; 8. root without tip; 9. immature male inflorescence (1 cm length); 10. mature male inflorescence (20 cm length); 11. immature female inflorescence (1 cm length); 12. immature embryo; 13. mature embryo; 14. embryogenic cell suspension; 15. non-embryogenic cell suspension. (**B**) Semi-quantitave RT-PCR was performed with mRNA from individual cells of the female gametophyte. EC. egg cell; ZY. zygote 24 hap; SY. synergid cell; CC. central cell; in the case of sperm cells (SC), 50 cells were used to perform RT-PCR; -. water control. Gel was blotted and hybridized with a *ZmEAL1* specific probe.

In order to study the onset of *ZmEAL1* expression during FG development 700 base pairs upstream of the *ZmEAL1* open reading frame were cloned as the *ZmEAL1* promoter. The promoter was then used to drive the expression of eGFP (P_{ZmEAL1}:*eGFP*) in transgenic maize plants. The two kilo base region upstream the open reading frame of *ZmEAL1* was used to drive the expression of a ZmEAL1-eGFP-fusion protein (P_{ZmEAL1}:*ZmEAL1-eGFP*) to get more insight into the sub-cellular localization of ZmEAL1 during FG development. To generate transgenic maize plants in total 2000 immature maize embryos were isolated and co-transformed with the P_{35S}:*PAT* construct and either with P_{ZmEAL1}:*eGFP* or with P_{ZmEAL1}:*ZmEAL1-eGFP* constructs via particle gun bombardment and sub-cultured to regenerate plantlets. For the assay in which the

P_{ZmEAL1}:*eGFP* construct was co-transformed with the P_{35S}:*PAT* construct 40 plantlets were acclimatized, 30 of which survived the glufosinate ammonium selection and genomic Southern blotting revealed that 14 lines carried both constructs (P_{35S}:*PAT* and P_{ZmEAL1}:*eGFP*) (Table 2). Southern blot analysis was also performed to select plants with full copy integration. Seven independent lines fulfilled this criterion and three of these showed eGFP expression (Table 3). On the other hand, for the co-transformation of P_{35S}:*PAT* and P_{ZmEAL1}:*ZmEAL1-eGFP* constructs 73 plantlets were acclimatized and 53 survived the glufosinate ammonium selection (Table 2). Eight plantlets showed co-transformation with P_{35S}:*PAT* and P_{ZmEAL1}:*ZmEAL1-eGFP* constructs, of which three had a full copy integration (Table 3). All three P_{ZmEAL1}:*ZmEAL1-eGFP* transgenic lines showed ZmEAL1-eGFP-fusion protein expression, although one line was misexpressing the fusion protein in the synergid cells (data not shown).

Table 2. Overview of maize transformation using *ZmEAL1* promoter constructs and regeneration of plantlets from immature embryos via tissue culture. P_{ZmEAL1}:*eGFP* and P_{ZmEAL1}:*ZmEAL1-eGFP* constructs were co-transformed with P_{35S}:*PAT* as selectable marker.

Construct	Transformed embryos (n)	Regenerated plants (n)	Glufosinate ammonium resistant lines (n)	Co-transformed lines (n)	Co-transformation efficiency (%)
P_{ZmEAL1}:*eGFP* + P_{35S}:*PAT*	1000	40	30	14	46,7
P_{ZmEAL1}:*ZmEAL1-eGFP* + P_{35S}:*PAT*	1000	73	53	8	15,1

Table 3. Integration and expression anlysis of P_{ZmEAL1}:eGFP and P_{ZmEAL1}:ZmEAL1-eGFP constructs in transgenic maize lines.

P_{ZmEAL1}:eGFP:NOSt transgenic maize lines		
Line #	Full copy integration	eGFP expression
3	+	-
6.1	+	-
6.2	+	+
10	+	-
11	-	-
12	+	+
14	+	+
23.2	-	-
25	+	-
26	-	-
27.2	-	-
28	-	-
29	-	-
30	-	-
P_{ZmEAL1}:ZmEAL1-eGFP:NOSt transgenic maize lines		
Line #	Full copy integration	ZmEAL1-eGFP expression
2	-	-
3	-	-
9	-	-
14	-	-
17	-	-
20	+	+
23	+	+[*]
35	+	+

∗ Transgenic line misexpressing ZmEAL1-eGFP in the synergid cells.

The T_1 generation of three independent lines (#6.2, #12 and #14) was used for *ZmEAL1* promoter activity analyses and two independent lines (#20 and #35) for ZmEAL1-eGFP-fusion protein localization studies. Sections of transgenic unfertilized maize ovules were analyzed and P_{ZmEAL1}:eGFP expression was first detected at early stage FG5, when the FG contains eight nuclei, with four nuclei located at the micropylar end and the other four at the chalazal end of the embryo sac. Cellularization has not taken place yet (Fig. 10A). At this stage the eGFP signal was distributed in a polar manner in the embryo sac, with stronger signals at the micropylar end, less in the middle and no signal at the chalazal end of the embryo sac. After cellularization, at late stage FG5, the eGFP signal was observed exclusively in the egg cell during stage FG6 and FG7 (Fig. 10B-C). After fertilization, the *ZmEAL1* expression decreased in zygotes 24 hours after pollination (Fig. 10D). When the first asymmetric zygotic division took place, eGFP signal was observed in both, apical and basal cells, nevertheless, the expression was reduced in comparison with the signals observed in zygotes (Fig. 10E). However, the eGFP signal increased again during embryo and suspensor development, at 3 days after pollination (dap) (Fig. 10F). *ZmEAL1* promoter activity could be observed until 7 dap in all cells of the embryo proper and suspensor (Fig. 10G-J) and

was completely gone at 8 dap. The ZmEAL1-eGFP-fusion protein was observed the first time after cellularization at late stage FG5 (Fig. 10K). In the same way like the promoter activity analyses ZmEAL1-eGFP-fusion protein was expressed exclusively in the egg cell (Fig. 10K-L). The pattern observed for *ZmEAL1* promoter activity in zygote and two-celled proembryo coincided also with the ZmEAL1-eGFP-fusion protein expression pattern (Fig. 10M-N). At 3 dap, however, the ZmEAL1-eGFP-fusion protein was visible only in the cells of the embryo proper and not in the suspensor cells and localized in small vesicles (Fig. 10O-P). From 4 until 7 dap the ZmEAL1-eGFP-fusion protein showed accumulation around the nucleus, with more protein concentration at one side of the nucleus. Expression of ZmEAL1-eGFP-fusion protein was not detected in the suspensor cells (Fig. 10Q-X). In summary, during the first steps of embryo development, from 3 until 5 dap (Fig. 10P-T), ZmEAL1-eGFP-fusion protein showed expression in all cell of the embryo proper. At 5 dap a group of cells placed in the middle of the embryo showed higher expression of ZmEAL1-eGFP-fusion protein (Fig. 10S-T). However, at 6 and 7 dap the ZmEAL1-eGFP-fusion protein was localized only at the center of the adaxial face of the embryo and at the embryonic protoderm, a single layer of homogenously sized cells surrounding the embryo proper (Fig. 10U-X). At 8 dap, when the embryo reaches the transition stage, neither promoter activity nor ZmEAL1-eGFP-fusion protein was detected any more (Fig. 10Z).
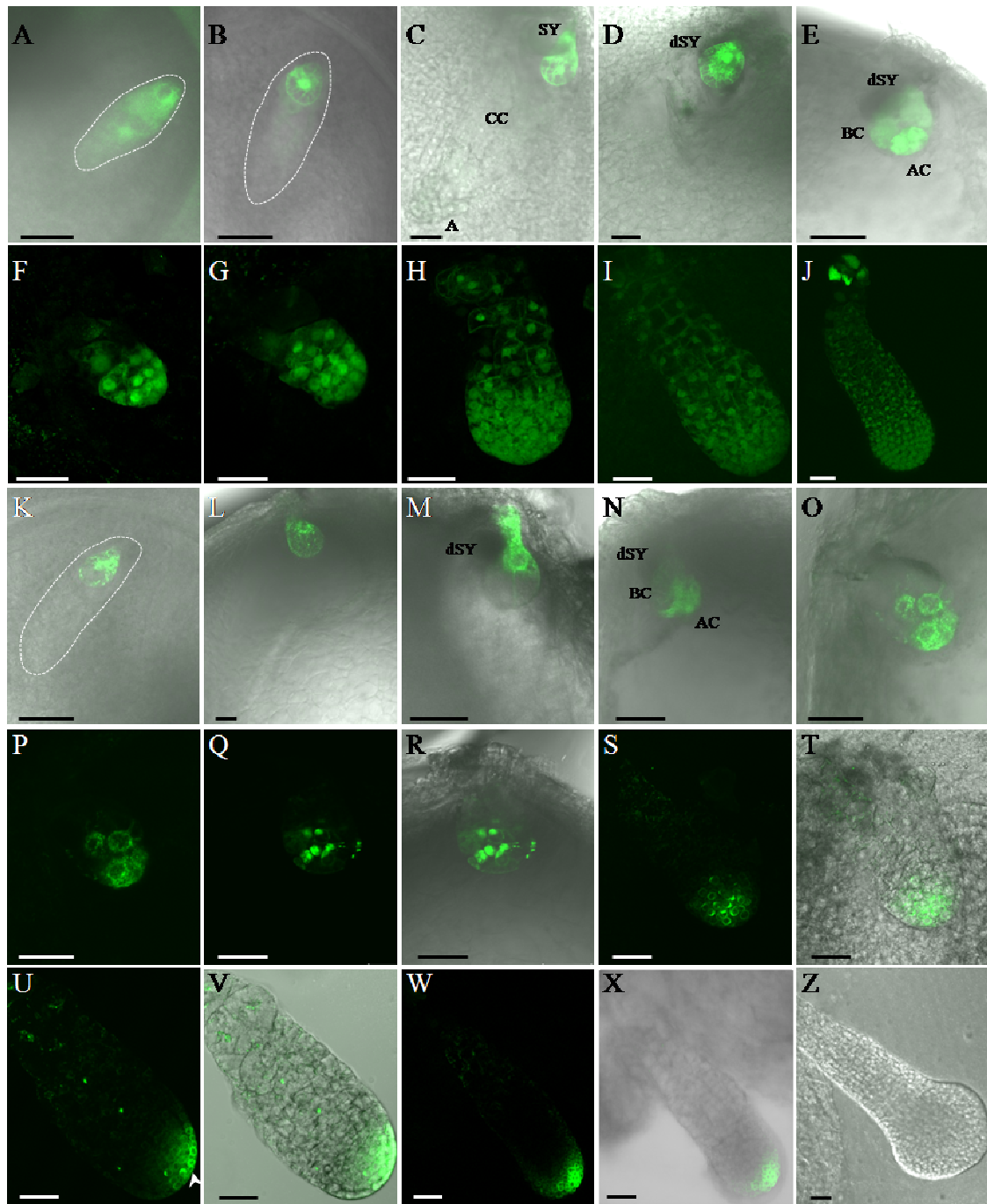
Figure 10. *ZmEAL1* **promoter activity and ZmEAL1-eGFP-fusion protein localization studies.** (**A-J**) Promoter activity analysis of stably transformed maize plants containing full length of P_{ZmEAL1}:*eGFP* construct. (**A**) Embryo sac at early stage FG5. (**B**) Early stage FG7. (**C**) Late stage FG7. (**D**) Zygote 24 hap. (**E**) Proembryo at 2 dap. (**F-J**) Embryos at 3, 4, 5, 6 and 7 dap, respectively. (**K-Z**) ZmEAL1-eGFP-fusion protein during FG development and zygotic embryogenesis in maize. (**K**) Embryo sac at early stage FG7. (**L**) Late stage FG7. (**M**) Zygote at 24 hap. (**N**) Proembryo at 2dap. (**O-P**) Embryo (EM) at 3 dap. (**Q-R**) EM at 4 dap. (**S-T**) EM at 5 dap. (**U-V**) EM at 6 dap; arrowhead indicates the protoderm (outer cell layer). (**W-X**) EM at 7 dap. (**Z**) EM at 8 dap. (A-E, K-O, R, T, V, X, Z) fluorescence microscopy images merged with its corresponding bright field microscopy image; (F-J, P-Q, S, U, W) fluorescence microscopy images. Dotted lines mark the FGs. Synergid cells (SY); central cell (CC); antipodal cells (A); degenerated synergid (dSY); basal cell (BC); apical cell (AC). Bars: 50µm.

3.4   ZmEAL1 is a small secreted peptide

In order to analyze the subcellular localization of ZmEAL1, ZmEAL1-eGFP-fusion protein was expressed under control of the endogenous *ZmEAL1* promoter in BMS maize suspension cells. Unexpectedly, the *ZmEAL1* promoter is active in some BMS maize suspension cells (Fig. 11A-B) revealing a powerful system for several *in vitro* assays. A plasmolysis study was carried out. Transient expression of $P_{ZmEAL1}:eGFP$ construct was used as negative control for the plasmolysis assay. An eGFP signal was not observed after plasmolysis treatment in cell walls of suspension cells transformed with $P_{ZmEAL1}:eGFP$ construct (Fig. 11C-D). Suspension cells expressing the ZmEAL1-eGFP-fusion protein showed protein localization at the endoplasmic reticulum surrounding the nucleus and in transvacuolar strands, mainly within small vesicles (Fig. 11E-F). ZmEAL1-eGFP-fusion protein was observed in the cell wall after plasmolysis treatment (Fig. 11G-H). Taken together ZmEAL1 is a protein secreted via the secretory pathway as predicted also through *in silico* analysis.
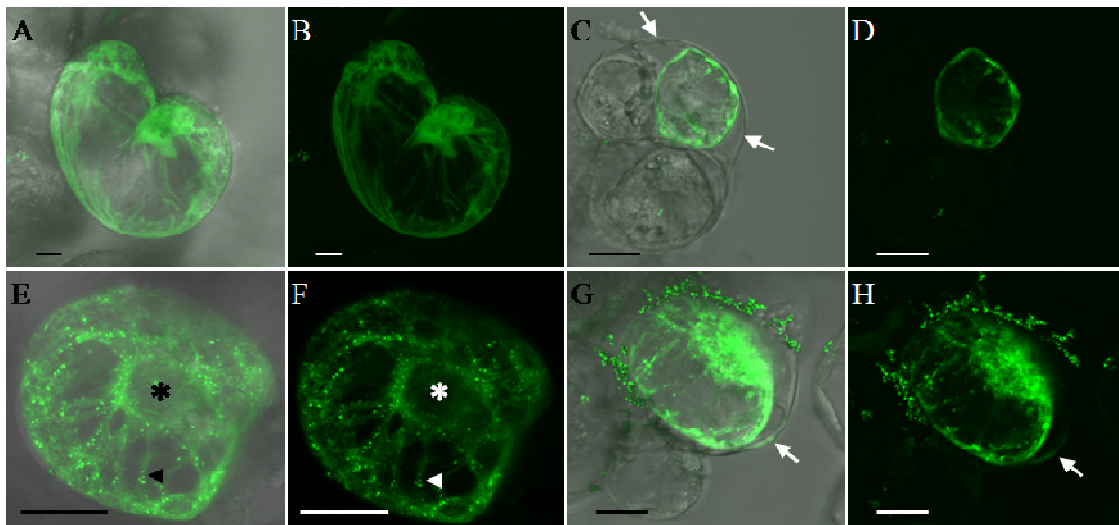

Figure 11. Fluorescent microscopy images of transiently transformed BMS cells. (**A**-**D**) BMS cells transiently transformed with $P_{ZmEAL1}:eGFP$ construct. (**A-B**) represent a cell before plasmolysis treatment; (**C**) and (**D**) show a cell after plasmolysis, eGFP signal is not visible in the cell wall (arrows). (**E-H**) BMS cells transiently transformed with $P_{ZmEAL1}:ZmEAL1-eGFP$ construct. (**E-F**) images of a cell before plasmolysis treatment, ZmEAL1-eGFP-fusion protein is visible around the nucleus (asterisk) and in small vesicles in the cytoplasm (arrowhead); (**G-H**) represent a cell after plasmolysis treatment; arrows indicate the cell wall with secreted ZmEAL1-eGFP-fusion protein. (A, C, E, G) fluorescence microscopy images merged with its corresponding bright field microscopy images; (B, D, F, H) fluorescence microscopy images. Bars: 20µm.

3.5 *ZmEAL1*-RNAi phenotypes

ZmEAL1-RNAi transgenic lines were generated and used as a tool for functional analyses. The expression of the *ZmEAL1*-RNAi construct was driven by the *Ubi1* promoter, which drives strong gene expression during megagametogenesis in maize (Srilunchang *et al.*, 2010). The genetic transformation assay was performed with 600 immature embryos which were co-transformed with P_{35S}:*PAT* and P_{UBI}:*ZmEAL1-AS:iF2intron:ZmEAL1:OCSt* constructs via particle gun bombardment. Embryos were sub-cultured and 15 plantlets were regenerated (Table 4). Only seven plantlets were glufosinate ammonium resistant and five lines showed to be co-transformed with P_{35S}:*PAT* and *ZmEAL1*-RNAi constructs.

Table 4. Overview of maize transformation and regeneration. P_{UBI}:*ZmEAL1-AS:iF2intron:ZmEAL1:OCSt* was co-transformed with P_{35S}:*PAT* in immature maize embryos.

Construct	Transformed embryos (n)	Regenerated plants (n)	Glufosinate ammonium resistant lines (n)	Co-transformed lines (n)	Co-transformation efficiency (%)
P_{UBI}:*ZmEAL1-AS:iF2intron:ZmEAL1:OCSt* + P_{35S}:*PAT*	600	15	7	5	71,4

Southern blot analyses further revealed that three lines showed full copy integration (Table 5). RT-PCR was carried out to verify the expression of the *ZmEAL1*-RNAi construct in transgenic maize plants. The transgenic lines #3, #7 and #9 were used for phenotypical analyses, because they showed expression of the *ZmEAL1*-RNAi construct, including line #3 that did not have a full copy integration. Besides expression of *ZmEAL1*-RNAi construct line #3 also showed a phenotype during FG development.

Table 5. Integration and expression analysis of P_{UBI}:*ZmEAL1-AS:iF2intron:ZmEAL1:OCSt* in transgenic maize plants.

P_{UBI}:*ZmEAL1-AS:iF2intron:ZmEAL1:OCSt* maize transgenic lines		
Line #	Full copy integration	*ZmEAL1*-RNAi expression
1	-	-
3	-	+
7	+	+
8	+	-
9	+	+
11	-	-
12	-	-

The T_0 and following T_1 generation developed normally besides some phenotypes that were observed on *ZmEAL1*-RNAi cobs (Fig. 12). Some seeds of the T_0 generation of *ZmEAL1*-RNAi line #3 showed development of embryos at the adaxial site of the cob axis (Fig. 12A-B). However, this phenotype was not observed in T_1 and T_2 generations, meaning that it was probably due to effects of the *in vitro* culture system. Pollination experiments were performed with cobs of *ZmEAL1*-RNAi lines #3, #7 and #9 showing incomplete seed set (Fig. 12A-D). On the other hand, when wild type cobs were pollinated with pollen of *ZmEAL1*-RNAi lines no effect from the male side was observed (Fig. 12E-F). The T_1 generation of *ZmEAL1*-RNAi showed seed abortion as well (Fig. 12H-L) besides *ZmEAL1*-RNAi line #3, which showed full seed set (Fig. 12G). In some cases kernel development started and seeds were aborted after some time (Fig. 12I). Cob of *ZmEAL1*-RNAi #9-21 showed a high number of aborted seeds, even before fertilization took place (Fig. 12L). Histological analysis were performed with cob of the next generation of *ZmEAL1*-RNAi #3R2, #7-3, #7-8, #9-14 and #9-21 seeds.
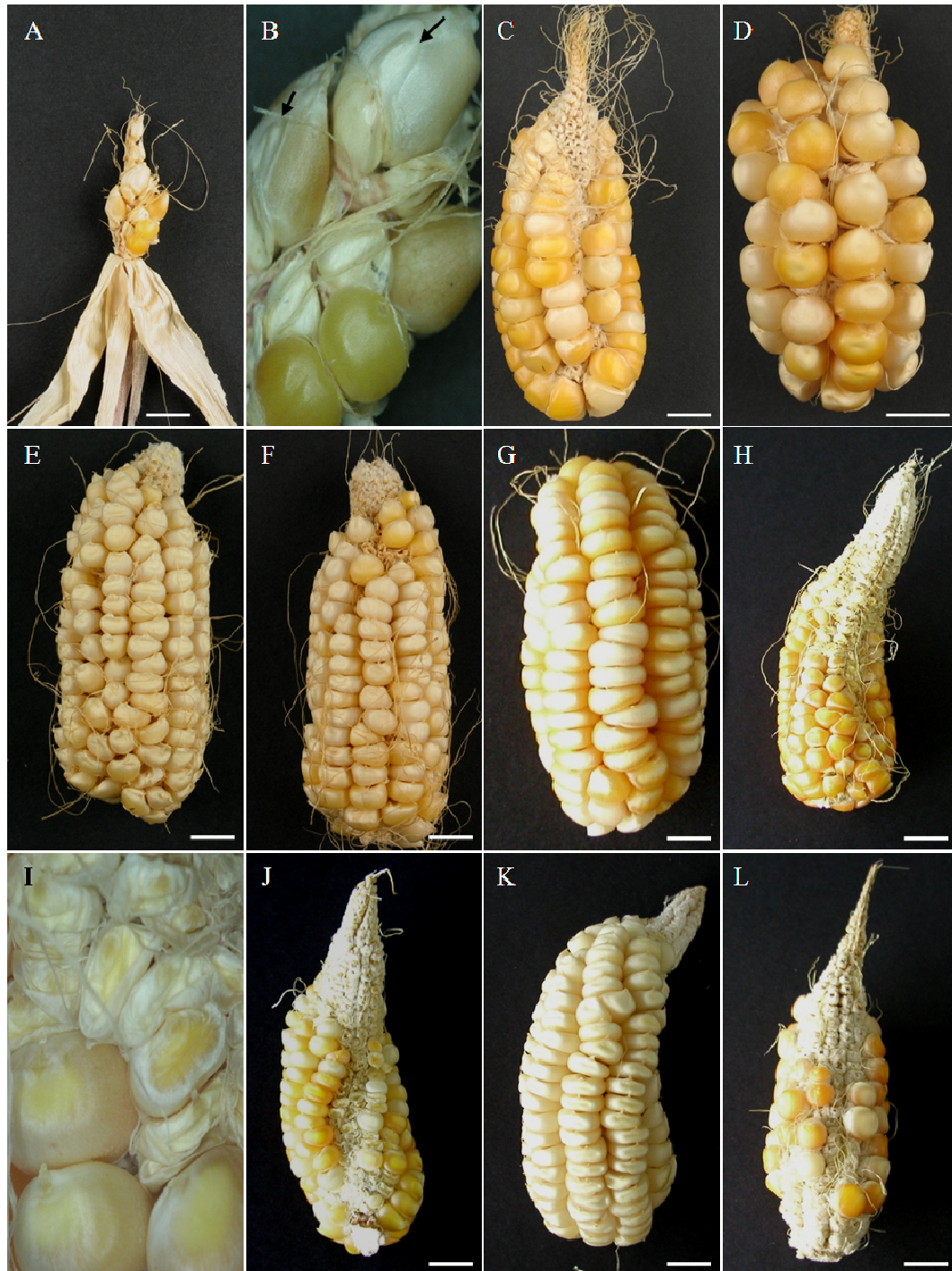
Figure 12. Pollination experiment with *ZmEAL1*-RNAi transgenic lines. (**A-F**) Pollination performed using cobs and pollen of the T_0 generation and of *ZmEAL1*-RNAi transgenic lines. (**G-L**) Pollination performed using cobs and pollen of the T_1 generation of *ZmEAL1*-RNAi transgenic lines. (**A**) *ZmEAL1*-RNAi line #3 pollinated with wild type (wt) pollen. (**B**) Closer look at seeds of *ZmEAL1*-RNAi line #3 showing development of embryos at the adaxial site of cob axis (arrows). (**C**) *ZmEAL1*-RNAi transgenic line #7 after self pollination. (**D**) *ZmEAL1*-RNAi transgenic line #9 pollinated with wt pollen. (**E-F**) Pollination of wt cobs with pollen of *ZmEAL1*-RNAi line #7 and #9, respectively. (**G**) Cob of a *ZmEAL1*-RNAi #3R2 plant pollinated with wt pollen. (**H-I**) Cob of *ZmEAL1*-RNAi #7-3 plant after self pollination. (**I**) Closer look at seeds, which were aborted at some point after fertilization. (**J**) Cob of *ZmEAL1*-RNAi #7-8 plant after self pollination. (**K**) Cob of *ZmEAL1*-RNAi #9-14 plant after self pollination. (**L**) Cob of *ZmEAL1*-RNAi #9-21 plant after self pollination. Bars: 1 cm.

In order to get more insight into the reasons of partial seed abortion, several *ZmEAL1*-RNAi cobs from the T_2 generation of three independent lines were analyzed at different developmental stages using the silk length as morphological feature to estimate the FG developmental stage as previously described (Srilunchang *et al.*, 2010). Srilunchang and co-workers have carried out their study using plants with the same genetic background and same growing conditions as used in the present study. FG development was analyzed by the Confocal Laser Scanning Microscopy (CLSM) from stage FG1 until mature stage FG7 as well as after the fertilization process until 2 dap. The T_2 generation of transgenic plants with glufosinate ammonium resistance lacking integration of the RNAi construct was used as a negative control to assure that the plants used as negative control had the same genetic background as *ZmEAL1*-RNAi lines. Additionally, these plants were also regenerated through a tissue culture procedure to evaluate possible phenotypical effects caused by somaclonal variation. The functional megaspore (stage FG1) of *ZmEAL1*-RNAi plants developed normally (Fig. 13A) and after the first nuclear mitotic division (stage FG2) two nuclei were separated from each other by a large vacuole with additional vacuoles at the chalazal and micropylar pole of the FG (Fig. 13B). The second mitotic division took place at stage FG4 (Fig. 13C). At stage FG5, the third mitotic division was completed and cellularization took place, giving rise to the synergid cells and egg cell at the micropylar pole, the central cell in the center and three antipodal cells at the chalazal pole of the FG. The two polar nuclei, which were located at distinct poles (micropylar and chalazal end of the FG), migrated to the center of the embryo sac at late stage FG5 (Fig. 13D). At stage FG6 the polar nuclei attached to each other, and then migrated to the micropylar end of the central cell adjacent to the egg cell (Fig. 13E). During early stage FG7 the cells of the FG entered the maturation process giving rise to the fully differentiated FG at late stage FG7 (Fig. 13F). During this stage the antipodal cells continued to divide reaching a final number of 20 to 100 cells. The first phenotype observed for the *ZmEAL1*-RNAi plants was the degeneration of the embryo sac (Fig. 13G). *ZmEAL1*-RNAi line #9 showed the most severe effect with 21,6% of degenerated embryo sacs. Wild type cobs showed only 4,9% of degenerated embryo sacs (Table 6). The *ZmEAL1*-RNAi line #3 and #7 showed less frequently degenerated embryos sacs of only 3,1 and 7,9%, respectively (Table 6). More interestingly, central cell-like structures developed at the chalazal end of the embryo sac, where usually only antipodals cells are present (Fig. 13H-M). Additionally, central cells often had multiple polar nuclei,

varying from 1 to 3 additional nuclei in comparison with the normal wild type condition (Fig. 13N-R). Taken together, the central cell-related phenotypes occurred at a frequency of 2,0% for *ZmEAL1*-RNAi line #3 and 2,5% for *ZmEAL1*-RNAi lines #7 and #9 (Table 6). The central cell-related phenotypes were never observed in wild type cobs (Table 6). The *ZmEAL1*-RNAi line #3 partially showed nuclei accumulation in the center of the embryo sac (Fig. 13S). This phenotype could be related to division of the "normal" polar nuclei giving rise to multiple polar nuclei or it could be related with autonomous development of endosperm observed in 0,8% of the cases for the *ZmEAL1*-RNAi line #3 (Fig. 13T-U and Table 6). The fertilization process itself seemed not severely affected in *ZmEAL1*-RNAi embryo sacs, as there were no differences between the fertilization rates of mutant and wild type cobs (Table 6). The two-celled-proembryo developed normally, as well as the endosperm (Fig. 13V). Embryo sacs with multiple polar nuclei could be normally fertilized. The same is true for embryo sacs with central cell-like structures at the chalazal end of the FG (Fig. 13W-Z).

Table 6. Analyses of female gametophytes of *ZmEAL1*-RNAi lines at mature stage FG7 and at 2 dap in comparison with wild type.

Line #	n	Mature stage FG7				n	2 dap
		Normal ES (%)	Degenerated ES (%)	Multiple CCs and multiple polar nuclei (%)	Endosperm developed autonomously (%)		Fertilized ES (%)
3	493	94,3	3,1	2,0*	0,8	425	73
7	1125	89,6*	7,9	2,5*	0,0	535	80,8
9	477	75,9*	21,6*	2,5*	0,0	364	72,3
wt	455	95,1	4,9	0,0	0,0	576	79,5

n, analyzed embryo sacs; ES, embryo sac; wt, wild type; CC, central cell; * represents $P \leq 0,05$ when compared with wild type.
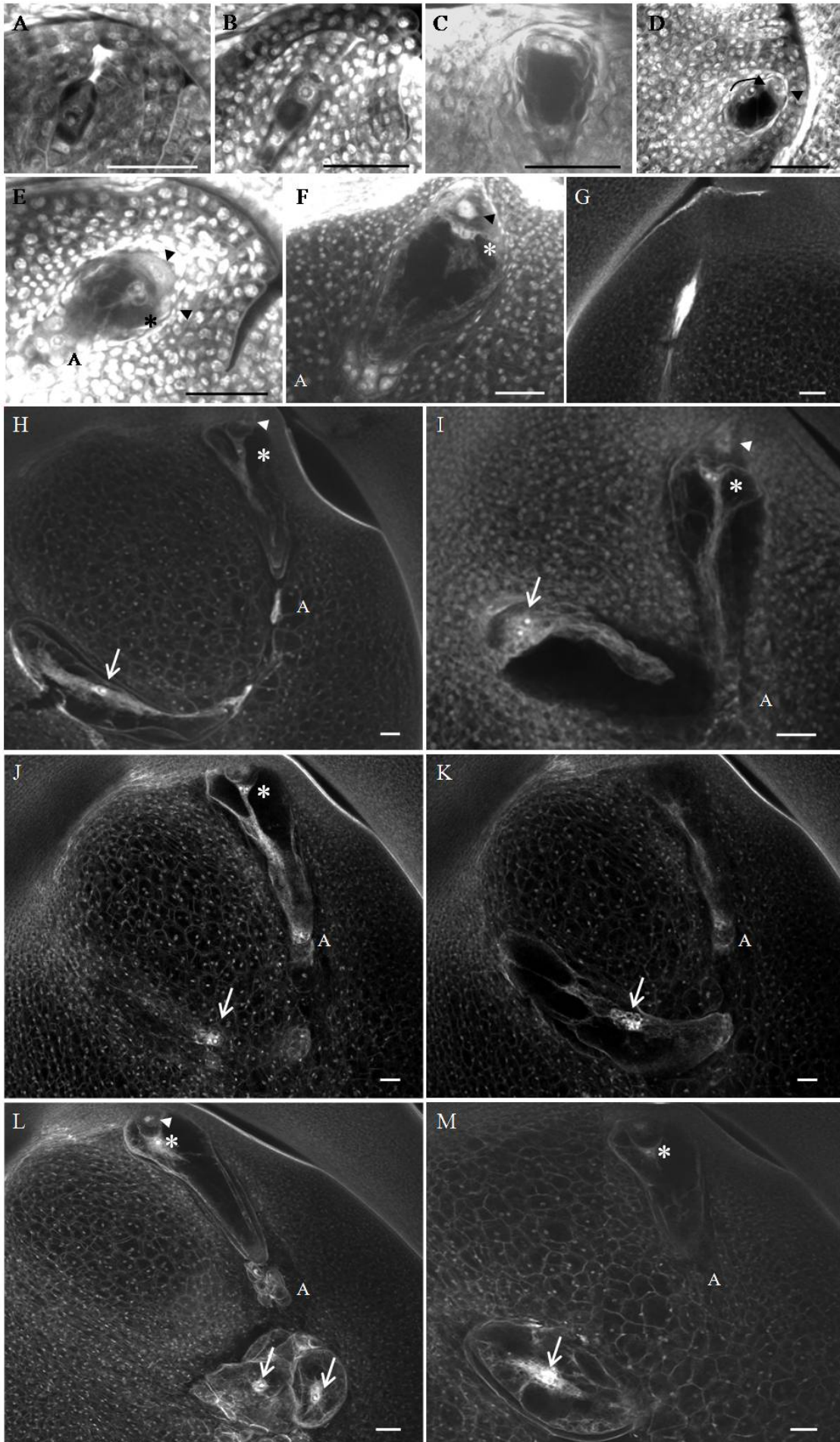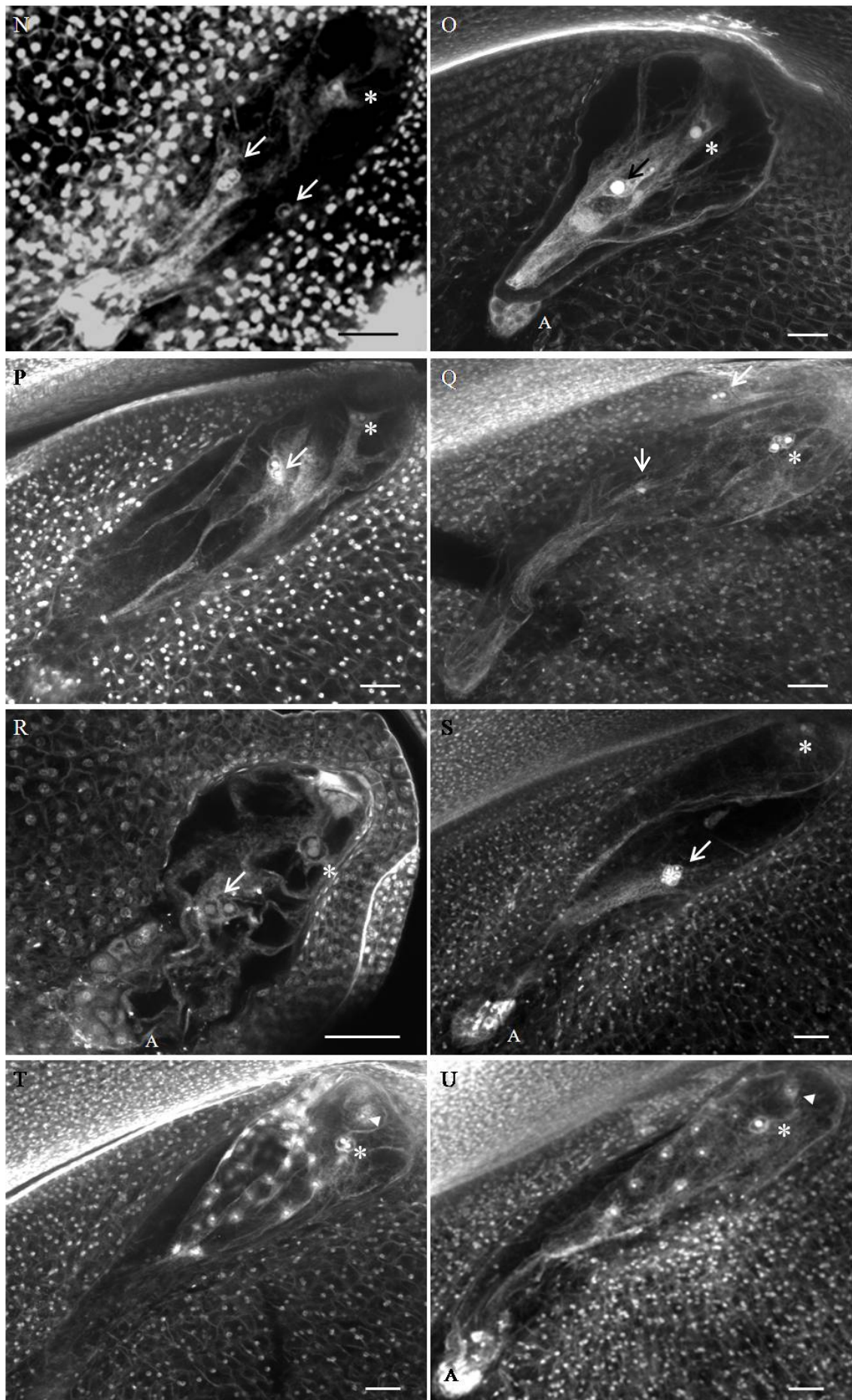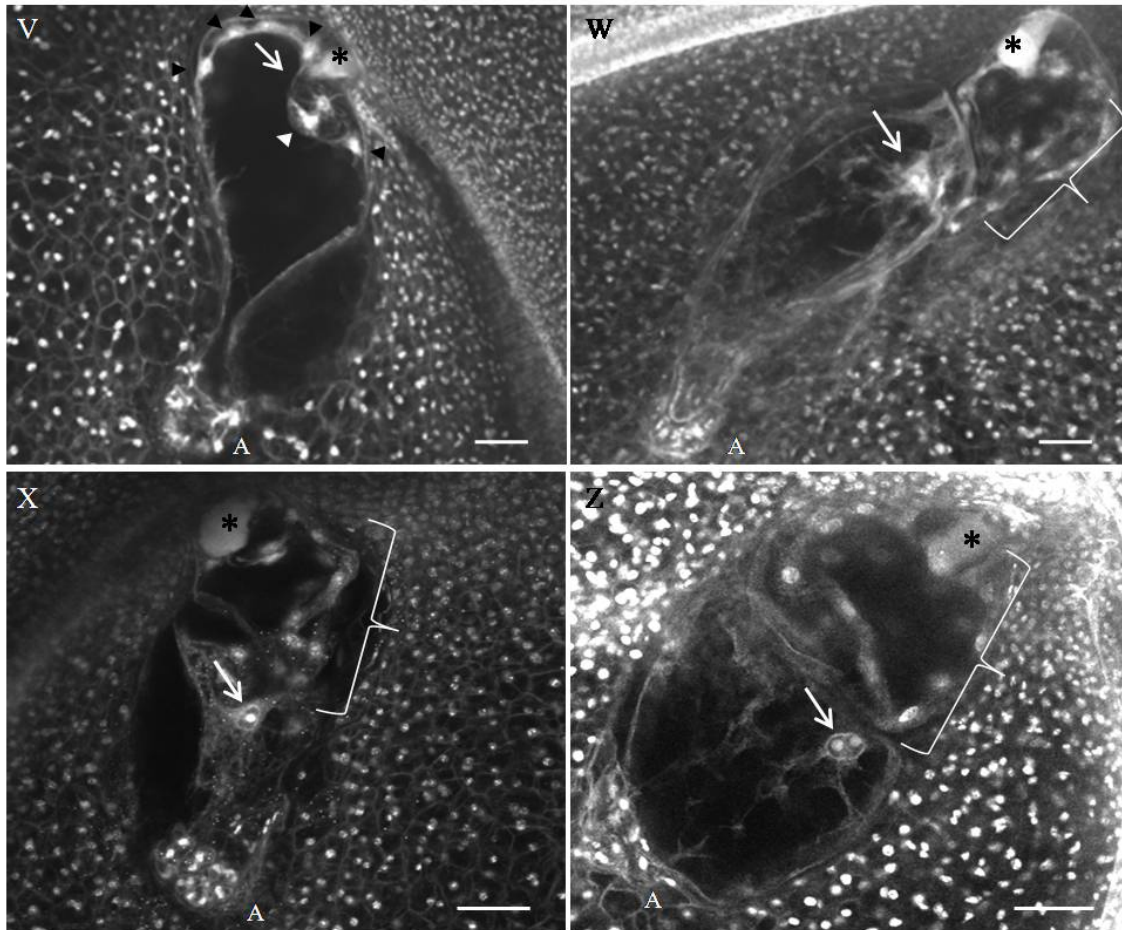
Figure 13. Megagametogenesis and phenotypes observed in mature ovules of *ZmEAL1-*RNAi mutants. (**A**) Stage FG1. (**B**) Stage FG2. (**C**) Stage FG4. (**D**) Late stage FG5: arrow indicates the migration of the polar nuclei to the micropylar end of the central cell adjacent to the egg cell; synergid and antipodal cells are not in focus on the picture. (**E**) Early stage FG7: arrowheads point toward nuclei of synergid cells; asterisk marks polar nuclei of the central cell; (A) antipodal cells; egg cell is not in focus on the picture. (**F**) Late stage FG7: arrowhead points toward egg cell nucleus; asterisk marks polar nuclei of central cell; (A) antipodal cells; synergid cells are not in focus on the picture. (**G**) Degenerated embryo sac. (**H-M**) Different examples of embryo sacs at late stage FG7 showing further development of some antipodals cells into central cell-like structures: arrowhead indicates egg cell nucleus; asterisk marks polar nuclei of central cell; (A) antipodal cells; arrow points toward polar nuclei of the central cell-like structure; synergid cells are not in focus on the pictures. Note that only one focus plane is shown for all examples and that additional central cell-like structures were always connected to antipodal cells. (**N-R**) Embryo sacs at late stage FG7 with several additional polar nuclei: asterisk marks "normal" polar nuclei, arrows indicate additional polar nuclei; (A) antipodal cells; synergid cells and egg cells are not in focus on the pictures. (**S**) Embryo sac at late stage FG7 with abnormal nuclei accumulation in the center. (**T-U**) Embryo sacs at late stage FG7 showing autonomous development of endosperm; arrowhead marks unfertilized egg cell; asterisk indicates "normal" polar nuclei; (A) antipodal cell; synergid cells are not in focus on the pictures. (**V**) Embryo sac at 2 days after pollination: asterisk points toward degenerated synergid cell; black arrowheads shows nuclei of endosperm; white arrowhead and arrow indicate the apical and basal cell of the two-celled proembryo, respectively; (A) antipodal cells. (**W-Z**) Ovules at 2 days after pollination, showing the phenotype where some antipodal cells developed into central cell-like structures; asterisk points to degenerated synergid cell, bracket indicates endosperm; arrow marks polar nuclei of the central cell-like structure; (A) antipodal cells. Note that the "normal" embryo sac could be fertilized and developed into embryo and endosperm. Bars: 50µm.

4   Discussion

EA1-box proteins might be involved in a broad spectrum of development processes. Until now only ZmEA1 has been shown to be involved in short range pollen tube guidance (Márton *et al.*, 2005). Recently, another EA1-box protein was identified to be expressed only after fertilization in wheat zygotes (Dunja Leljak personal communication) indicating a function different from pollen tube guidance. Besides that, one additional EA1-box proteins in maize (ZmEAL2), six hypothetical proteins in *Oryza sativa* and one hypothetical protein in *Sorghum bicolor* showed homology to ZmEAL1, revealing an interesting research field to identify the common characteristic and functions of those genes. ZmEAL1 described here plays a role in cell identity maintenance during female gametophyte development. The function of the protein during zygotic embryogenesis remains to be determined.

BLAST searches revealed significant similarity between ZmEAL1 and ZmEA1 proteins. Further on, *ZmEAL1* and *ZmEA1* are both expressed in the egg cell opening the possibility to search for similar *cis*-regulatory sequences, which could activate transcription in the egg cell. For that reason, DNA sequences of *ZmEAL1* and *ZmEA1* promoters were aligned showing 42,9% sequence identity. Three conserved motifs were identified. Motifs 1 and 2 have a quite similar core sequence, namely TTCTCA for motif 1 and TTCT(G)CA for motif 2. The sequence TTCTCA is also found in both *ZmMAB1* (Leljak-Levanić *et al.*, unpublished data) and *ZmDSUL* promoters (Srilunchang *et al.*, 2010), which are expressed in the egg cell. A fourth element, showing quite high sequence identity, was identified when *ZmEAL1*, *ZmEA1*, *ZmMAB1* and *ZmDSUL* promoters were compared. A number of *cis*-regulatory sequences have been identified being involved in several aspects of plant biology (for review see Priest *et al.*, 2009). Promoter deletions of the identified conserved motifs should be aspects of future research to determine whether the sequences are indeed necessary to regulate transcription in the egg cell.

Nothern blot analysis performed with a *ZmEAL1* probe revealed the expression of two transcripts, one with 500 and another with 700 nt. All tissues examined showed a low expression pattern besides embryogenic cell suspension, in which the expression of the 500 nt transcript was higher. However, after analyses of P_{ZmEAL1}:*eGFP* plants eGFP signals were not detected in any of the tissues with relative higher expression according to Northern blot analysis (data not shown). Moreover, when *ZmEAL1*-RNAi plants were analysed, no phenotypes were observed in these tissues indicating that the protein is not

required. The divergent results observed for Northern blot analysis and the expression of *ZmEAL1* visualized with eGFP could be explained, first, due to cross hybridization with similar genes. Cordts (2000) reported already the gene *ZmEC135*, expressed in the egg cell, *ZmEC135* and *ZmEAL1* have 50% sequence identity and the whole cDNA of *ZmEAL1* was used as probe for Nothern blot hybridization. Alternatively, a detection limit of promoter-eGFP activity in comparison to radioactive Northern blot should be considered. Further analysis could be performed with a more sensitive marker, like the GUS (β-glucuronidase) (Jefferson *et al*., 1987) marker under the control of *ZmEAL1* promoter.

The expression of *ZmEAL1* in embryogenic cell suspension could be related to similarities between those cells and maize embryos, in which the gene is as well expressed. In the same way, *ZmEAL1* promoter activity was detected in BMS suspension cells, which are derived from maize embryos (Quayle *et al*., 1991).

The *ZmEAL1* transcript was isolated 26 times after the analysis of about 1000 ESTs from an egg cell cDNA library (Dresselhaus *et al*., 1994). Single cell RT-PCR analysis revealed high expression of *ZmEAL1* in egg cells, with down-regulation of about 50% after fertilization in zygotes 24 hours after pollination. The gene is also slightly expressed in central cells (detected only after blotting PCR products) and sperm cells, for which 50 cells were used to perform the experiment. An eGFP signal was not detected in central cells and sperm cells of P_{ZmEAL1}:*eGFP* plants. Taken together, it seems that, before fertilization, *ZmEAL1* is exclusively expressed in the egg cell. Moreover, *ZmEAL1* is generally expressed at developmental stages when fate determination takes place, during megagametogenis and zygotic embryogenesis. During female gametophyte development ZmEAL1 protein is translated only after cellularization is completed, at late stage FG5 onward. Kägi and Groß-Hardt (2007) discussed that cell-specific marker gene expression is only initiated after cellularization suggesting that only then distinct cell fates are manifested. After fertilization ZmEAL1 is still expressed in the zygote, and after asymmetric zygotic division, both apical and basal cell of two-celled embryo showed a ZmEAL1-eGFP-fusion protein signal. Further on, protein expression is detected in the embryo proper but not in the suspensor until the late transition stage. At the late transition stage the embryo starts to differentiate and forms both shoot and root apical meristems (Forestan *et al.,* 2010). Interestingly, *ZmEAL1* promoter activity is detected in suspensor cells from the two-celled proembryo until the late transition stage and eGFP signal are observed in all cells of the embryo

proper. Probably the 5' UTR of *ZmEAL1* transcript possess regulatory elements responsible for translational control, explaining the differences between expression of P_{ZmEAL1}:*eGFP* and P_{ZmEAL1}:*ZmEAL1-eGFP*. Translation regulatory elements at 5' UTR of mRNAs have been extensively reported for animals (for review see Hughes, 2006).

The knowledge about how non-cell autonomous signaling is mediated in the embryo sac is very limited. However, symplastic connections, between the embryo sac cells, via plasmodesmata were identified in *Torenia* (Han *et al.*, 2000; Okuda *et al.*, 2009) and in maize (Diboll and Larson, 1966). Additionally, several studies characterized small gametophytic secreted peptides to play an important role during the double fertilization process (Dresselhaus, 2006) highlighting the importance of apoplastic communication. ZmEAL1 has a predicted signal peptide and according subcellular localization experiment performed with BMS suspension cells ZmEAL1-eGFP-fusion protein is localized at the endoplasmic reticulum surrounding the nucleus, in transvacuolar strands, mainly within small vesicles, being the first evidence for ZmEAL1 secretion. In maize embryos, from 4 until 7 dap, the protein accumulates around the nucleus, with more protein concentration at one side of the nucleus. This structure probably corresponds to the endoplasmic reticulum. Further on, plasmolysis assays were carried out with BMS suspension cells transformed with P_{ZmEAL1}:*ZmEAL1-eGFP* allowing the detection of ZmEAL1-eGFP-fusion protein in the cell wall of those cells.

The observation that embryo sacs of *ZmEAL1*-RNAi plants showed the development of central cell-like structures at the chalazal end of the embryo sac, thus opposite of the ZmEAL1 secreting egg cell suggests a non-cell-autonomous action of the secreted protein. Cell-to-cell communication is believed to play an important role during female gametophyte development and during fertilization process (Dresselhaus, 2006) and ZmEAL1 seems to represent the signaling peptide identified to be related with cell fate maintenance of embryo sac cells.

The female gametophyte developed normally from stage FG1 to early stage FG7. At late stage FG7 phenotypes were observed, which are related with loss of cell identity. First, the development of central cell-like structures was observed at the chalazal end of the embryo sac, were normally only antipodal cells develop. The central cell showed the presence of additional polar nuclei, varying from one to three additional polar nuclei in comparison with the normal wild type condition. A similar phenotype was observed in *ig1* (*indeterminate gametophyte1*) mutants of maize. The *ZmIG1* gene

encodes a LATERAL ORGAN BOUNDARIES domain protein with high similarity to ASYMMETRIC LEAVES2 of *Arabidopsis thaliana*. In *ig1* mutant embryo sacs, the proliferative phase is prolonged resulting in extra rounds of free nuclear divisions, which resulted in extra egg cells, central cells and polar nuclei (Evans, 2007). Although the *ig1* and *ZmEAL1*-RNAi resulting phenotypes partially overlap, the expression pattern of both proteins is quite different. *ZmIG1* is expressed from stage FG1 onwards meaning that nuclear proliferation was observed before cellularization while ZmEAL1 is expressed only after cellularization took place. Similar results were achieved with the analysis of *AtRBR1* (RETINOPLASTOMA-RELATED PROTEIN1) knockdown mutants. Megagametophytes of *rbr1* mutants developed normally during early stages, from stage FG1 to FG5. However, at stage FG7 the female gametophytes had supernumerary nuclei cluster at the micropylar end of the embryo sac. *rbr1* mutant ovules lack the expression of mitotic cyclin B1 in the egg apparatus suggesting that these cells are either arrested in G1 or G2 (Ebel *et al*., 2004).

Nuclear proliferation in the central cell observed in *ZmEAL1*-RNAi ovules suggests that the central cell is not differentiated, which would in turn result in insufficient/disrupted communication between central cell and antipodal cells. This hypothesis would explain the phenotype in which central cell-like structures developed at the chalazal end of the embryo sac, where only antipodals cells are observed in wild type ovules. Similar results were achieved by the knockdown of a gene which encodes a splicing factor PRP4 protein in the *lis* (*lachesis*) mutant in *Arabidopsis thaliana*, in which the central cell is misspecified and its identity is shifted towards antipodal cells (Groß-Hardt *et al.*, 2007). Furthermore, in *clo* (*clotho*) and *ato* (*atropos*) mutant embryo sacs in *Arabidopsis* the synergids and central cell adopted attributes of egg cell identity. *CLOTHO* and *ATROPOS* encode the *Arabidopsis* homologue of Snu114 (component of the spliceosome) and of SF3a60 (implicated in pre-spliceosome formation), respectively (Moll *et al.*, 2008). Another example is the *eostre* mutant in *Arabidopsis* that mis-expresses the homeodomain gene *BEL1-like homeodomain1* (*BLH1*) in the embryo sac resulting in a cell fate switch of a synergid cell towards an egg cell (Pagnussat *et al*., 2007). These findings suggest that there are various levels of cell fate regulation, (i) between the gametic cells and accessory cell (synergid and antipodal cells), (ii) between the two female gametes (egg cell and central cell), and (iii) all gametophytic cells are competent to adopt gametic cell fate (Kägi and Groß-Hardt, 2007). Another phenotype observed in *ZmEAL1*-RNAi ovules was autonomous proliferation of endosperm. Similar

results were observed for *rbr1* mutant ovules, as described above. Probably AtRBR1 acts upstream of FIS (FERTILIZATION INDEPENDENT SEED) or together with MEA-FIE (MEDEA-FERTILIZATION INDEPENDENT ENDOSPERM) PcG complex to control female gametophyte cell arrest (Ebel *et al*., 2004).

The fertilization process itself was not affected in *ZmEAL1*-RNAi lines. Female gametophytes showing central cell-like structure development at the chalazal end of the embryo sac as well as megagametophytes with one or several additional polar nuclei in the central cell could be normally fertilized. In summary, pollen tube guidance and interactions between gametes was not affected in *ZmEAL1*-RNAi lines.

Degeneration of embryo sacs was also observed. However, for *ZmEAL1*-RNAi lines #3 and #7 the number of degenerated female gametophytes did not differ statistically from the wild type situation. Only for *ZmEAL1*-RNAi line #9 21,6% of degenerated embryo sac was observed. The self pollinated cobs of T_1 generation of *ZmEAL1*-RNAi line #9 showed reduced seed set with kernels that were aborted early before fertilization, correlating with histological analysis, which revealed a high number of degenerated embryo sacs. A common phenotype observed for *ZmEAL1*-RNAi lines was that kernels started to developed, grains started to fill but at some time they were aborted. This phenotype occurred in a low frequency and could be related to embryo sacs showing more than one polar nuclei in the central cell. It was already reported that maize endosperm development is very sensitive to a deviation from the normal 2 maternal:1 paternal genome ratio in the endosperm. Consequently, when an embryo sac with three or more polar nuclei is fertilized by a sperm cell, the resulting development of endosperm is reduced (Lin, 1984).

Taken together, ZmEAL1 is a signaling molecule that probably regulates the cell cycle in the central cell, inhibiting proliferation and promoting cell differentiation. The receptor of ZmEAL1 and the stage at which the cell cycle of central cell nuclei is arrested before fertilization remains to be determined. Also the signaling cascade downstream of ZmEAL1 remains to be determined and the molecules that are probably secreted from the differentiated central cell to the antipodal cells to repress their ability to generate gametic cells (central cells) have to be identified as well.

Analysis of *cis*-acting elements in the *ZmEAL1* promoter revealed the presence of an auxin responsive element (AuxRE) containing the sequence 5'-TGTCTC-3'. This consensus core sequence was identified in promoters of primary auxin response genes (Guilfoyle, 1999; Hagen and Guilfoyle, 2001). ARF (<u>A</u>uxin <u>R</u>esponse <u>F</u>actor) proteins

can bind to these elements and regulate the expression of promoters containing this AuxRE (Ulmasov *et al.*, 1999). Besides that, the *ZmEAL1* gene is located close to a predicted *SAUR* (*Small Auxin-Up RNA*) gene and to *ZmEA1*, whose promoters contain the identical AuxRE identified in the *ZmEAL1* promoter. Similar findings were achieved in soybean (*Glycine max*) with the characterization of a gene cluster comprising five genes that encode a group of auxin regulated RNAs (McClure *et al.*, 1989). Three of those genes are transcriptionally regulated by auxin. Besides that, the genes were spaced at intervals of about 1,25 kb in the genome and transcribed in alternate directions. *ZmEA1* and the predicted *SAUR* gene are located at about 1000 and 500 bp upstream of *ZmEAL1*, respectively. *ZmEA1* and the predicted *SAUR* gene are transcribed in opposite direction of *ZmEAL1*. The predicted *SAUR* gene located in the vicinity of *ZmEAL1* showed 71% of sequence identity with the ORF of *ZmSAUR1* (Yang and Poovaiah, 2000). Initially isolated from soybean (McClure and Guilfoyle, 1987), *SAUR* genes have also been characterized in mung bean (Yamamoto *et al.*, 1992), *Arabidopsis* (Gil *et al.*, 1994), apple (Watillon *et al.*, 1998), maize (Yang and Poovaiah, 2000; Knauss *et al.*, 2003) and rice (Jain *et al.*, 2006). Yang and Poovaiah (2000) described the existence of two additional *ZmSAUR1*-related gene loci in the maize genome. The exact function of SAUR proteins is still unknown, but CaM (calmodulin) was shown to bind to ZmSAUR1 (Yang and Poovaiah, 2000) and ZmSAUR2 (Knauss *et al.*, 2003) in a calcium-dependent manner.

Another indication that *ZmEAL1* might be induced by auxin is the finding that the promoter is active the first time at early stage FG5 with transcript distribution in a polar manner, with highest expression at micropylar end, less in the middle and almost no expression at the chalazal end of the embryo sac. Recently, an auxin gradient in the syncytial embryo sac (early stage FG5) with a concentration maximum at the micropilar end of the embryo sac was shown to play a key role in gametic cell specification in *Arabidopsis* (Pagnussat *et al.*, 2009). Additionally, down-regulation of *ARF*s or ectopic expression of the auxin biosynthesis gene *YUCCA1* alters gametophytic cell identity. Specifically, synergid cells adopt egg cell fate when *ARF*s are down-regulated in the embryo sac and ectopic expression of *YUCCA1* results in micropylar cells (egg cell and synergid cells) with abnormal polarities, misexpression of cell-specific marker genes, failure of antipodals cells to degenerate as well as unfused polar nuclei. In the same way, *ZmEAL1*-RNAi embryo sacs showed altered cell identity namely central cell-like

structures developed at the chalazal end of the embryo sac, where usually only antipodals cells are present.

Interestingly, during the first steps of embryo development, from 3 until 5 dap, ZmEAL1-eGFP-fusion protein expression was observed in all cells of the embryo proper, but the fusion protein was not observed in the suspensor. At 5 dap, when the embryos are in the globular stage, a group of cells placed in the center of the embryo proper showed higher expression of ZmEAL1-eGFP-fusion protein. However, at 6 and 7 dap, when the embryos are in the early and late transition stage, respectively, the protein is localized only at the embryonic protoderm and at the center of the adaxial face of the embryo proper. Forestan *et al.* (2010) observed similar patterns in auxin accumulation during maize embryo development. Embryos at the globular stage were characterized by high auxin accumulation at the top of the embryo proper, while low signal was detected in the suspensor. At early transition stage auxin maximum was evident in the protodermal layer. At late transition stage, auxin accumulation was still detectable in the protodermal layer and inner cells of the embryo proper. It has been reported earlier that the protoderm is the first evidence of differentiation in the maize embryo (Elster *et al.*, 2000) and that this differentiation is correlated with high auxin accumulation (Forestan *et al.,* 2010).

In conclusion, the presence of AuxRE in the *ZmEAL1* promoter, the similarities between *ZmEAL1* expression and auxin accumulation at early stage FG5 as well as the ZmEAL1-eGFP-fusion protein expression pattern and auxin accumulation during zygotic embryogenesis indicates that *ZmEAL1* might be activated by auxin representing the first apoplastic signal molecule mediating the auxin response, which is involved in cell differentiation during megagametogenesis and probably in early embryo development as well.

4.1   Outlook

The *ZmEAL1* gene encodes a small secreted protein involved in cell fate maintenance. The identification of the receptor of ZmEAL1 is relevant to understand the whole pathway in which it is involved. Co-IP (co-ImmunoPrecipitation) of proteins from cellular fractions was reported to be the most convincing evidence that two or more proteins interact *in vivo* (Monti *et al.*, 2005; Phee *et al.*, 2006; Ren *et al.*, 2003). Protein extract of the membrane fraction could be obtained from microdissected embryos of P_{ZmEAL1}:*ZmEAL1-eGFP* plants at 7 days after pollination. The clarified homogenate of this protein extract could be incubated with the GFP antibody

chemically cross-linked to protein G beads to perform immunoprecipitation. Chemical cross-linking of antibodies to protein G was reported to improve the efficiency of co-IP (Miernyk and Thelen, 2008). The immunoprecipitated sample would subsequently be subjected to MALDI-TOF mass spectrometry. Further validation of the identified receptor could be performed using FRET (Förster-Resonance-Energy-Transfer) or knockdown mutants to phenocopy the *eal1* phenotypes. Proteins acting downstream of ZmEAL1 could be identified through microarray analysis. To proceed so, ovules of *ZmEAL1*-RNAi, showing the phenotypes described before, could be microdissected and the transcriptome compared with that of wild type ovules. After the identification of candidate knockdown mutants, it should be verified whether *eal1* knockdown phenotypes are observed. In the same way, ZmEAL1 could be synthesized or expressed and purified using recombinant DNA techniques (*Escherichia coli* or *Pichia pastoris*). ZmEAL1 could then be used for *in vitro* studies. One possibility would be the application of the protein on BMS suspension cells and observation of possible phenotypes. Once again, transcriptome analysis could be performed comparing BMS suspension cells before and after treatment with ZmEAL1.

Several conserved motifs were identified in the promoters of *ZmEAL1*, *ZmEA1* and other egg cell expressed genes. Promoter deletion studies could be performed to proof whether the sequences are necessary to activate transcription in the egg cell.

Finally, there are evidences that *ZmEAL1* is activated by auxin. To determine whether this theory is true $P_{ZmEAL1}:eGFP$ plants could be treated with NPA (N-1-Naphthylphthalamic Acid), an inhibitor of auxin transport, via daily watering for two weeks starting from the tasseling stage as described previously (Wu and McSteen, 2007). Subsequently, $P_{ZmEAL1}:eGFP$ embryos could be scanned to determine whether eGFP signal is reduced after NPA treatment. Forestan *et al*. (2010) reported recently altered auxin accumulation patterns in the embryo by the use of NPA treatment according to Wu and McSteen (2007).

5   Summary

In plants, haploid spores divide mitotically to generate multicellular gametophytes. The development of the female gametophyte of most flowering plants follows a well defined pattern. Extensive studies were carried out to unravel the molecular mechanisms underlying megagametogenesis. However, the means by which cell-cell communication contributes to female gametophyte development are poorly understood. The aim of the present study was to identify the function of a small peptide, which was predicted to be secreted from the egg cell. This small peptide was identified through the analysis of a maize egg cell cDNA library (Dresselhaus *et al.*, 1994) as one of the most abundant transcript in the egg cell. The protein was named ZmEAL1 (Zea mays EA1 Like1) due to the presence of an EA1-box (Márton *et al.*, 2005). The ZmEAL1 precursor consists of 74 amino acids containing a signal peptide that compromises 26 amino acids resulting in a mature protein of 48 amino acids. Subcellular location of a ZmEAL1-eGFP-fusion protein in BMS suspension cells revealed protein localization to the endoplasmic reticulum surrounding the nucleus and in transvacuolar strands mainly within small vesicles. After plasmolysis ZmEAL1-eGFP-fusion protein was detected in the cell wall of these cells. Maize was stably transformed with a ZmEAL1-eGFP-fusion protein construct to study protein localization in the female gametophyte under the endogenous promoter. ZmEAL1-eGFP-fusion protein was detected exclusively in the egg cell as soon as cellularization took place. After fertilization the expression of ZmEAL1-eGFP-fusion decreases in zygotes, with additional decline of expression in the apical and basal cells. Between 3 and 7 days after pollination the eGFP signal increased again with localization of ZmEAL1-eGFP-fusion protein restricted to the embryo proper. Transgenic maize plants were stably transformed with an eGFP marker construct to study *ZmEAL1* promoter activity. eGFP signal were first detected at early stage FG5. Promoter activity detected with eGFP and expression of ZmEAL1-eGFP-fusion protein correlate from the mature embryo sac stage until two days after pollination when the two-celled proembryo is formed. In contrast to the fusion protein eGFP expression alone was detected in suspensor cells from the two-celled proembryo until late transition stage and eGFP signal were observed in all cells of the embryo proper. At 8 days after pollination, neither eGFP alone nor ZmEAL1-eGFP-fusion protein was detected anymore. Promoter activity in vegetative tissues was never detected.

Functional analysis of ZmEAL1 was performed through the analysis of *ZmEAL1*-RNAi ears. The female gametophyte developed normally before cellularization. Conversely, at late stage FG7 the development of central cell-like structures was observed at the chalazal end of the embryo sac at the position of antipodals cells in wild type gametophytes. The central cell showed the presence of additional polar nuclei varying from one to three additional nuclei in comparison with normal wild type embryo sacs. The ZmEAL1 peptide secreted from the egg cell is probably responsible to control cell cycle and/or to maintain cell identity in the central cell. Moreover, the development of central cell-like structures in detriment of antipodals cells might be due to the incapacity of the immature central cell to repress the development of antipodals into gametic cells, according to the "lateral inhibition model". Finally, degeneration of the whole embryo sac was as well observed. The fertilization process seemed not affected in *ZmEAL1*-RNAi ears. However, at low frequency seeds were aborted shortly after fertilization. The function of ZmEAL1 after fertilization during zygotic embryogenesis remains to be determined.

6   References

Acosta-García G, Vielle Calzada J-P (2004) A classical arabinogalactan protein is essential for the initiation of female gametogenesis in *Arabidopsis. Plant Cell* 16, 2614-2628.

Amien S, Kliwer I, Márton ML, Debener T, Geiger D et al. (2010) Defensin-like ZmES4 mediates pollen tube burst in maize via opening of the potassium channel KZM1. *PLoS Biol.* 8, e1000388.

Bailey TL, Elkan C (1994) Fitting a mixture model by expectation maximization to discover motifs in biopolymers. *Proceedings of the Second International Conference on Intelligent Systems for Molecular Biology*. California:AAAI Press, 28-36.

Becker D, Brettschneider R, Lörz H (1994) Fertile transgenic wheat from microprojectile bombardment of scutellar tissue. *Plant J.* 5, 299-307.

Bedinger PA, Fowler JE (2009) The maize male gametophyte. In: Bennetzen JL, Hake SC (eds.) *Handbook of maize: its biology*. NY: Springer Science and Business Media, 57-78.

Bemer M, Wolters-Arts M, Grossniklaus U, Angenent GC (2008) The MADS domain protein DIANA acts together with AGAMOUS-LIKE80 to specify the central cell in *Arabidopsis* ovules. *Plant Cell* 20, 2088-2101.

Brettschneider R, Becker D, Lörz H (1997) Efficient transformation of scutellar tissue of immature maize embryos. *Theor. and Appl. Genet.* 94, 737-748.

Capron A, Serralbo O, Fulop K, Frugier F, Parmentier Y et al. (2003) The *Arabidopsis* anaphase-promoting complex or cyclosome: molecular and genetic characterization of the APC2 subunit. *Plant Cell* 15, 2370-2382.

Capron A, Gourgues M, Neiva LS, Faure JE, Berger F et al. (2008) Maternal control of male-gamete delivery in *Arabidopsis* involves a putative GPI-anchored protein encoded by the *LORELEI* gene. *Plant Cell* 20, 3038-3049.

Christensen CA, King EJ, Jordan JR, Drews GN (1997) Megagametogenesis in *Arabidopsis* wild type and the Gf mutant. *Sex. Plant Reprod.* 10, 49-64.

Christensen CA, Gorsich SW, Brown RH, Jones LG, Brown J et al. (2002) Mitochondrial GFA2 is required for synergid cell death in *Arabidopsis. Plant Cell* 14, 2215-2232.

Colombo M, Masiero S, Vanzulli S, Lardelli P, Kater MM et al. (2008) *AGL23*, a type I MADS-box gene that controls female gametophyte and embryo development in *Arabidopsis. Plant J.* 54, 1037-1048.

Cordts S (2000) Isolierung und Charakterisierung von Genen, die in der Eizelle von Mais (*Zea mays* L.) spezifisch hochreguliert sind. *Dissertation*, Universität Hamburg, Shaker Verlag, Aachen, ISBN 3-8265-7139-8.

D'Halluin K, Bonne E, Bossut M, De Beuckeleer M, Leemans J (1992) Transgenic maize plants by tissue electroporation. *Plant Cell* 4, 1495-1505.

Diboll A, Larson D (1966) An electron microscopic study of the mature megagametophyte in *Zea mays. Am. J. Bot.* 53, 391-402.

Dresselhaus T, Lörz H, Kranz E (1994) Representative cDNA libraries from few plant cells. *Plant J.* 5, 605-610.

Dresselhaus T (2006) Cell–cell communication during double fertilization. *Curr. Opin. Plant Biol.* 9, 41-47.

Ebel C, Mariconti L, Gruissem W (2004) Plant retinoblastoma homologues control nuclear proliferation in the female gametophyte. *Nature* 429, 776-780.

Elster R, Bommert P, Sheridan WF, Werr W (2000) Analysis of four embryo specific mutants in *Zea mays* reveals that incomplete radial organization of the proembryo interferes with subsequent development. *Dev. Genes Evol.* 210, 300-310.

Escobar-Restrepo JM, Huck N, Kessler S, Gagliardini V, Gheyselinck J et al. (2007) The FERONIA receptor-like kinase mediates male-female interactions during pollen tube reception. *Science* 317, 656-660.

Evans MMS (2007) The *indeterminate gametophyte1* gene of maize encodes a LOB domain protein required for embryo sac and leaf development. *Plant Cell* 19, 46-62.

Evans MMS, Grossniklaus U (2009) The maize megagametophyte. In: Bennetzen J, Hake S (eds) *Handbook of maize: its biology*. NY: Springer Science and Business Media, 79-104.

Forestan C, Meda S, Varotto S (2010) ZmPIN1-mediated auxin transport is related to cellular differentiation during maize embryogenesis and endosperm development. *Plant Physiol.* 152, 1373-1390.

Gallois JL, Guyon-Debast A, L´ecureuil A, Vezon D, Carpentier V et al. (2009) The *Arabidopsis* proteasome RPT5 subunits are essential for gametophyte development and show accession-dependent redundancy. *Plant Cell* 21, 442-459.

Gil P, Liu Y, Orbovic V, Verkamp E, Poff KL, Green PJ (1994) Characterization of the auxin-inducible *SAUR-AC1* gene for use as a molecular genetic tool in *Arabidopsis*. *Plant Physiol.* 104, 777-784.

Groß-Hardt R, Kägi C, Baumann N, Moore JM, Baskar R et al. (2007) *LACHESIS* restricts gametic cell fate in the female gametophyte of *Arabidopsis*. *PLoS Biol.* 5, 494-500.

Guignard L (1899) Sur les anthérozoïdes et la double copulation sexuelle chez les végé taux angiospermes. *Rev. Gén. Bot.* 11, 129-135.

Guilfoyle TJ (1999) Auxin-regulated genes and promoters. In: Hooykaas PJJ, Hall M, Libbenga KL (eds) *Biochemistry and Molecular Biology of Plant Hormones*. Leiden: Elsevier, 423-459.

Hagen G, and Guilfoyle T (2001) Auxin-responsive gene expression: genes, promoters, and regulatory factors. *Plant Mol. Biol.* 15, 1985-1997.

Han Y-Z, Huang B-Q, Zee S-Y, Yuan M (2000) Symplastic communication between the central cell and the egg apparatus cells in the embryo sac of *Torenia fournieri* Lind. before and during fertilization. *Planta* 211, 158-162.

Higashiyama T, Yabe S, Sasaki N, Nishimura Y, Miyagishima S-y et al. (2001) Pollen tube attraction by the synergid cell. *Science* 293, 1480-1483.

Higashiyama, T (2002) The synergid cell: attractor and acceptor of the pollen tube for double fertilization. *J. Plant Res.* 115, 149-160.

Huang B-Q, Russel SD (1992) Female germ unit: organization, isolation and function. *Int. Rev. Cytol.* 140, 233-292.

Huang B-Q, Fu Y, Zee S Y, Hepler P K (1999) Three-dimensional organization and dynamic changes of the actin cytoskeleton in embryo sacs of *Zea mays* and *Torenia fournieri. Protoplasma* 209, 105-119.

Hughes TA (2006) Regulation of gene expression by alternative untranslated regions. *Trends in Genetics* 22, 119-122.

Jain M, Tyagi AK, Khurana JP (2006) Genome-wide analysis, evolutionary expansion, and expression of early auxin-responsive *SAUR* gene family in rice (*Oryza sativa*). *Genomics* 88, 360-371.

Jefferson RA, Kavanagh TA, Bevan MW (1987) GUS fusions: β-glucuronidase as a sensitive and versatile gene fusion marker in higher plants. *EMBO J.* 6, 3901-3907.

Jensen, WA (1964) Observations on the fusion of nuclei in plants. *J. Cell Biol.* 23**,** 669-672.

Johnston AJ, Matveeva E, Kirioukhova O, Grossniklaus U, Gruissem W (2008) A dynamic reciprocal RBR-PRC2 regulatory circuit controls *Arabidopsis* gametophyte development. *Curr. Biol.* 18, 1680-1686.

Joshi, CP (1987) An inspection of the domain between the putative TATA box and translation start site in 79 plant genes. *Nucl. Acids Res.* 15, 6643-6653.

Kägi C, Groß-Hardt R (2007) How females become complex: cell differentiation in the gametophyte. *Curr. Opin. Plant Biol.* 10, 633-638.

Kasahara RD, Portereiko MF, Sandaklie-Nikolova L, Rabiger DS, Drews GN (2005) MYB98 is required for pollen tube guidance and synergid cell differentiation in *Arabidopsis*. *Plant Cell* 17, 2981-2992.

Kasten FH (1981) Kasten's fluorescent Feulgen method for DNA. In Clark G (ed): *Staining Procedures*. Baltimore: Williams and Wilkins, 59-61.

Knauss S, Rohrmeier T, Lehle L (2003) The auxin-induced maize gene *ZmSAUR2* encodes a short-lived nuclear protein expressed in elongating tissues. *J. Biol. Chem.* 278, 23936-23943.

Krautwig B, Lörz H (1995) Single androgenetic structures of maize *(Zea mavs L.)* for the initiation of homogeneous cell suspension and protoplast cultures. *Plant Cell Rep.* 14, 477-481.

Kranz E, Bautor J, Lörz H (1991) *In vitro* fertilization of single, isolated gametes of maize mediated by electrofusion. *Sex. Plant Reprod.* 4, 12-16.

Kwee HS, Sundaresan V (2003) The *NOMEGA* gene required for female gametophyte development encodes the putative APC6/CDC16 component of the Anaphase Promoting Complex in *Arabidopsis*. *Plant J.* 36, 853-866.

Lescot M, Déhais P, Moreau Y, De Moor B, Rouzé P, Rombauts S (2002) PlantCARE: a database of plant *cis*-acting regulatory elements and a portal to tools for *in silico* analysis of promoter sequences. *Nucleic Acids Res.*, Database issue, 30, 325-327.

Lin BY (1984) Ploidy barrier to endosperm development in maize. *Genetics* 107, 103-115.

Logemann J, Schell J, Willmitzer L (1987) Improved method for the isolation of RNA from plant tissues. *Anal Biochem.* 163, 16-20.

Luo M, Bilodeau P, Koltunow A, Dennis ES, Peacock WJ, Chaudhury AM (1999) Genes controlling fertilization-independent seed development in *Arabidopsis thaliana. Proc. Natl. Acad. Sci. USA* 96, 296-301.

Maeda E, Miyake H (1997) Ultratructure of antipodal cells of rice (*Oryza sativa*) before anthesis with special reference to concentric configuration of endoplasmic reticula. *J. Crop Sci.* 66, 488-496.

Márton ML, Cordts S, Broadhvest J, Dresselhaus T (2005) Micropylar pollen tube guidance by Egg Apparatus 1 of maize. *Science* 307, 573-576.

McClure BA, Guilfoyle TJ (1987) Characterization of a class of small auxin-inducible soybean polyadenylated RNAs. *Plant Mol. Biol.* 9, 611-623.

McClure BA, Hagen G, Brown CS, Gee MA, Guilfoyle TJ (1989) Transcription, organization, and sequence of an auxin-regulated gene cluster in soybean. *Plant Cell* 1, 229-239.

Miernyk JA, Thelen JJ (2008) Biochemical approaches for discovering protein-protein interactions. *Plant J.* 53, 597-609.

Moll C, von Lyncker L, Zimmermann S, Kägi C, Baumann N et al. (2008) CLO/GFA1 and ATO are novel regulators of gametic cell fate in plants. *Plant J.* 56, 913-921.

Monti M, Orru S, Pagnozzi D, Pucci P (2005) Interaction proteomics. *Biosci. Rep.* 25, 45-56.

Moretti S, Armougom F, Wallace IM, Higgins DG, Jongeneel CV, Notredame C (2007) The M-Coffee web server: a meta-method for computing multiple sequence alignments by combining alternative alignment methods. *Nucl. Acids Res.* 35, 645-648.

Murashige T, Skoog F (1962) A revised medium for rapid growth and bioassays with tobacco tissue cultures. *Physiol. Plant* 15, 473-497.

Nicholas KB, Nicholas HB Jr., Deerfield, DWII (1997) GeneDoc: analysis and visualization of genetic variation. *Embnew News* 4, 14.

Nawaschin S (1898) Resultate einer Revision der Befruchtungsvorgänge bei *Lilium martagon* und *Fritillaria tenella*. *Bull Acad. Imp. Sci. St Pétersbourg* 9, 377-382.

Niewiadomski P, Knappe S, Geimer S, Fischer K, Schulz B et al. (2005) The *Arabidopsis* plastidic glucose 6-phosphate/phosphate translocator GPT1 is essential for pollen maturation and embryo sac development. *Plant Cell* 17, 760-775.

Nonomura K, Miyoshi K, Eiguchi M, Suzuki T, Miyao A et al. (2003) The *MSP1* gene is necessary to restrict the number of cells entering into male and female sporogenesis and to initiate anther wall formation in rice. *Plant Cell* 15, 1728-1739.

Nonomura KI, Morohoshi A, Nakano M, Elguchi M, Mlyao A et al. (2007) A germ cell-specific gene of the ARGONAUTE family is essential for the progression of pre-meiotic mitosis and meiosis during sporogenesis in rice. *Plant Cell* 19, 2583-2594.

Okuda S, Tsutsui H, Shiina K, Sprunck S, Takeuchi H et al. (2009) Defensin-like polypeptide LUREs are pollen tube attractants secreted from synergid cells. *Nature* 458, 357-361.

Pagnussat GC, Yu HJ, Sundaresan V (2007) Cell-fate switch of synergid to egg cell in *Arabidopsis eostre* mutant embryo sacs arises from misexpression of the *BEL1-Like Homeodomain* gene *BLH1*. *Plant Cell* 19, 3578-3592.

Pagnussat GC, Alandete-Saez M, Bowman JL, Sundaresan V (2009) Auxin-dependent patterning and gamete specification in the *Arabidopsis* female gametophyte. *Science* 324, 1684-1689.

Pallotta MA, Graham GC, Langridge P, Sparrow DHB, Barker SJ (2000) RFLP mapping of manganese efficiency in barley. *Theor. Appl. Genet.* 101, 1100-1108.

Pang SZ, DeBoer D, Wan Y, Ye C, Layton JC, Neher MK, Armstrong C (1996) An improved green fluorescent protein gene as a vital marker in plants. *Plant Physiol.* 112, 893-900.

Pastuglia M, Azimzadeh J, Goussot M, Camilleri C, Belcram K et al. (2006). γ-Tubulin is essential for microtubule organization and development in *Arabidopsis*. *Plant Cell* 18, 1412-1425.

Pawlowskia PW, Wang CJR, Golubovskaya IN, Szymaniaka JM, Shi L et al. (2009) Maize *AMEIOTIC1* is essential for multiple early meiotic processes and likely required for the initiation of meiosis. *Proc. Natl. Acad. Sci. USA* 106, 3603-3608.

Perez-Perez JM, Serralbo O, Vanstraelen M, Gonzalez C, Criqui MC et al. (2008) Specialization of CDC27 function in the *Arabidopsis thaliana* anaphase-promoting complex (APC/C). *Plant J.* 53, 78-89.

Phee BK, Shin DH, Cho JH, Kin SH, Kim JI et al. (2006) Identification of phytochrome-interacting protein candidates in *Arabidopsis thaliana* by co-immunoprecipitation coupled with MALDI-TOF MS. *Proteomics* 6, 3671-3680.

Portereiko MF, Lloyd A, Steffen JG, Punwani JA, Otsuga D et al. (2006) AGL80 is required for central cell and endosperm development in *Arabidopsis*. *Plant Cell* 18, 1862-1872.

Priest HD, Filichkin SA, Mockler TC (2009) *cis*-Regulatory elements in plant cell signaling. *Curr. Opin. Plant Biol.* 12, 643-649.

Punwani JA, Rabiger DS, Drews GN (2007) MYB98 positively regulates a battery of synergid-expressed genes encoding filiform apparatus–localized proteins. *Plant Cell* 19, 2557-2568.

Quayle TJA, Hetz W, Feix G (1991) Characterization of a maize endosperm culture expressing zein genes and its use in transient transformation assays. *Plant Cell Rep.* 9, 544-548.

Randolph LF (1936) Developmental morphology of the cariopsis in maize. *J. Ag. Res.* 53, 881-916.

Ravi M, Marimuthu MPA, Siddiqi I (2008) Gamete formation without meiosis in *Arabidopsis*. *Nature* 451, 1121-1124.

Ren L, Emery D, Kaboord B, Chang E, Qoronfleh MW (2003) Improved immunomatrix methods to detect protein–protein interactions. *J. Biochem. Biophys. Methods* 57, 143-157.

Richert J, Kranz E, Lörz H, Dresselhaus T (1996) A reverse transcriptase polymerase chain reaction assay for gene expression studies at the single cell level. *Plant Sci.* 114, 93-99.

Russell SD (1979) Fine structure of megagametophyte development in *Zea mays*. *Can. J. Bot.* 57, 1093-1110.

Sheridan WF, Avalkina NA, Shamrov II, Batygina TB, Golubovskaya IN (1996) The *mac1* gene: controlling the commiment to the meiotic pathway in maize. *Genetics* 142, 1009-1020.

Shimizu KK, Ito T, Ishiguro S, Okada K (2008) *MAA3* (*MAGATAMA3*) helicase gene is required for female gametophyte development and pollen tube guidance in *Arabidopsis thaliana*. *Plant Cell Physiol.* 9, 1478-1483.

Shimizu KK, Okada K (2000) Attractive and repulsive interactions between female and male gametophytes in *Arabidopsis* pollen tube guidance. *Development* 127, 4511-4518.

Southern EM (1975) Detection of specific sequences among DNA fragments separation by gel electrophoresis. *J. Mol. Biol.* 98, 503-517.

Srilunchang K-o, Krohn NG, Dresselhaus T (2010) DiSUMO-like DSUL is required for nuclei positioning, cell specification and viability during female gametophyte maturation in maize. *Development* 137, 333-345.

Stirn S, Mordhorst AP, Fuchs S, Lörz H (1995) Molecular markers for embryogenic potential and regenerative capacity of barley *(Hordeum vulgare* L.) cell cultures. *Plant Sci.* 106, 195-206.

Ulmasov T, Hagen G, Guilfoyle TJ (1999) Activation and repression of transcription by auxin-response factors. *Proc. Natl. Acad. Sci. USA* 96, 5844-5849.

Ulmasov T, Murfett J, Hagen G, Guilfoyle TJ (1997) Aux/IAA proteins repress expression of reporter genes containing natural and highly active synthetic auxin response elements. *Plant Cell* 9, 1963-1971.

Vollbrecht E, Hake S (1995) Deficiency analysis of female gametogenesis in maize. *Dev. Genet.* 16, 44-63.

Walbot V, Evans MMS (2003) Unique features of the plant life cycle and their consequences. *Nature Rev. Genet.* 4, 369-379.

Watillon B, Kettmann R, Arredouani A, Hecquet JF, Boxus P, Burny A (1998) Apple messenger RNAs related to bacterial lignostilbene dioxygenase and plant *SAUR* genes are preferentially expressed in flowers. *Plant Mol. Biol.* 36, 909-915.

Wu X, McSteen P (2007) The role of auxin transport during inflorescence development in maize (*Zea mays*, Poaceae). *Am. J. Bot.* 94, 1745-1755.

Yamamoto KT, Mori H, Imaseki H (1992) cDNA cloning of indole-3-acetic acid-regulated genes: *Aux22* and *SAUR* from mung bean *(Vigna radiata)* hypocotyl tissue. *Plant Cell Physiol.* 33, 93-97.

Yang WC, Shi DQ, Chen YH (2010) Female gametophyte development in flowering plants. *Ann. Rev. Plant Biol.* 61, 89-108.

Yang T, Poovaiah BW (2000) Molecular and biochemical evidence for the involvement of calcium/calmodulin in auxin action. *J. Biol. Chem.* 275, 3137-3143.

Young B, Sherwood RT, Bashaw EC (1979) Cleared-pistil and thick-sectioning techniques for detecting aposporous apomixis in grasses. *Can. J. Bot.* 57, 1668-1672.

DiSUMO-like DSUL is required for nuclei positioning, cell specification and viability during female gametophyte maturation in maize

1 Introduction

Reversible posttranslational modifications are widely used to dynamically regulate protein activity and degradation. Proteins can be modified by small chemical groups, sugars, lipids, and even by covalent attachment of other polypeptides. The highly conserved ubiquitin consisting of 76 amino acids is the best-known and studied example of a polypeptide modifier (Herrmann *et al.*, 2007). It was shown that conjugation of polyubiquitin chains (polyubiquitination) involving lysine residue K48 has a well-established role in marking proteins for degradation by a multi-enzyme complex called the 26S proteasome (Müller *et al.*, 2001). K29 and K63 polyubiquitination leads to endosome formation and modification of protein function. Monoubiquitination and multiubiquitination can also direct target proteins toward the endosome-lysosome pathway (Haglund and Stenmark, 2006).

After the discovery of ubiquitin, several related small proteins displaying structural similarity to ubiquitin have been reported (Gill, 2004; Herrmann *et al.*, 2007; Kirkin and Dikic, 2007). These small ubiquitin-like proteins (called UBLs) include small ubiquitin-like modifiers (SUMOs), related-to-ubiquitin-1 (RUB-1/NEDD-8), autophagy defective-8 (APG-8) and APG-12, homologous to ubiquitin-1 (HUB-1/UBL-5), ubiquitin-fold-modifier-1 (UFM-1), ubiqitin related modifier-1 (URM-1) and Fau ubiquitin-like protein-1 (FUB-1). Moreover, two UBLs containing two head-to-tail ubiquitin-like domains have been reported: interferon-stimulated gene-15 (ISG-15) and antigen–F-adjacent transcript-10 (FAT-10). Human SUMO-1-3 (corresponding to yeast SMT3C, B and A, respectively) have been studied most intensively (Kirkin and Dikic, 2007).

SUMOs, which were first described in 1996, constitute a highly conserved protein family found in all eukaryotes (Johnson, 2004). Although SUMO shares only about 18% sequence identity to ubiquitin, the protein structure is quite similar (Gill, 2004). SUMO and ubiquitin share the overall mechanistic principles of substrate

selection and attachment, including a flexible carboxy (C) terminus, which is generally a glycine residue that forms an isopeptide linkage to a lysine side chain within the target protein (Schwartz and Hochstrasser, 2003). The most prominent difference between members of the SUMO family and other ubiquitin-related proteins (including ubiquitin) is a very flexible N-terminal extension and an extension of amino acids at the C-terminus in SUMO (Melchior, 2000). The C-terminus is processed by limited proteolysis to expose a C-terminal glycine residue for target linkage (Kerscher, 2007). While yeast and invertebrates studied to date contain a single *SUMO* gene, vertebrates contain four genes (*SUMO-1-4*) and plants even more. For example, eight *SUMO* genes are found in the *Arabidopsis thaliana* genome (Saracco *et al*., 2007). Human SUMO-2 and SUMO-3 polypeptides are ~96% identical to each other (and are referred to collectively as SUMO-2/-3), whereas they share only ~45% identity with SUMO-1 (Zhang *et al*., 2008). Interestingly, while human SUMO-1 is apparently unable of self-conjugation, SUMO-2/-3 can lead to chain formation (Tatham *et al*., 2001; Ulrich, 2008)

The reversible attachment of SUMO to their target proteins (SUMOylation) proceeds in analogy to ubiquitin. In an initial ATP-dependent process, SUMO forms a thioester bond with the heterodimeric SUMO-activating enzyme (SAE) (Desterro *et al*., 1999). The activated SUMO moiety is subsequently passed to SUMO-conjugating enzyme (SCE), which acts in concert with E3 ligases to attach SUMO to its targets through an isopeptide bond. In contrast to ubiquitin, the SUMO system utilizes only a single E2 enzyme, UBC-9 (ubiquitin-conjugating Enzyme 9), and probably fewer E3 ligases (Anckar and Sistonen, 2007). Moreover, Ubc-9 can recognize the substrate itself and directly transfers activated SUMO by the formation of an isopeptide bond between the C-terminal carboxyl group of SUMO and the ε-amino group of lysine in substrate proteins (Welchman *et al*., 2005). DeSUMOylation is catalyzed by cysteine proteases, called ubiquitin-like-protein-specific protease-1 and -2 (Ulp-1 and Ulp-2) in yeast as well as sentrin/SUMO-specific proteases (SENP) in human. While SENP-1 and -2 are able to process all three SUMOylating isoforms without distinction, SENP-3 and SENP-5 display a preference for SUMO-2/-3. Interestingly, all of these proteases are located at distinct subcellular localizations matching the function of their substrates: SENP-1 localizes to the nucleus, SENP-3 and SENP-5 to the nucleolus and SENP-2 to the cytoplasm, nuclear pore or nuclear body (for review Herrmann *et al*., 2007).

Compared to ubiquitin, SUMO has much fewer cellular substrates but, intriguingly, several indentified targets turned out to be important cellular and especially transcriptional regulators (Geiss-Friedlander and Melchior, 2007; Gill, 2004; Müller *et al*., 2001; Vertegaal *et al*., 2006). Lately, it has become clear that SUMOylation is involved in surprisingly diverse biological pathways, such as genome integrity, chromosome packing and dynamics, transcriptional regulation, nucleocytoplasmic translocalization and various aspects of signal transduction acting *via* modulation of protein–protein interactions as well as protein–DNA binding (Hay, 2005). Through biochemical and proteomic approaches over 200 proteins have been identified as SUMO substrates (Vertegaal *et al.*, 2006; Zhang *et al*., 2008), implicating SUMOylation as a post-translational modification mechanism of a wide range of cellular and developmental functions, predominately associated with the nucleus (Seeler and Dejean, 2003). Genetic studies identified roles for SUMOylation in regulating chromosome condensation and segregation via sister chromatid cohesion, kinetochore function as well as mitotic spindle elongation and progression through mitosis (Watts, 2007).

The proper function of these processes is a major prerequisite for cell specification and fate determination during development of higher eukaryotes. In order to understand the underlying molecular mechanisms of cell polarity establishment and cell identity in flowering plants (angiosperms), we are studying the development of the haploid female gametophyte, or embryo sac, as a model. After meiosis, development of the angiosperm embryo sac begins with a phase of free nuclear division to produce an eight-nuclei coecytium during a process called megagametogenesis. During this process, embryo sac nuclei undergo a stereotypical number of mitotic divisions. Migration and asymmetric positioning of nuclei is highly regular. The embryo sac then cellularizes and differentiates to produce four cell types: an egg cell, usually two synergids, a homodiploid central cell and, depending on the plant species, up to around 40 antipodals (Brukhin *et al*., 2005; Drews and Yadegari, 2002). Embryo sac development thus provides an ideal system to study fundamental cellular processes such as asymmetric nuclei position and migration as well as position dependent cell fate determination. As SUMOylation plays a prevalent role in functions associated with the mitotic nucleus, we searched maize and wheat egg cell EST data (Márton *et al*., 2005; Sprunck *et al*., 2005) for transcripts encoding SUMO and SUMO related proteins for further functional studies during female gametophyte development. Here, we report the

identification of ubiquitously expressed *SUMO* genes and of a diSUMO-like (DSUL) protein gene displaying a highly specific expression pattern during embryo sac development and early embryogenesis in maize. Unlike FAT10 and ISG15 that contain two UBL domains, DSUL contains two head-to-tail SUMO-like domains thus represents the first protein displaying such a protein structure. We further analysed DSUL phylogeny, processing, subcellular localization, expression pattern as well as its role during female gametophyte development.

2   Material and Methods

2.1   EST sequencing and bioinformatic analyses

988 EST sequences derived from a cDNA library of maize egg cells (Dresselhaus *et al.*, 1994) were clustered and analyzed for the presence of transcripts encoding SUMO/SMT3 proteins. ZmSUMO1a (GenBank accession # FJ515939), ZmSUMO1b (GenBank accession # FJ515940) and ZmDSUL (GenBank accession # FJ515941) sequences were compared online and aligned by ClustalW (Thompson *et al.*, 1994). Alignment data were used to generate a phylogram (Figure 2) with Treeview (version 1.6.6; Page, 1996). Protein alignments were drawn by GeneDoc, version 2.6.02 (Nicholas *et al.*, 1997), using ClustalW alignment data. Prediction of 3-dimensional protein structures was performed using HHpred (http://toolkit.tuebingen.mpg.de/hhpred) based on PDB 1Z2M structural data. Based on hits to known protein structures from HsISG15, the structure of ZmDSUL was modeled by using Accelrys discovery studio 1.7.

2.2   Plant growth, isolation of cells from the female gametophyte and *in vitro* suspension culture

Maize (*Zea mays*) inbred lines A188 (Green and Phillips, 1975) and H99 (D'Halluin *et al.*, 1992) and transgenic lines were grown under standard greenhouse conditions at 26ºC with 16 h light and a relative air humidity of about 60%. Cells of the maize embryo sac before fertilization were isolated according to Kranz *et al.* (1991) and after fertilization according to Cordts *et al.* (2001) with the exception that ears were kept on wet paper instead of MS medium. Tobacco (*Nicotiana benthamiana*) plants were grown at 22ºC with 16 h light and at 18ºC in the dark with a relative air humidity of about 70%. Black Mexican Sweet (BMS) maize cells were cultivated in MS (Murashige and Skoog, 1962) medium containing 2 mg/l 2,4D. Stock cultures on solid and suspension cultures in liquid MS medium were maintained in the dark at 26ºC on a shaker at 60-70 rpm and sub-cultured into fresh medium every 3 weeks and 4 days, respectively.

2.3   DNA and RNA extraction, Southern blots and SC RT-PCR

Extraction of genomic DNA from plant tissues was performed according to Pallotta *et al.* (2000). Total RNA was extracted from all samples with TRIzol® reagent (Invitrogen) according to the manufacturer's specifications. Before RT-PCR, 1 μg of total RNA was digested with DNaseI (DNaseI amp grade, Invitrogen) and used for first-

strand cDNA synthesis using Oligo (dT)$_{18}$ (MBI Fermentas) and reverse transcriptase (RevertAid^{TM} M-MuLV Reverse Transcriptase, MBI Fermentas) following the manufacturer's protocol. Quality and amount of generated cDNAs was analyzed by PCR using maize *GAPDH* (*Glyceraldehyde 3-phosphate dehydrogenase*)-specific primers ZmGap1 (5'-AGGGTGGTGCCAAGAAGGTTG-3') and ZmGap2 (5'-GTAGCCCCACTCGTTGTCGTA-3'). For detection of transgenic plants, mRNA from plant leaves was isolated using Dynabead$^{®}$ oligo (dT)$_{25}$ (Invitrogen) following the manufacturer's guidelines. cDNA was generated as described above.

For Southern blot analysis, genomic DNA (gDNA) was digested with *Bsp*TI and *Not*I. This enzyme combination cuts out the full-length *ZmDSUL* cDNA from the pZmDSUL-RNAi vector described below. Restricted DNA was separated in 1% agarose gels and transferred with 20xSSC onto Hybond-XL membranes (GE Healthcare). DNA was cross-linked to membranes with 300 mJ radiation in a UV Stratalinker 1800 (Stratagene). Hybridization, washing and exposure were performed according to the procedure described for DNA gel blots according to the specifications of the manufacturer (Roche).

Single cell RT-PCR analysis (SC RT-PCR) was performed as described by Cordts *et al.* (2001) with minor modifications: SC reverse transcription (RT) was performed using the primers ZmDSULRev (5'-GCTGCCATCAATGATGGAGCAG-3'), ZmSUMO1aRev (5'-GTCCCTCAGCAATGGCACAAG-3') or ZmSUMO1bRev (5'-CAAGGAGCCAGAGCATCACAAG-3') in addition to ZmGap2 (5'-GTAGCCCCACTCGTTGTCGTA-3') for cDNA synthesis. After RT, each reaction was split into two reaction tubes and 38 PCR cycles were conducted with each reaction using *ZmDSUL*-specific primers ZmDSULFor (5'- CGATCAGGCTTCAGGCATGGC-3') and ZmDSULRev, *ZmSUMO1a*-specific primers ZmSUMO1aFor (5'-CGCCCGGAAACTGACCTCTACC-3') and ZmSUMO1aRev, *ZmSUMO1b*-specific primers ZmSUMO1bfor (5'-ATCGATCGCCGGAAAACTAACC-3') and ZmSUMO1bRev as well as *GAPDH*-specific primers ZmGap1 (5'-AGGGTGGTGCCAAGAAGGTTG-3') and ZmGap2. Twenty-five micro liters of the *ZmDSUL, ZmSUMO1a* and *ZmSUMO1b* as well as 15 µl of the *GAPDH* PCR products were each separated in 1% agarose gels. The size of the amplified *ZmDSUL* transcript was 753 bp, 440 bp for the *ZmSUMO1a* transcript, 415 for *ZmSUMO1b* and 622 bp for *GAPDH*. While maize *SUMO* and *DSUL* genes do not contain introns, *GAPDH* derived

genomic amplificates are approximately 1.2–1.3 kbp in size and were used as a control to visualize genomic DNA contaminations.

2.4   Generation of constructs, biolistic transformation and regeneration of transgenic maize plants

pZmDSUL-RNAi construct (*UBI*p::*ZmDSUL-AS*::*iF2intron*::*ZmDSUL*::*OCSt*): for this construct, the *ZmDSUL* cDNA was PCR amplified from vector pUbi-IF2-15 (DNA Cloning Service) using primers F15Eco (5'-CGCG<u>GAATTC</u>ACGATCAGGCTTCA) and R15Bam (5'-CAGT<u>GGATCC</u>GGTTCTCAATCGATGT) and cloned in anti-sense orientation into the *Bam*HI and *Eco*RI restriction sites of the vector *pUbi-ZmDSUL* (DNA Cloning Service). In a second cloning step, *ZmDSUL* cDNA was PCR amplified using the primers F15Bsr (5'-GCGGCC<u>TGTACA</u>CGATCAGGCTTCA) and R15Bss (5'-CAGT<u>GCGCGC</u>GGTTCTCAATCGATGT) from vector pUbi-IF2-15, and cloned in sense-orientation into the *Bsr*GI and *Bss*HII restriction sites of the vector pUbi-ZmDSUL, generating the pZmDSUL-RNAi construct.

pZmDSUL:ZmDSUL-GFP (*ZmDSULp*::*ZmDSUL-GFP*::*NOSt*) and *pZmDSUL:GFP* (*ZmDSULp*::*GFP*::*NOSt*) vectors: for the first construct, the open reading frame (ORF) of *ZmDSUL* together with 1566 bp upstream of the ORF were PCR-amplified from genomic DNA with primers 15Fgen (5'-CTCT<u>GCGGCCGC</u>TTTGCTCACAG-3') and 15Rgen (5'CC<u>GGATCC</u>AATAAAAATTATTAGCTGCC) containing *Not*I and *Bam*HI restriction sites, respectively, which were then used for cloning the fragment between the *Not*I and *Bam*HI restriction sites of the vector *pLNU-GFP-Neu* (DNA Cloning Service) to generate the *pZmDSUL:ZmDSUL-GFP* construct. For the shorter promoter construct, a PCR fragment was generated with the primers pZm15_fw-SpeI (5'-GCATACTAGTGCTTTGCTCACAGGTGATTCAG-3') and pZm15_rev-EcoRI (5'-CGATGAATTCGCCTGAAGCCTGATCGTCCTTC-3'). The PCR fragment was inserted in front of the *Nos* terminator in the plasmid *pNos-AM* (DNA Cloning Service) using *Spe*I and *Eco*RI. In order to generate a short version of the promoter the resulting plasmid was cut with the enzymes *Eco*RV and *Stu*I and religated, resulting in a shortened promoter of 511 bp upstream of the start codon. The GFP reporter cDNA was inserted in between the promoter and terminator resulting in the reporter construct.

pN-DSUL-GFP and *pC-DSUL-GFP* constructs (*35S*p:*GFP*::*ZmDSUL*::*35S*t and *35S*p::*ZmDSUL*::*GFP*::*35St*): for these constructs, the ORF of *ZmDSUL* DNA was

PCR-amplified from the plasmid *pZmDSUL-ZmDSUL-GFP* (see above) with modified primers ZmDSULgateFor (5'-<u>CACC</u>ATGGCGTCCCCTGGCCGG-3') and ZmDSULgateRev (5'-<u>GGATCC</u>ATAAAAATTATTAG-3') generating CACC and *Bam*HI restriction sites, respectively. PCR products were cloned using the pENTR™ Directional TOPO® cloning kit (Invitrogen). Entry clones were generated using the Gateway system (Gateway® LR Clonase™ II Enzyme Mix, Invitrogen) and the destination vectors pB7FWG2.0 for C-terminal GFP fusion to ZmDSUL and pB7WGF2.0 for N-terminal GFP fusion to ZmDSUL, respectively (Karimi *et al*., 2002). Plasmids were generally isolated with a plasmid mini prep kit (Avegene) and fully sequenced. 0,1 μg was generally used for transformation of *E. coli* cells or cells of *Agrobacterium tumefaciens* strain GV3101 (Holsters *et al*., 1980) according to standard procedures.

Biolistic transformation of BMS suspension cells was performed as follows: cells were grown at 26ºC in a dark chamber with 60-70 rpm shaking. Before transformation cells were sterile filtrated through a 500 μm metal net and then passed through a 100 μm pore sized nylon mesh to spread a uniform cell layer on solid MS medium. Before biolistic transformation, cells were incubated at 26ºC for 1 to 2 h. After transformation, plates were incubated overnight in the dark at 26ºC. Cells were transferred to fresh liquid medium and cultivated in darkness using a shaker (60-70 rpm) for at least 4 h before microscopic observations. Photos were taken immediately after a transfer of 100 μl of medium containing individual cells or cell clusters showing GFP fluorescence onto glass slides.

Transformation of immature maize embryos using biolistic particle bombardment was performed as follows: immature hybrid embryos of the maize inbred lines A188 and H99 were isolated 11 to 13 days after pollination (DAP). The constructs *pZmDSUL*-RNAi, *pZmDSUL:GFP* and *pZmDSUL:ZmDSUL-GFP* were each co-transformed with the vector *35S*p:*PAT* carrying the selectable marker PAT for glufosinate ammonium resistance (Becker *et al*., 1994). Particle bombardment, tissue culture, and selection of transgenic maize plants were performed according to Brettschneider *et al*. (1997).

2.5   Recombinant protein expression in *Nicotiana benthamiana*

To express recombinant ZmDSUL fusion proteins in *Nicotiana benthamiana, Agrobacterium tumefaciens* strain GV3101 was grown at 28ºC in LB medium with 40 μg·ml^{-1} gentamycin and 50 μg·ml^{-1} spectomycin to the stationary phase. Bacteria were

sedimented by centrifugation at 3500 xg for 15 min at room temperature and resuspended in infiltration buffer (10 mM $MgCl_2$, 10 mM MES-KOH pH 5,7 and 100 µM Acetosyringone). Cells were left in this medium for 2 h and then infiltrated into the abaxial air spaces of 2-4 week old *Nicotiana benthamiana* plants. The *Agrobacterium* cultures carrying ZmDSUL-fusion protein (N- and C-terminal GFP versions) and a p19 construct to suppress post-transcriptional gene silencing (PTGS) of the host silencing response and thus to increase transient gene expression (Voinnet *et al.*, 2000; 2003). These two constructs were brought to an optical density (OD_{600}) of a maximum of 1,0 to avoid toxicity.

For total protein extraction, 1 g of *N. benthamiana* leaves was each collected after 2 days infiltration. Leaf samples were grinded to powder by a Retsch homogenizer MM200 for 2 min at 30 Hz speed. 300-500 µl of protein extraction buffer [20 mM Tris-Cl pH 7,5, 150 mM NaCl, 1 mM EDTA, 10 mM DTT and 1 cocktail protease inhibitor tablet (per 10 mL of extraction buffer)] were added to the grinded sample. Samples were centrifuged at 48000 xg for 1 hour at 4ºC. Protein concentrations were determined by a standard Bradford assay (Bio-Rad). Thirty micrograms of the supernatant was then loaded onto a 12% SDS gel or stored at -20ºC for later analyses. Proteins were separated and transferred onto PVDF membranes (Millipore) by wet electro-blotting. For detection of GFP, a mouse IgG κ monoclonal GFP antibody (Roche) and an anti-mouse IgG-POD antibody conjugated to peroxidase (Roche) were used at 1:5000 dilutions for both antibodies. Signals were detected using an ECL detection kit (GE Healthcare).

2.6   Histological studies, GUS staining and GFP imaging

For phenotypical analysis of wild-type and *ZmDSUL*-RNAi embryo sacs, immature and mature cobs were harvested from green-house grown maize plants. Whole cobs were treated according to a fixing/clearing method using Kasten's fluorescent periodic acid-Schiff's reagent decscribed by Vollbrecht and Hake (1995). The phases for hydration and dehydration of ears was prolonged from 20 to 30 minutes in each step and ears were dissected after they were cleared with methyl salicylate (Young *et al.*, 1979). Samples were mounted in methyl salicylate on glass slides under a cover slip and analysed with a LSM 510-META confocal laser scanning microscopy (CLSM, Zeiss) with 488 nm excitation and a LP 505 filter.

GUS staining of maize ovaries at various stages of FG development was performed as follows: the various stages were dissected and incubated in GUS staining buffer according to Bantin *et al.* (2001) with the exception that the staining solution was

prepared in water. After 1-2 hours incubation at 37ºC, dissected ovules were washed in 100mM sodium phosphate buffer (pH 7,0) and placed on glass slide with a drop of Hoyer's clearing solution for 15-20 min before microscopy. GFP fluorescence from BMS suspension cells and embryo sacs of maize were monitored by CLSM with 488 nm excitation and a BP 505-550 filter for selective GFP visualization. Image capture and processing were done using the AxioCam HRc camera, the Zeiss LSM 510 META software, and the Zeiss LSM image browser version 3.5.0.359.

3   Results

3.1   *DSUL* encodes a diSUMO-like protein localized to nucleoplasm and cytoplasm

Previous studies from our and other labs indicated that post-translational protein modification by ubiquitination and SUMOylation might play a major role in gametophyte development in plants (for example Sprunck *et al.*, 2005; Borges *et al.*, 2008; Kim *et al.*, 2008; Liu *et al.*, 2008). To study the role of SUMO during female gametophyte development, we searched for transcripts encoding SUMO in an EST collection from maize egg cells (Dresselhaus *et al.*, 1994; Márton *et al.*, 2005). Among the 30 largest EST clusters, we identified three genes encoding proteins with homology to SUMO (Suppl. Tab. 1). A more detailed analysis (Fig. 1A and Fig. 2) comparing these proteins with highly conserved ubiquitin and SUMOs from man (HsUbi, 76 amino acids, and HsSUMO1-4 consisting of 95-103 amino acids) as well as *Arabidopsis* AtSUM1-6 (100-117 amino acids) revealed two highly similar proteins, called *Zea mays* SUMO1a/b (ZmSUMO1a and ZmSUMO1b; precursor lengths of 99 and 109 amino acids, respectively), homologous to *Arabidopsis* AtSUM1 and 2 (Fig. 2). Interestingly, the third protein contained two head-to-tail SUMO-like domains and was named *Zea mays* diSUMO-like (ZmDSUL). For alignments and phylogenetic investigations, the ZmDSUL sequence, consisting of 250 amino acids (aa), was split into two domains [ZmDSUL-N (126 aa) and ZmDSUL-C (124 aa)] after a putative di-glycine (GG) cleavage site typically found at the C-terminal end of all SUMO proteins. The GG motif for SUMOylation is boxed in red in Figure 1A. Until now, dimeric SUMO-like proteins have not been described. However, FAT10 and ISG15 (each 165 amino acids) contain two ubiquitin-like domains. As shown in Suppl. Tab. 1, the sequence homology of both domains in FAT10 and ISG15 is higher compared with ubiquitin (27/34% and 28/36%, respectively) than to SUMO (15/11% and 12/18%, respectively), while ZmDSUL shows a higher sequence homology to SUMO (25/22%) compared with ubiquitin (17/15%). Thus ZmDSUL represents the first dimeric SUMO-like protein. Another transcript for a diSUMO-like protein consisting of 204 aa was identified in a wheat egg cell EST collection (*Triticum aestivum* diSUMO-like: TaDSUL; Fig. 1A) (Sprunck *et al.*, 2005). Various plant genomes were then analyzed for the presence of DSUL encoding genes. While *Sorghum bicolour* contains a gene most similar to maize *DSUL,* two less related *DSUL* genes were identified in the rice genome (Fig. 2). Dicotyledonous plant species including *Arabidopsis thaliana*, poplar

or vine grape as well as the moss *Physcomitrella patens* do not contain *DSUL* genes indicating that it represents a Gramineae or monocot specific gene. Phylogenetic analyses showed that DSUL proteins form an own clade, while dimeric FAT10 and ISG15 form a clade with ubiquitin (Fig. 2). ZmSUMO1a and ZmSUMO1b cluster into the same group with Arabidopsis AtSUM1 and AtSUM2.

The common sites for ubiquitin polymerization at Lys 29 and Lys 63 are missing in SUMO and DSUL sequences, indicating that polymerization does not occur. The conserved Lys 48 residue found in ZmDSUL and SbDSUL is not present in wheat and rice DSUL. This indicates that also this site might not be involved in polymerization, although biochemical proof is missing. With the exception of OsDSUL2, DSUL proteins contain two conserved predicted di-glycine (GG) processing sites, one in the middle and the second at the C-terminal region of the protein. SUMO-specific proteases cleave after the GG site to expose these residues for activation and SUMOylation (Herrmann *et al*., 2007). The lack of this motif in OsDSUL2 may indicate that it represents a pseudogene, while OsDSUL1 is the active rice protein. 3D structure modeling of ZmDSUL (Fig. 1B, left) based on the X-ray crystal structure of HsISG15 (1Z2M; Narasimhan *et al*., 2005; Fig. 1B, middle) not only showed that the structure of ZmDSUL is highly conserved and strongly overlapping with HsISG16 (Fig. 1B, right), but also consists of two globular domains linked by a long stretch containing the predicted GG processing site in the middle of the protein as well as an exposed second GG site at the very C-terminus. In order to determine whether ZmDSUL is processed at either or both predicted cleavage sites, we fused GFP N- or C-terminally to ZmDSUL and transiently expressed the fusion proteins in tobacco leaves (*Nicotiana benthamiana*). Two days after infection, crude protein extracts were separated by SDS-PAGE and analyzed by immunoblotting using an anti-GFP antibody (Fig. 3A). Lack of processing should generate 54 kDa bands. Processing behind the central GG-site between both SUMO-like domains should give a 42 kDa band, and cleavage after the C-terminal GG-site should generate a 52 kDa band for the N-terminal and a 32 kDa band for the C-terminal GFP-fusions. A 31 kDa ER-GFP was used as a positive control for comparison. The N-terminal fusion showed a 52 kDa band and the C-terminal fusion a weak band at 32 kDa (Fig. 3A). Additionally, 34 kDa bands and a 31 kDa band for the N-terminal fusion were visible probably derived from degradation products. A 42 kDa band was never detected. We thus conclude that ZmDSUL is only processed at the C-terminus, but not in the middle of the protein thus generating a naturally occurring

diSUMO-like protein with an exposed di-glycine at the very C-terminus. The GFP degradation products always observed with both chimeric proteins suggests that maize DSUL might not possess a very long half-life in tobacco leaves.

We used the same constructs in order to study the sub-cellular localization of ZmDSUL in maize BMS (Black Mexican Sweet) suspension cells. As shown in Figure 3B-E, GFP signals from the N-terminal fusion protein were evenly distributed in the cytoplasm and nucleoplasm excluding the nucleolus. About one third of the cells showed a stronger accumulation inside the nucleus (Fig. 3B). Interestingly, when GFP was fused to the C-terminus of ZmDSUL, from where it is cut (Fig. 3A), fluorescence signals were exclusively detected polar at one cytoplasmic site of the nuclear surface, but neither in the nucleoplasm nor in the remainder of the cytoplasm (Fig. 3F-I). Similar protein localization and aggregation has been described previously for animal cells that accumulate unfolded or misfolded proteins at the pericentriolar region in immediate vicinity to the cell nucleus. This region was also shown to contain many proteasome complexes and was called aggresome in animal cells (Hatakeyama and Nakayama, 2003). Similar protein localization was neither observed when GFP was fused to the N-terminus of ZmDSUL nor in cells expressing very high amounts of free GFP. Free GFP always showed equal fluorescence in the cytoplasm and nucleus excluding the nucleolus (Fig. 3J and K).

A

B

Figure 1. Primary structure alignment of ubiquitin, diubiquitin-like, SUMO and DSUL proteins, and predicted 3-D structure of ZmDSUL. (**A**) Protein sequences encoded by human (Hs), Arabidopsis (At), wheat (Ta) and maize (Zm) *Ubi (ubiquitin)*, *SUMO* and *DSUL* genes were aligned using ClustalW and processed with GeneDoc. See Figure 2 for protein accession numbers. Letters in black blocks indicate identical amino acid residues/conserved substitutions, amino acid residues with more than 80% conservation are highlighted in dark grey, and those with more than 60% conservation are shown as light grey boxes. The dimeric SUMO-like proteins DSUL from maize and wheat as well as dimeric human ubiquitin-like FAT10 and ISG15 were split into an N-terminal and a C-terminal domain for alignment. Stars label Lys 29, Lys 48 and Lys 63 in HsUbi, which serve as common sites for ubiquitin polymerization. The predicted cleavage sites (arrow) exposing C-terminal glycine-glycine (GG in red boxes) residues to generate mature SUMO and DSUL proteins are indicated and the length of precursor proteins is given. The N-terminal polySUMOylation motif of HsSUMO-2/3 and HsSUMO-4 is boxed in blue. (**B**) Predicted 3-D structure of ZmDSUL (left) based on the NMR-structure of HsISG15 (middle; PDB IZ2M). N- and C-terminal ends of proteins are indicated. ZmDSUL (left) forms two globular domains that are connected by a linker containing a putative SUMO-cleavage site (blue GGs). Each domain consists of a β-sheet (light-blue) and two α-helices (red). Loops/turns are indicated in green. GGs at the C-terminus are in red. An overlay of ZmDSUL and HsISG15 3-D projections is shown at the right.

Figure 2. **Phylogenetic relationship of selected members of the ubiquitin (Ubi), diubiquitin-like (FAT10 and ISG15), SUMO and DSUL protein families.** Protein sequences were aligned by ClustalW and the unrooted tree was drawn by Tree-View. Branch lengths are proportional to phylogenetic distances and the scale bar represents 10% substitutions per site. Protein accession numbers at GenBank are as follows: *Zea mays* ZmSUMO1a (FJ515939), ZmSUMO1b (FJ515940), ZmDSUL (FJ515941), *Sorghum bicolor* SbDSUL (EER97428), *Triticum aestivum* TaDSUL (FJ515942), *Oryza sativa* OsDSUL1 (NP_001060074) and OsDSUL2 (EAZ04433), *Arabidopsis thaliana* AtSUM1-6 (NP_194414, NP_200327, NP_200328, NP_199682, NP_565752, and NP_199681) and *Homo sapiens* HsSUMO1-4 (AAC50996, AAH71645, NP_008867 and NP_001002255), HsFAT10 (NP_006389), HsISG15 (NP_005092) as well as HsUbi (P62988). Genes encoding DSUL proteins have only been detected in Poaceae genomes and form an own clade (colored in green). Maize SUMO proteins (ZmSUMO1a and ZmSUMO1b) form a highly homologous clade with Arabidopsis SUM1 and SUM2 proteins (light grey circle). HsFAT10 and HsISG15 are most closely related to ubiquitin (HsUbi as an example; dark grey circle).
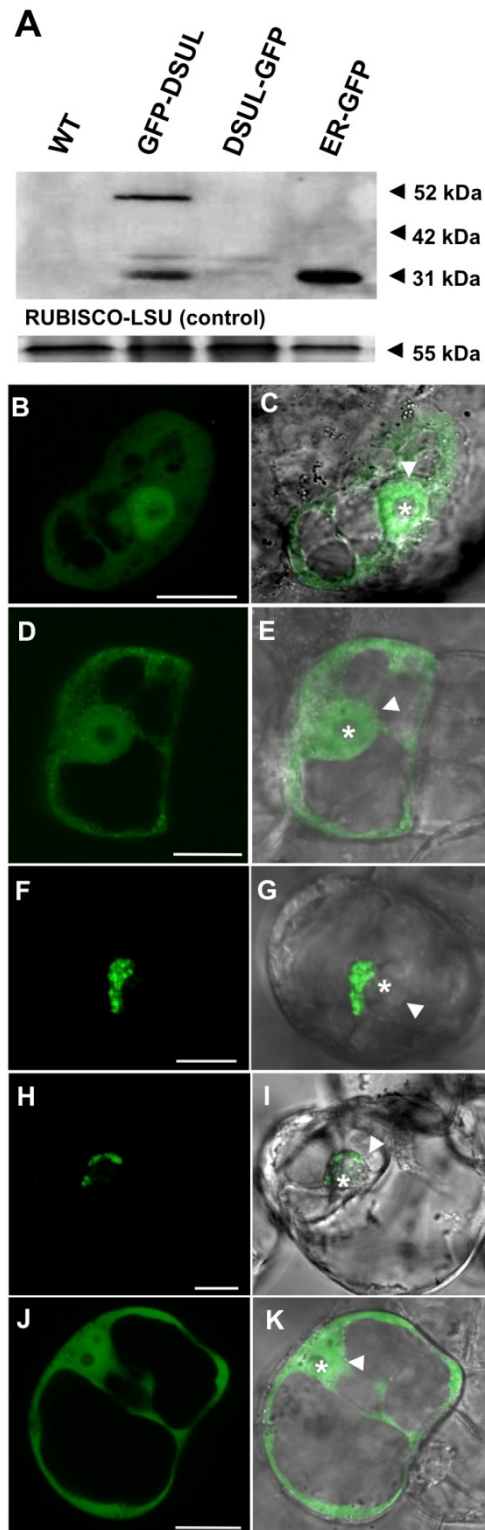
Figure 3. Processing and subcellular localization of ZmDSUL. Processing of ZmDSUL was studied two days after infection in *Nicotiana benthamiana* leaves and subcellular localization in maize suspension cells after transient transformation. (**A**) Dimeric ZmDSUL is processed at the C-terminus, but is not cleaved to generate monomeric DSUL protein domains. Two days after infiltration (infection) with constructs described below, tobacco leaf protein extracts were blotted and the length of GFP-fusion proteins detected with an anti-GFP antibody. The full length fusion protein (52 kD) was only detectable when GFP was fused to the N-terminus (GFP-DSUL). GFP cleaved from the predicted C-terminal diglycine motif generates a band at 32 kDa. A fusion protein containing a monomeric ZmDSUL domain containing GFP either attached to the N- or C-terminus (42 kD) was never detectable. ER-GFP (31 kDa) was loaded as a positive control. (**B-E**) BMS suspension cells bombarded with gold particles carrying a construct *p35S:GFP-ZmDSUL* encoding GFP fused to the N-terminus of ZmDSUL. (**B** and **C**) In some cells GFP signals were predominantly visible in the nucleus (arrow head), but not in the nucleolus (asterisk). Strong GFP-ZmDSUL fluorescence was also visible in the cytoplasm, while the majority of cells showed an even distribution between nucleus and cytoplasm (**D** and **E**). (**F-I**) BMS suspension cells bombarded with gold particles harboring a *p35S:ZmDSUL-GFP* construct. Signals were exclusively detected in the cytoplasm polar at the nuclear surface (**F** and **H**). (**J** and **K**) BMS suspension cells were bombarded with gold particles carrying a *pUbi:GFP* construct as a control. GFP signals are visible at equal intensities in the nucleus and cytoplasm excluding the nucleolus. Nuclei in the images are indicated by arrowheads and nucleoli by asterisks. B, D, F, H and J: UV microscopy images and C, E, G, I and K UV images merged with respective bright field microscopy images. Scale bars are 20μm.

3.2   *ZmDSUL* is exclusively expressed in the micropylar region of the immature female gametophyte and restricted to egg cell and zygote after cellularization

We first analyzed the expression pattern of *ZmSUMO1a*, *ZmSUMO1b* and *ZmDSUL* in various maize tissues and cells of the female gametophyte (FG) by RT-

PCR. As shown in Fig. 4A, *ZmSUMO1b* is ubiquitously expressed in all tissues analyzed, while *ZmSUMO1a* is particularly expressed in vegetative and male reproductive tissues. In contrast, expression of *ZmDSUL* could not be detected in any of the vegetative and reproductive tissues analyzed. A more detailed expression analysis of these genes in isolated cells of the FG before and after fertilization (Fig. 4B) indicated relatively low transcript amounts of *ZmSUMO1a* and *ZmSUMO1b* in both egg cells and zygotes (24 hours after pollination). Transcripts derived from synergids were detected after Southern blotting (data not shown). In contrast, *ZmDSUL* is highly expressed in egg cells and even stronger in zygotes confirming the egg cell EST cluster data, where *ZmDSUL* was identified as one of the most abundant ESTs present in the maize egg cell. Significant expression was also detected after 38 PCR cycles in synergids, while expression in central cells and sperm cells was not even detectable after Southern blotting. Due to its specific expression pattern in the female gametophyte, we have restricted further analyses to *ZmDSUL*.
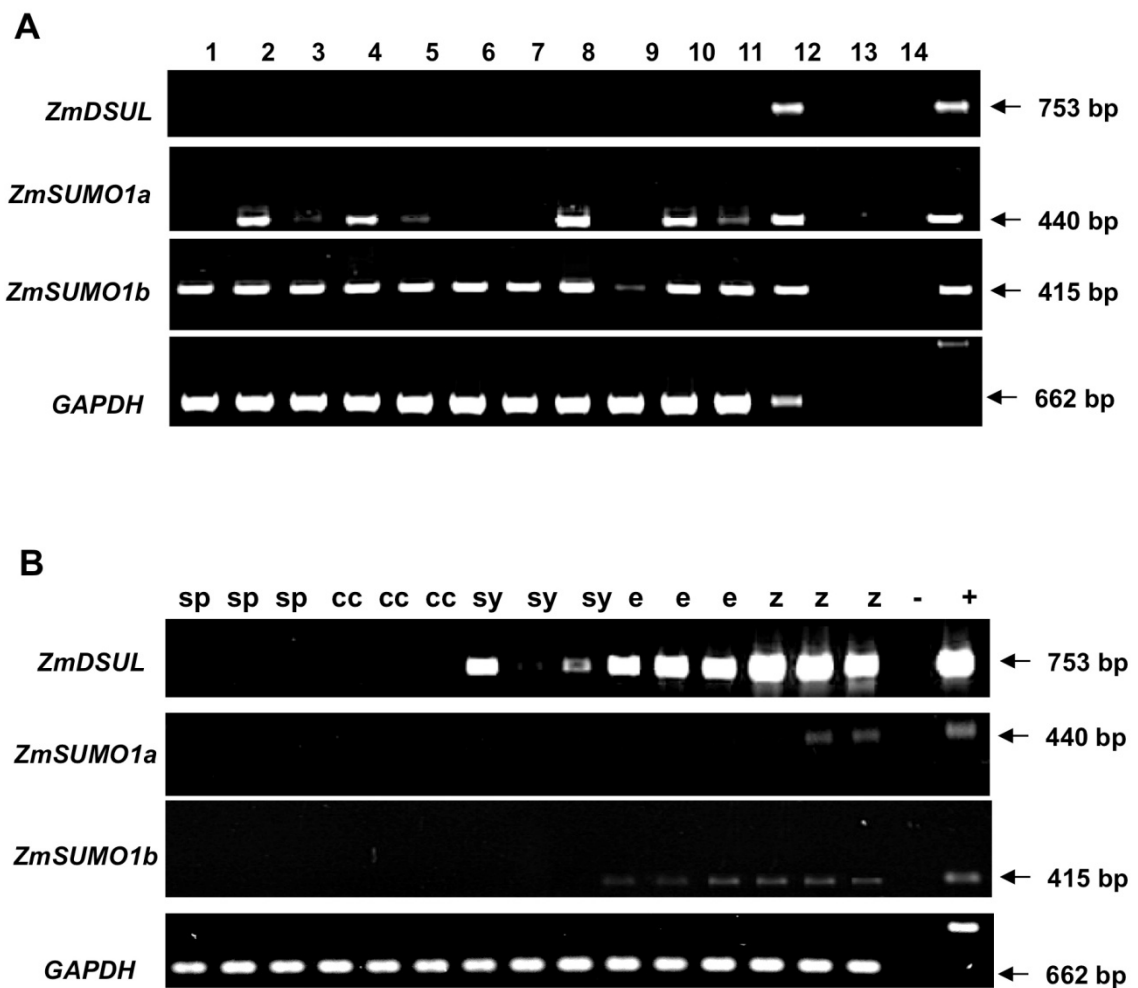
Figure 4. Expression of *ZmDSUL, ZmSUMO1a* and *ZmSUMO1b* in various tissues and microdissected cells of the female gametophyte of maize before and after fertilization. (A) RT-PCR was performed from various maize tissues by using *ZmDSUL, ZmSUMO1a,*

ZmSUMO1b and *GAPDH* specific primers. Tissues are as follows: 1: embryo 10 days after pollination; 2: mature leaf; 3: root tips; 4: roots; 5: internodes; 6: nodes; 7: mature tassels; 8: mature pollen; 9: mature ovules; 10: mature anthers; 11: embryo 25 days after pollination; 12, egg cell; 13: water (negative control); 14: blank lane and 15: PCR from genomic DNA. (**B**) RT-PCR was performed on mRNA from individual cells of the female gametophyte (cc: central cell; e: egg cell; sp: sperm cells; sy: synergid; z: zygote, isolated 24 hours after pollination; -: blank line; +: PCR from genomic DNA). The length of the PCR products is indicated.

In order to study the onset of *ZmDSUL* expression during FG development, we cloned 511 base pairs upstream of its open reading frame (ORF) as the short version of the *ZmDSUL* promoter (*ZmDSULp*). This promoter region was then used to drive expression of GFP as a marker in transgenic maize ovaries. As shown in Figure 5A, GFP signals were first detectable at stage FG 5/6 when cellularization and nuclei migration takes place (see Fig. 6 for stages of FG development). GFP signals are visible in the micropylar most region where it accumulated in two of the four nuclei. After cellularization, GFP signals are exclusively detectable in the immature egg cell (Fig. 5B). While signal intensity slightly decreases during FG and egg cell maturation (Fig. 5C), an about five time increase in signal intensity was observed in the zygote after fertilization (Fig. 5D) and signals completely vanished after the first asymmetric cell division (Fig. 5E). An expression at later stages during embryo development or outside the FG was never observed. With the aim to analyze the formation of aggresome-like structures described above also during FG development, we have cloned 1,566 base pairs upstream of the ZmDSUL-ORF as a long promoter version. This promoter region was then used to control the expression of GFP fused C-terminally to ZmDSUL. The GFP expression pattern (Fig. 5F-J) was almost identical with that of free GFP with the exception that GFP signals were first observed at the most micropylar spindle pole region excluding the nuclei. At later stages GFP signals were most strongly visible in the nucleus of egg cell and zygote, respectively, indicating that GFP might have been cleaved from the C-terminus of ZmDSUL and was then able to penetrate the nucleus. Occasionally slight background signals were visible at early stage FG7 in the antipodal region (Fig. 5B and G), but these were also visible in wt ovules of the same stages. In conclusion, 0.51 and 1.57 kbp versions of the *ZmDSUL* promoter display the same activity during FG development beginning in stage FG 5/6, restricted to the egg cell after cellularization and strongly induced again after fertilization before being turned off before/during zygote division. Moreover, aggresome formation was not observed when the endogenous promoter was used to study marker protein expression.
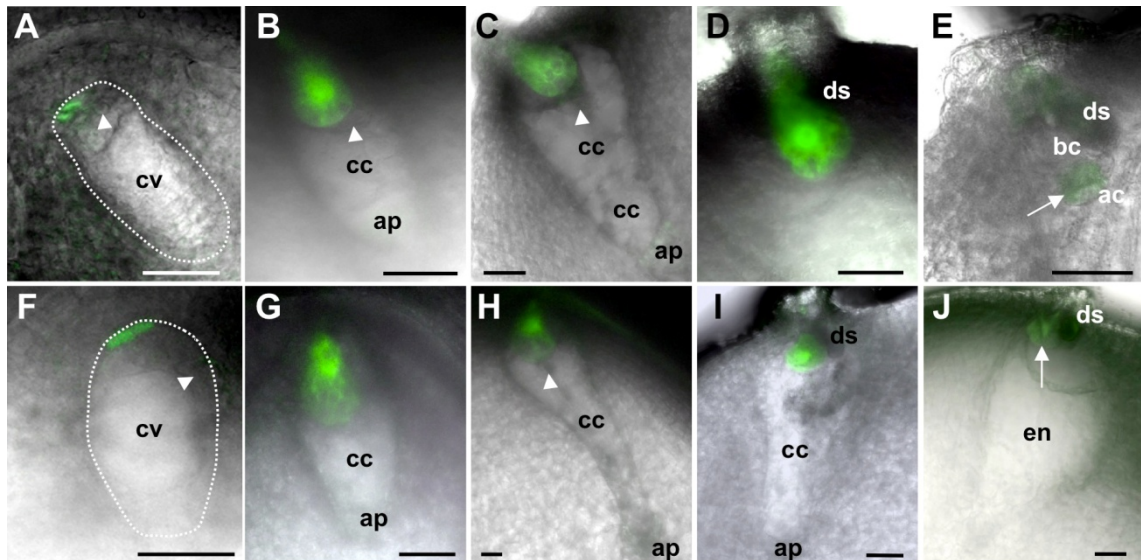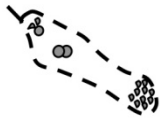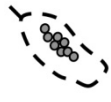
Figure 5. *ZmDSUL* **promoter activity is detectable in the micropylar region of the maize female gametophyte from stage FG 5 onward and restricted to egg cell and zygote after cellularization.** Transgenic maize ovules expressing either GFP (**A-E**) or a C-terminal DSUL-GFP fusion protein (**F-J**) under the control of *ZmDSUL* promoters of 1.5 and 0.7 kbp, respectively, were manually sectioned and scanned by CLSM. Please note that free GFP is able to enter and thus label nuclei at various FG stages. (**A**) GFP signals are first detectable at stage FG 5/6 (whole FG encircled) and label the two uppermost of the four micropylar nuclei. A nucleus localized closer to the large central vacuole is not labeled (arrowhead) and signals in the chalazal region of the FG were never observed. (**B**) After cellularization and nuclei migration was completed (early stage FG 7), strong GFP signals were restricted to the mature egg cell and (**C**) slightly decrease in intensity during FG maturation (late stage FG 7) The arrowheads label the unfused polar nuclei of the central cell. (**D**) Strongest signals were detected after fertilization in the zygote and (**E**) signals completely vanished at the 2-cell-zygote (1-cell-proembryo) stage. The arrow indicates the first asymmetric zygote cell division plane. (**F**) Similar to GFP, DSUL-GFP signals were first detectable in the most micropylar region of the FG at stage FG 5/6 (encircled) still excluded from nuclei. (**G**) Strongest signals before fertilization were detected in the egg cell at stage FG 7 (early) and (**H**) signal intensity slightly decreases during FG maturation (late stage FG 7). (**I**) Similar to free GFP, signals obtained from DSUL-GFP were strongest in the zygote and (**J**) vanished after the first zygotic division (arrow). Note that GFP signals label the egg and zygote nucleus indicating that GFP was cleaved from the C-terminal end of DSUL. Abbreviations: ac, apical cell; ap, antipodal cells; bc; basal cell; cc, central cell; cv, central vacuole; degenerated synergid cell; en, endosperm. Scale bars are 50µm.

3.3   ZmDSUL is required for polar nuclei positioning, cell specification and viability during female gametophyte maturation

In order to investigate the role of ZmDSUL during FG and zygote/early embryo development, we first established a method to visualize megasporogenesis and megagametogenesis in maize. The size of the female inflorescence and silk length was measured and correlated with developmental stages as described by Huang and Sheridan (1994). We adapted a method originally described by Young *et al*. (1979) with modifications by Vollbrecht and Hake (1995). In order to understand whole FG structures, cleared ovules were sectioned and pieces containing FGs scanned by CLSM.

Only sections with a cut face longitudinally to the mature FG could be fully scanned and taken into consideration to quantify phenotypes (Tab. 1).

Table 1. Developmental defects of maize female gametophytes (FGs) in _ZmDSUL_-RNAi lines. Sporophytic tissues of the ovary were fully differentiated in WT and RNAi lines. FG: female gametophyte.

	n[1]	Fully differentiated FGs (%)	Nuclei accumul. in FG center (%)	Unequal nuclei size (%)	Collapsed FG (%)	Empty FG (%)
WT [a/b]	63	96	0	0	4	0
RNAi #1[a]	97	74	7	5	14	0
RNAi #2[a]	129	74	4	8	14	0
RNAi #2[b]	110	67	0	2	16	15

Sporophytic tissues of the ovary were fully differentiated in wild-type and RNAi lines. *Silk length 3-6 mm. †Silk length >6 mm. _n_, number of scanned embryo sacs. FG, female gametophyte.

Meiotic stages could be observed at a silk/female inflorescence length of 0-0.5 mm. Fig. 6A shows an enlarged sub-epidermal megaspore mother cell (archesporial cell). During progression of differentiation and enlargement, the nucleus is positioned towards the micropylar pole and the chromatin becomes condensed (pachytene stage in Fig. 6B). The nucleolus is still visible at the diplotene stage (Fig. 6C). Figure 6D shows the ten homologous chromosome pairs aligned at the equatorial plate and the spindle apparatus is visible. Female meiosis finally results in a linear tetrad of four megaspores. The three megaspores orientated towards the micropyle degenerate (Fig. 6E and F). The functional megaspore (stage FG 1) forms the mature FG after three mitotic nuclear divisions. At stage FG 1 silk length of 0.5-1 mm was measured. After the first mitotic nucleus division (stage FG 2), both nuclei are separated from each other by a large vacuole (Fig. 6G). The micropylar and chalazal poles are occupied by additional vacuoles. Further mitotic nuclei divisions occur at both poles first generating a four nucleate (stage FG 3-4; silk length 1-4 mm, in Fig. 6H) and later eight nucleate immature FG (stage FG 5; silk length 4-5 mm, in Fig. 6I). Between stage FG 5 and 6, one nucleus from each pole moved towards the center of the FG (Fig. 5I) to approach each other and to stay in direct contact. An eight-nucleate immature at late stage 6

FG/early stage FG 7 (silk length 5-7 mm) is shown in Fig. 6J. Polar nuclei have approached each other, egg and two synergid nuclei are visible in the micropylar region and antipodal cells are beginning to form at the chalazal pole. Finally, a fully mature and differentiated FG (at late stage FG 7; silk length 7 mm onwards) is shown in Fig. 6K. Egg cell and two synergids have been specified, polar nuclei of the central cell are positioned close to the egg cell, large vacuoles have formed inside the central cell and antipodals have divided to form a cluster of at least 20 cells.
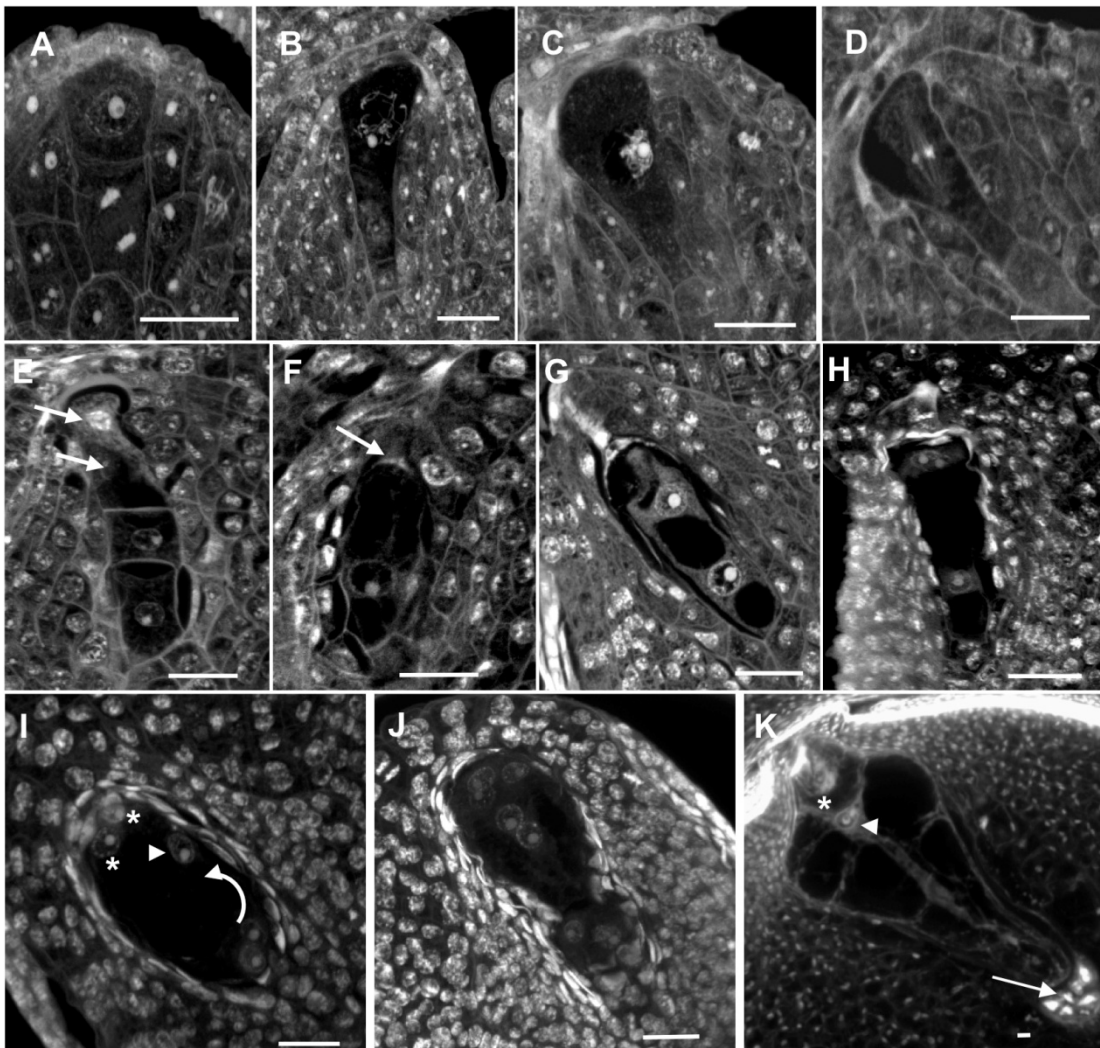
Figure 6. Longitudinal CLSM sections of maize ovules to visualize nuclei division and migration during megasporogenesis and megagametogenesis. (**A**) Sub-epidermal megaspore mother cell (MMC) before the first meiotic division. MMC at pachytene stage (**B**), at diplotene stage (**C**) and at metaphase I (**D**). (**E**) Quartet megaspore stage formed after meiosis. The two micropylar megaspores have started to degenerate (arrows). (**F**) The three micropylar megaspores are degenerated (arrow). The remaining large nucleus represents the functional megaspore (stage FG 1). (**G**) Two-nucleate female gametophyte (FG) stage (stage FG 2). Nuclei are separated by a large vacuole. (**H**) Four-nucleate FG (stage FG 3/4). (**I**) Eight-nucleate immature FG (stage FG 5/6) shortly before the polar nuclei approached each other. A nucleus from the micropylar region moved towards the upper center of the FG (arrowhead) to meet the second polar nucleus migrating at a longer distance (arrow) from the chalazal region of the immature FG. Egg and one synergid nuclei (asterisks) are visible in the micropylar region

of the FG. (**J**) Eight-nucleate immature FG (late stage FG 6). Polar nuclei have approached each other, egg and two synergid nuclei are visible in the micropylar region and antipodal cells are beginning to form at the chalazal pole. (**K**) Mature FG (late stage FG 7). Egg cell (asterisk) and synergids are fully differentiated, polar nuclei (arrowhead) are positioned close to the egg cell and antipodals have divided to form a cluster of cells (arrow). Large vacuoles have formed in the cytoplasm of the central cell. Scale bars are 20 µm.

An RNAi silencing approach was conducted to down-regulate *ZmDSUL* gene activity and to study its role during FG development, maturation and function. In contrast to WT plants (Fig. 7A), seed set was impaired in a number of independent transgenic *ZmDSUL*-RNAi lines. The RNAi lines # 1 (accession #1513) and RNA line # 2 (accession # 1515) showed the most severe effect with about 35 to 44% undeveloped seeds in the T1 generation (Fig. 7B). Ears from these two independent heterozygous *ZmDSUL*-RNAi lines of the T2 generation (Tab. 1) were collected at maturity (silk length of about 5 cm onwards) and subjected to a cytological analysis using the fixing/clearing method described above. Maternal sporophytic tissues of all ovaries were fully developed to maturity and we could not observe morphological differences between WT and *ZmDSUL*-RNAi ovaries. WT control plants contained about 96% fully differentiated FGs (Fig. 6K; Tab. 1). In contrast, heterozygous *ZmDSUL*-RNAi ovaries only contained about 67-74% differentiated FGs (Tab. 1). A more detailed analysis revealed a variation of phenotypes, but meiotic and mitotic nuclei division seemed to be completed as all FGs contained eight nuclei (Fig. 7C-J) or a degenerated FG at a later stage of maturation (Fig. 7K-N). Including stage FG4, FGs from mutant ovules were indistinguishable from that of wt plants (Fig. 7C and D). However at stage FG 5 a number of ovules contained eight nuclei in the center of the FG (Fig. 7E-H) that were positioned at opposite poles in WT ovules (Fig. 6I). Additionally the large central vacuole was missing. Moreover, nuclei were not properly separated from each other, a prerequisite for cell specification occurring at this stage of FG maturation. We also observed a number of FGs displaying a more polar distribution of four nuclei towards each pole at a slightly later developmental stage (Fig. 7H-J), but also in these FGs polar localization was not completed, nuclei were directly attached to each other and started to degenerate. Degeneration of the micropylar most nuclei specifying egg apparatus cells (two synergid cell and the egg cell) occurred first (Fig. 7H-J), while initiation of nuclei degeneration at the chalazal region was slightly delayed. When very mature ovaries at late stage FG 7 were analyzed, a relative large number of ovaries showed disintegration of FG nuclei and cytoplasm, were collapsed or appeared empty (Fig. 7K-N). The frequency of phenotype occurrence is shown in Tab. 1. The RNAi lines #1 and

#2 were analyzed while silks from the ears had a maximum length of about 6 mm corresponding to FG maturation stage FG7. Mutant ovaries displayed a developmental arrest at stage FG 5/6. Very mature mutant ovaries (RNAi line # 2 with a silk length >6mm) analyzed at late stage FG 7 showed one/third collapsed or empty FGs. In summary, we conclude that megagametogenesis is not affected by *ZmDSUL* down-regulation until stage FG 5, which correlates with the onset of *ZmDSUL* promoter activity. All mitotic divisions were completed, but nuclei neither properly positioned at FG poles nor sufficiently separated from each other. As a consequence, egg cell, synergid-, central cell- and antipodal cell-specification could not take place and the FG instead disintegrated without affecting maturation of surrounding maternal tissues.
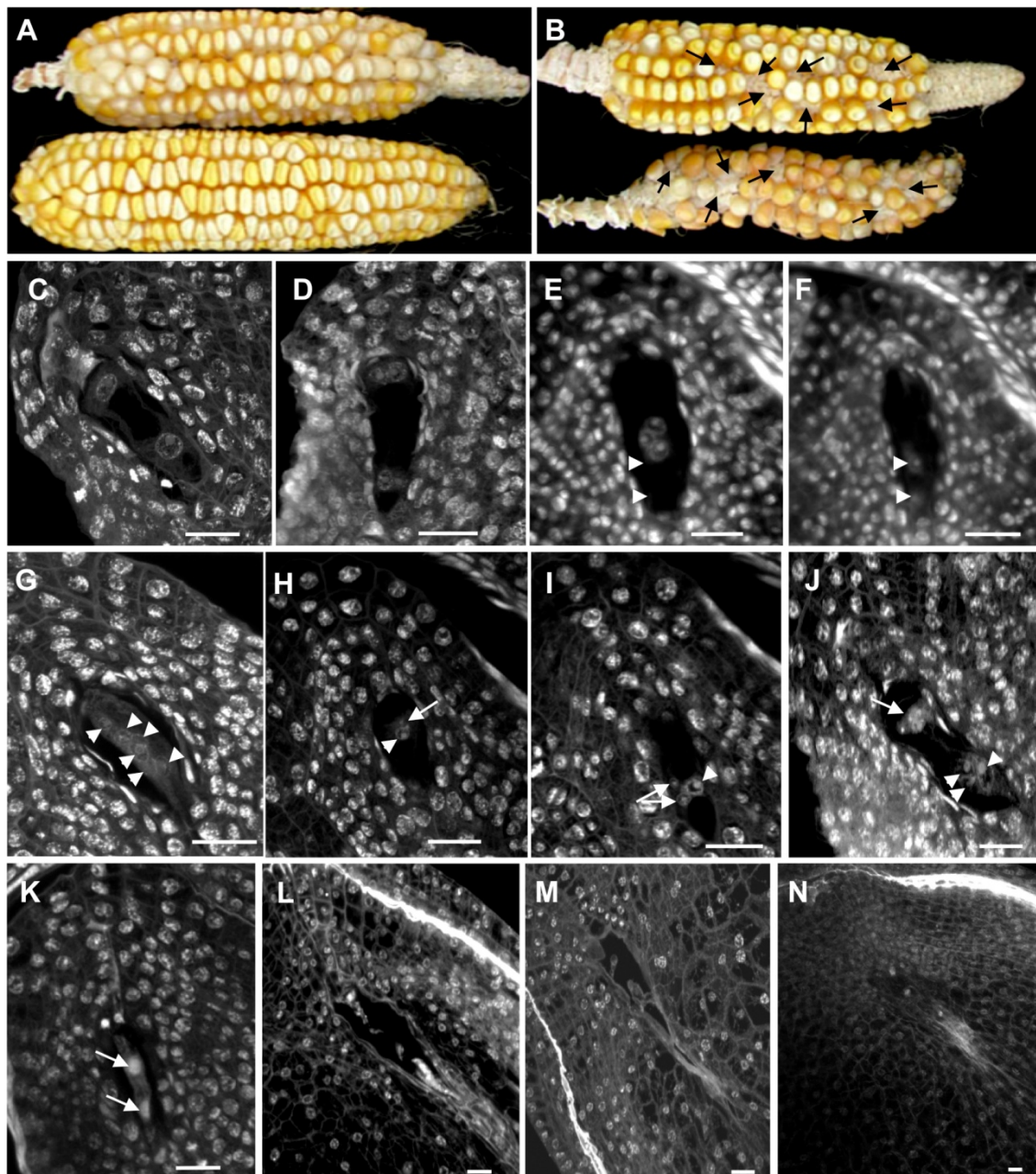
Figure 7. Longitudinal CLSM sections of *ZmDSUL*-RNAi ovules display lack of polar nuclei positions and nuclei degeneration at stage FG5/6 during megagametogenesis. (**A**) Ears from an A188 wild-type plants. (**B**) Ears from *ZmDSUL*-RNAi mutant plants line #1 (accession 1513, top) and line #2 (accession 1515, bottom), respectively. Example arrows point towards ovaries that did not initiate seed development. Ovules of heterozygous *ZmDSUL*-RNAi plants were analyzed after silk emergence. At this stage, wt ovule contained fully differentiated and mature embryo sacs (stage late FG 7). FG development until stage FG 5/6 was identical with that of wt ovules as indicated by FGs from mutant plants at stage FG2 (**C**) and FG 4 (**D**). (**E-J**) Mutant ovules are arrested at stage FG 5/6. Nuclei are not properly positioned in the micropylar region of the FG, egg apparatus and antipodal regions are not specified. (**E** and **F**) Two focus plains of one mutant FG showing three (E) and two (F) of eight nuclei localized to the center of the FG (nuclei are indicated by arrowheads). (**G**) An example of six of eight nuclei (indicated by arrowheads) lined up from the micropylar to chalazal pole of the FG. Nuclei are not completely positioned at the poles. (**H** and **I**) Two focus plains of one mutant FG. (H) Three (arrow) of the four micropylar nuclei are already degenerated and not positioned in the most micropylar region. One nucleus seems still intact (arrowhead). (I) Two of the four nuclei are already smaller and degenerating (arrows). The arrowhead marks an intact nucleus. (**J**) Similar phenotype as in (H/I): a group of four nuclei at each pole are attached to each other; three of the four nuclei are not properly localized to the micropylar pole and are already degenerated (arrow), while nuclei at the chalazal pole seem to be still intact (arrowheads mark three of them in the focus plain shown). (**K**) Progression of nuclei degeneration at both poles (arrows). (**L** and **M**) Further progression of FG degeneration culminated in a tiny collapsed FG lacking nuclei. (**N**) Overview of an ovule with a fully differentiated nuclear cone (top left) and inner integument containing an empty FG. Scale bars are 20 µm.

4   Discussion

4.1   Cell specification and viability of the female gametophyte

Although the maturation of the angiosperm female gametophyte is an attractive system to study fundamental cellular and developmental processes such as asymmetric nuclei position and migration as well as position dependent cell fate determination, until recently little progress has been made due to the deep embedding of the embryo sac in the maternal tissues of the ovary. The establishment of powerful forward and reverse genetics methods combined with a toolkit of cellular markers now enables to study these processes in the model plant Arabidopsis (Pagnussat *et al.*, 2005; Jones-Rhoades *et al.*, 2007; Berger *et al.*, 2008) and led researchers to the conclusion that the 'angiosperm female gametophyte is no longer the forgotten generation' (Brukhin *et al.*, 2005). However, until now only few genes expressed in the female gametophyte have been studied at the functional level and we are just beginning to uncover the genes involved, for example, in cell specification during embryo sac maturation (Groß-Hardt *et al*., 2007). In other plants such as maize, which, due to the large size of its embryo sac, is especially suited for these studies, until now only one report described the molecular identity of a gene involved in position-based determination of female gametophyte cell identity. IG1 encoding a LOB domain protein restricts nuclei division before cellularization (Huang and Sheridan, 1996; Evans, 2007). In contrast to *dsul* mutant phenotypes described in this report, the *ig1* mutant is viable in most genetic backgrounds. A large scale genetic deficiency screen was conducted to characterize female gametogenesis in maize (Vollbrecht and Hake, 1995). Although this screen did not result in the identification of the genes involved, genetically separable female gametogenesis programs were identified and it was further demonstrated that embryo sac development requires postmeiotic gene expression. In conjunction with the *dsul* phenotypes it is noteworthy that many mutant embryo sacs described were degenerated and degeneration often began at the micropylar pole where *DSUL* is expressed. Moreover, some mutant embryo sacs defective in cellular patterning/cell specification contained nuclei of a different size and occasionally partly degenerated micronuclei similar to findings in *dsul* mutant ovaries. The cytological analysis of partly sterile *indica/japonica* hybrids in rice indicated that sterility was mainly caused by female gametophyte development defects (Zeng *et al*., 2009). The described phenotypes partly overlapped with those described for *dsul* mutant ovaries: the eight-nucleate stage was shown to be most severely affected by asynchronous nuclear migration and abnormal

positioning of nuclei as well as egg apparatus or complete female gametophyte degeneration. Due to our observations using young and very mature ovaries, we suggest that the latter phenotypes are likely a consequence of abnormal nuclei positioning as well as a failure of cell specification.

4.2   Does DSUL play a role for spindle elongation and asymmetry?

A detailed investigation of *dsul* mutant ovaries showed that mitotic nuclei division cycles were completed, but the eight nuclei of the immature female gametophyte were localized either centrally in the FG or not properly distributed towards the micropylar and chalazal poles. Moreover, nuclei often were not separated from each other, a prerequisite for cell specification. A similar phenotype has been described for Arabidopsis embryo sacs of double heterozygous F1 mutants defective in both *γ-tubulin* genes. About 16% abnormal female gametophytes were observed at the eight-nucleate stage displaying abnormal number, position and appearance of nuclei. Spindle and phragmoplast structures associated with cytokinesis were aberrant (Pastuglia *et al*., 2006). Highly conserved γ-tubulin plays a major role for microtubule nucleation at MTOCs (microtubule organizing centers) and thus the establishment and organization of the mitotic spindle apparatus (Hendrickson *et al*., 2001).

SUMO has recently been reported to be a key of regulating miotic spindle-asymmetry in yeast (Leisner *et al*., 2008). It was shown that SUMOylation of the spindle-orientation protein Kar9 regulates its asymmetric localization and thus positioning of both the spindle poles and the daughter nuclei. A number of reports showed an important role of SUMOylation for chromosome segregation in yeast (for review Watts 2007). In mammalian cells, it was shown that SUMO-2/3 localized to centromeres and condensed chromosomes, whereas SUMO-1 localizes to the mitotic spindle and spindle midzone (Zhang *et al*., 2008). In summary the various reports indicate that SUMOylation is essential for mitotic chromosome condensation, sister chromatid cohesion, kinetochore function, mitotic spindle elongation and asymmetry. Regarding that *dsul* mutant embryo sacs contained eight nuclei, although not completely distributed to the poles and attached to each other, we suggest that DSUL might be involved in the regulation of spindle elongation and asymmetry during megagametogenesis, and perhaps the asymmetric zygote division, but that it is not or less important for chromosome segregation itself.

4.3 ZmDSUL localization to the nucleoplasm, cytoplasm and aggresome formation

The subcellular localization of the unprocessed N-terminal ZmDSUL-GFP fusion protein displayed localization in both nucleoplasm and cytoplasm, with a stronger accumulation in the nucleus excluding the nucleolus of some cells. A similar pattern has been described for the diubiquitin-like protein FAT10 (Kalveram *et al*., 2008). SUMO and SUMOylation substrates are predominately nuclear, although a number of targets are also exclusively cytoplasmic (Herrmann *et al*., 2007; Seeler and Dejean, 2003; Vertegaal *et al*., 2006; Zhao, 2007). The subcellular localization pattern of GFP-ZmDSUL suggests that it might also be involved to modify target proteins both in the cytoplasm and nucleoplasm. A very interesting subcelluar localization pattern was observed when GFP was C-terminally fused to ZmDSUL and overexpressed in maize suspension cells. The fusion protein localized exclusively perinuclear at one site of the nuclear surface. Such a protein accumulation pattern has been reported previously to occur when cytosolic GFP-fusion proteins are either overexpressed, misfolded, inappropriately assembled, aberrant modified or induced by environmental stress and has thus been termed aggresome formation (Johnston *et al*., 1998; García-Mata *et al*., 1999; Kawaguchi *et al*., 2003). The aggresome represents a huge proteasome complex in immediate proximity to the centrosome in animal cells. In animal cells, the cytoplasmic protein histone deacetylase 6 (HDAC6), which mediates the transport of polyubiquitylated cargo to the aggresome (Hubbert *et al*., 2002; Kawaguchi *et al*., 2003) was recently found to also interact with FAT10. Endogenous and ectopically expressed FAT10 as well FAT10-GFP localized to the aggresome under proteasome inhibiting conditions in a microtubule-dependent manner (Hipp *et al*., 2005; Kalveram *et al*., 2008). However, in contrast to our observations, N- and C-terminal fusion of GFP to FAT10 both displayed aggresome localization only under proteasome inhibiting conditions, suggesting that ZmDSUL might possess other or additional functions than labeling proteins for degradation. Moreover, we did not observe aggresome formation in the FG using the *ZmDSUL* promoter providing further evidence that the observed phenotype is solely correlated to overexpression of a cytosolic GFP-fusion protein similar to observations in animal cells (Johnston *et al*., 1998; García-Mata *et al*., 1999; Kawaguchi *et al*., 2003).

4.4   ZmDSUL structure and maturation

Based on the data presented we conclude that both ZmSUMO1a/b and ZmDSUL preproteins are carboxy-terminally truncated to expose a diglycine (GG) motif for SUMOylation and DSULylation, respectively. In contrast to the diubiquitin-like proteins FAT10 and ISG15, diSUMO-like DSUL from grasses contain the conserved GG motif also centrally and exposed between both SUMO-like domains. Biochemical studies in tobacco have revealed that DSUL is not cleaved at this position. Therefore, we conclude that DSUL represents a third member of the family of dimeric ubiquitin-related proteins. Another open question is related to the occurrence of polyDSULylation: while SUMO-1 generally leads to monomodification, SUMO-2/3 can lead to chain formation via the N-terminally located and conserved SUMOylation motif ψKxE/D (where ψ is a large hydrophobic residue such as Val, Leu, Ile, Phe or Met and x is any kind of amino acid; Tatham *et al*., 2001; Matic *et al*., 2008). While ZmDSUL and SbDSUL contain this motif only once in the middle of the C-terminal and not N-terminal SUMO-like domain, TaDSUL and OsDSUL1 do not contain this motif indicating that polyDSULylation likely does not occur.

Although ZmDSUL is only about 13% homologous to HsISG at the amino acid level, we were able to predict a 3-D model based on the available X-ray diffraction data for ISG15 (Narasimhan *et al*., 2005), conserved core amino acid positions and a very similar predicted secondary structure. The predicted DSUL structure is amazingly similar to that of ISG15 and it will be interesting to find out whether similar enzymes used for ISGylation/deISGylation, which are different from those required for SUMOylation/deSUMOylation, are also involved in conjugation/deconjugation of DSUL. ISG15 utilizes, for example, the E2 enzyme UBC8 while SUMO utilizes the single E2 enzyme UBC9 (Kim *et al*., 2004; Zhao, 2007). UBC7 as well as UBC9, the latter of which is likely involved in ZmSUMO1a/b conjugation, are expressed in the maize embryo sac (de Vries *et al*., 1998; Yang *et al*., 2006), but a gene encoding UBC8 was not yet reported. Future work should thus include the detection of the enzymatic DSUL maturation, activation, conjugation as well as deconjugation machinery. However, due to very specific and restricted expression pattern of *DSUL* in the female gametophyte, these efforts are biochemically limited and a technical challenge.

4.5   Outlook

In summary, *ZmDSUL* promoter activity was observed the first time at stage FG5 when cell differentiation takes place. Moreover, *ZmDSUL*-RNAi ovules developed normally until stage FG5, meaning that all mitotic divisions were completed. However, nuclei positioning was affected in the female gametophyte at this stage. This phenotype indicates that ZmDSUL might be involved in regulating spindle elongation and asymmetry during megagametogenesis. Yeast two-hybrid assays could now be performed to identify proteins conjugated or interacting with ZmDSUL. Validation of the interaction between ZmDSUL and candidate proteins could be performed using FRET (Förster-Resonance-Energy-Transfer) or by the generation of knockdown mutants, which phenocopy the *ZmDSUL*-RNAi phenotype. Furthermore, *ZmDSUL* promoter activity was observed in the mature egg cell and in the zygote. To investigate the role of ZmDSUL in the zygote *ZmDSUL*-RNAi transgenic plants could be generated, in which the expression of the *ZmDSUL*-RNAi-construct could be driven specifically in the egg cell or zygote to analyze the function of the protein in these cells.

5   Summary

Reversible post-translational modification of numerous proteins by small ubiquitin-related modifiers (SUMO) represents a major regulatory process in various eukaryotic cellular and developmental processes. With the aim to study the role of SUMOylation during female gametophyte (FG) development in maize, we identified three *Zea mays* genes encoding SUMO (ZmSUMO1a and ZmSUMO1b) and a di<u>SUMO-l</u>ike protein called ZmDSUL that contains two head-to-tail SUMO-like domains. While *ZmSUMO1a* and *ZmSUMO1b* are almost ubiquitously expressed, *ZmDSUL* transcripts were detected exclusively in the egg apparatus and zygote of maize. The latter gene was selected for detailed studies. ZmDSUL is processed close to the C-terminus generating a dimeric protein similar to animal FAT10 and ISG15 that contain two ubiquitin-like domains. While GFP fused to the ZmDSUL N-terminus was located in the cytoplasm and predominately in the nucleoplasm of some transiently transformed maize suspension cells, C-terminal GFP fusions exclusively accumulated at the nuclear surface. GFP or ZmDSUL-GFP under control of the ZmDSUL promoter displayed earliest GFP signals in the micropylar-most position of the FG at stage 5/6 when migration of polar nuclei and cellularization occurs. Mature FGs displayed GFP signals exclusively in the egg cell, but strongest signals were observed shortly after fertilization and completely vanished during the first asymmetric zygote division. RNAi silencing of *ZmDSUL* showed that it is required for female gametophyte viability. Moreover, nuclei segregation and positioning defects occurred at stage FG 5 after mitotic nuclei divisions were completed. In summary, we report a diSUMO-like protein that appears to be essential for nuclei segregation and positioning, the prerequisite for cell specification during FG maturation.

6   References

Alkuraya FS, Saadi I, Lund JJ, Turbe-Doan A, Morton CC, Maas RL (2006) SUMO1 haploinsufficiency leads to cleft lip and palate. *Science* 313, 1751.

Anckar J, Sistonen L (2007) SUMO: getting it on. *Biochem. Soc. Trans.* 35, 1409-1413.

Bantin J, Matzk F, Dresselhaus T (2001) *Tripsacum* as a natural model system to study parthenogenesis. *Sex. Plant Reprod.* 14, 219-226.

Becker D, Brettschneider R, Lörz H (1994) Fertile transgenic wheat from microprojectile bombardment of scutellar tissue. *Plant J.* 5, 299-307.

Berger F, Hamamura Y, Ingouff M, Higashiyama T (2008) Double fertilization - caught in the act. *Trends Plant. Sci.* 13, 437-443.

Borges F, Gomes G, Gardner R, Moreno N, McCormick S, Feijó JA, Becker JD (2008) Comparative transcriptomics of *Arabidopsis* sperm cells. *Plant Physiol.* 148, 1168-1181.

Brettschneider R, Becker D, Lörz H (1997) Efficient transformation of scutellar tissue of immature maize embryos. *Theor. Appl. Genet.* 94, 737-748.

Brukhin V, Curtis MD, Grossniklaus U (2005) The angiosperm female gametophyte: no longer the hidden generation. *Curr. Sci.* 89, 1844-1852.

Canaan A, Yu X, Booth CJ, Lian J, Lazar I et al. (2006) FAT10/diubiquitin-like protein-deficient mice exhibit minimal phenotypic differences. *Mol. Cell Biol.* 26, 5180-5189.

Cordts S, Bantin J, Wittich PE, Kranz E, Lörz H, Dresselhaus T (2001) *ZmES* genes encode peptides with structural homology to defensins and are specifically expressed in the female gametophyte of maize. *Plant J.* 25, 103-114.

Desterro JM, Rodriguez MS, Kemp GD, Hay RT (1999) Identification of the enzyme required for activation of the small ubiquitin-like protein SUMO-1. *J. Biol. Chem.* 274, 10618-10624.

de Vries A, Cordts S, Dresselhaus T (1998) Molecular characterization of a cDNA encoding an ubiquitin carrier protein (UBC7) isolated from egg cells of maize (Accession No. AJ002959) (PGR98-177). *Plant Physiol.* 118, 1011.

D'Halluin K, Bonne E, Bossut M, De Beuckeleer M, Leemans J (1992) Transgenic maize plants by tissue electroporation. *Plant Cell* 4, 1495-1505.

Dresselhaus T, Lörz H, Kranz E (1994) Representative cDNA libraries from few plant cells. *Plant J.* 5, 605-610.

Drews GN, Yadegari R (2002) Development and function of the angiosperm female gametophyte. *Annu. Rev. Genet.* 36, 99-124.

Evans MM (2007) The *indeterminate gametophyte1* gene of maize encodes a LOB domain protein required for embryo sac and leaf development. *Plant Cell* 19, 46-62.

García-Mata R, Bebok Z, Sorscher EJ, Sztul ES (1999) Characterization and dynamics of aggresome formation by a cytosolic GFP-chimera. *J. Cell Biol.* 146, 1239-1254.

Gross-Hardt R, Kagi C, Baumann N, Moore JM, Baskar R, Gagliano WB, Jurgens G, Grossniklaus U (2007) LACHESIS restricts gametic cell fate in the female gametophyte of *Arabidopsis*. *PLoS Biol.* 5, e47.

Geiss-Friedlander R, Melchior F (2007) Concepts in sumoylation: a decade on. *Nat. Rev. Mol. Cell Biol.* 8, 947-956.

Gill G (2004) SUMO and ubiquitin in the nucleus: different functions, similar mechanisms? *Genes Dev.* 18, 2046-2059.

Green CE, Phillips RL (1975) Plant regeneration from tissue cultures of maize. *Crop Sci.* 15, 417-421.

Haglund K, Stenmark H (2006) Working out coupled monoubiquitination. *Nat Cell Biol.* 8, 1218-1219.

Hatakeyama S, Nakayama KI (2003) Ubiquitylation as a quality control system for intracellular proteins. *J. Biochem.* 134, 1-8.

Hay RT (2005) SUMO: a history of modification. *Mol. Cell* 18, 1-12.

Hendrickson TW, Yao J, Bhadury S, Corbett AH, Joshi HC (2001) Conditional mutations in gamma-tubulin reveal its involvement in chromosome segregation and cytokinesis. *Mol. Biol. Cell* 12, 2469-2481.

Herrmann J, Lerman LO, Lerman A (2007) Ubiquitin and ubiquitin-like proteins in protein regulation. *Circ. Res.* 100, 1276-1291.

Hipp MS, Kalveram B, Raasi S, Groettrup M, Schmidtke G (2005) FAT10, a ubiquitin-independent signal for proteasomal degradation. *Mol. Cell Biol.* 25, 3483-3491.

Holsters M, Silva B, Van Vliet F, Genetello C, De Block M et al. (1980) The functional organization of the nopaline *A. tumefaciens* plasmid pTiC58. *Plasmid* 3, 212-230.

Huang B-Q, Sheridan WF (1994) Female gametophyte development in maize: microtubular organization and embryo sac polarity. *Plant Cell* 6, 845-861.

Hubbert C, Guardiola A, Shao R, Kawaguchi Y, Ito A, Nixon A, Yoshida M, Wang XF, Yao TP (2002) HDAC6 is a microtubule-associated deacetylase. *Nature* 417, 455-458.

Ihara M, Stein P, Schultz RM (2008) UBE2I (UBC9), a SUMO-conjugating enzyme, localizes to nuclear speckles and stimulates transcription in mouse oocytes. *Biol. Reprod.* 79, 906-913.

Johnson ES (2004) Protein modification by SUMO. *Annu. Rev. Biochem.* 73, 355-382.

Johnston JA, Ward CL, Kopito RR (1998) Aggresomes: a cellular response to misfolded proteins. *J. Cell Biol.* 143, 1883-1898.

Jones-Rhoades MW, Borevitz JO, Preuss D (2007) Genome-wide expression profiling of the *Arabidopsis* female gametophyte identifies families of small, secreted proteins. *PLoS Genet.* 3, 1848-1861.

Kalveram B, Schmidtke G, Groettrup M (2008) The ubiquitin-like modifier FAT10 interacts with HDAC6 and localizes to aggresomes under proteasome inhibition. *J. Cell Sci.* 121, 4079-4088.

Karimi M, Inze D, Depicker A (2002) GATEWAY vectors for *Agrobacterium*-mediated plant transformation. *Trends Plant Sci.* 7, 193-195.

Kawaguchi Y, Kovacs JJ, McLaurin A, Vance JM, Ito A, Yao TP (2003) The deacetylase HDAC6 regulates aggresome formation and cell viability in response to misfolded protein stress. *Cell* 115, 727-738.

Kerscher O (2007) SUMO junction-what's your function? New insights through SUMO-interacting motifs. *EMBO Rep.* 8, 550-555.

Kim KI, Giannakopoulos NV, Virgin HW, Zhang DE (2004) Interferon-inducible ubiquitin E2, Ubc8, is a conjugating enzyme for protein ISGylation. *Mol. Cell Biol.* 24, 9592-9600.

Kim HJ, Oh SA, Brownfield L, Hong SH, Ryu H et al. (2008) Control of plant germline proliferation by SCF (FBL17) degradation of cell cycle inhibitors. *Nature* 455, 1134-1137.

Kirkin V, Dikic I (2007) Role of ubiquitin- and Ubl-binding proteins in cell signaling. *Curr. Opin. Cell Biol.* 19, 199-205.

Kranz E, Bautor J, Lörz H (1991) In vitro fertilization of single, isolated gametes of maize mediated by electrofusion. *Sex. Plant Reprod.* 4, 12-16.

La Salle S, Sun F, Zhang XD, Matunis MJ, Handel MA (2008) Developmental control of sumoylation pathway proteins in mouse male germ cells. *Dev. Biol.* 321, 227-237.

Leisner C, Kammerer D, Denoth A, Britschi M, Barral Y, Liakopoulos D (2008) Regulation of mitotic spindle asymmetry by SUMO and the spindle-assembly checkpoint in yeast. *Curr. Biol.* 18, 1249-1255.

Liu J, Zhang Y, Qin G, Tsuge T, Sakaguchi N et al. (2008) Targeted degradation of the cyclin-dependent kinase inhibitor ICK4/KRP6 by RING-type E3 ligases is essential for mitotic cell cycle progression during *Arabidopsis* gametogenesis. *Plant Cell* 20, 1538-1554.

Márton ML, Cordts S, Broadhvest J, Dresselhaus T (2005) Micropylar pollen tube guidance by egg apparatus 1 of maize. *Science* 307, 573-576.

Matic I, van Hagen M, Schimmel J, Macek B, Ogg SC et al. (2008) In vivo identification of human small ubiquitin-like modifier polymerization sites by high accuracy mass spectrometry and an in vitro to in vivo strategy. *Mol. Cell Proteomics* 7, 132-144.

Melchior F (2000) SUMO--nonclassical ubiquitin. *Annu. Rev. Cell. Dev. Biol.* 16, 591-626.

Miura K, Jin JB, Hasegawa PM (2007) Sumoylation, a post-transcriptional regulatory process in plants. *Curr. Opin. Plant Biol.* 10, 495-502.

Müller S, Hoege C, Pyrowolakis G, Jentsch S (2001) SUMO, ubiquitin's mysterious cousin. *Nat. Rev. Mol. Cell Biol.* 2, 202-210.

Murashige T, Skoog F (1962) A revised medium for rapid growth and bioassays with tobacco tissue cultures. *Physiol. Plant* 15, 473-497.

Narasimhan J, Wang M, Fu Z, Klein JM, Haas AL, Kim JJ (2005) Crystal structure of the interferon-induced ubiquitin-like protein ISG15. *J. Biol. Chem.* 280, 27356-27365.

Nicholas KB, Nicholas HB Jr, Deerfield DWII (1997) GeneDoc: analysis and visualization of genetic variation. *Embnew News*, 4, 14.

Page RD (1996). TreeView: an application to display phylogenetic trees on personal computers. *Comput. Appl. Biosci.* 12, 357-358.

Pagnussat GC, Yu HJ, Ngo QA, Rajani S, Mayalagu S et al. (2005) Genetic and molecular identification of genes required for female gametophyte development and function in *Arabidopsis*. *Development* 132, 603-614.

Pagnussat, G. C., Alandete-Saez, M., Bowman, J.L. and Sundaresan, V. (2009) Auxin-dependent patterning and gamete specification in the *Arabidopsis* female gametophyte. *Science* 324, 1684-1689.

Pallotta MA, Graham RD, Langridge P, Sparrow DHB, Barker SJ (2000) RFLP mapping of manganese efficiency in barley. *Theor. Appl. Genet.* 101, 1100-1108.

Pastuglia M, Azimzadeh J, Goussot M, Camilleri C, Belcram K et al. (2006) Gamma-tubulin is essential for microtubule organization and development in *Arabidopsis*. *Plant Cell* 18, 1412-1425.

Saracco SA, Miller MJ, Kurepa J, Vierstra RD (2007) Genetic analysis of SUMOylation in Arabidopsis: conjugation of SUMO1 and SUMO2 to nuclear proteins is essential. *Plant Physiol.* 145, 119-134.

Schwartz DC, Hochstrasser M (2003) A superfamily of protein tags: ubiquitin, SUMO and related modifiers. *Trends Biochem. Sci.* 28, 321-328.

**Seeler JS, Dejean A** (2003) Nuclear and unclear functions of SUMO. *Nat Rev Mol. Cell Biol.* 4, 690-699.

Sprunck S, Baumann U, Edwards K, Langridge P, Dresselhaus T (2005) The transcript composition of egg cells changes significantly following fertilization in wheat (*Triticum aestivum* L.). *Plant J.* 41, 660-672.

Tatham MH, Jaffray E, Vaughan OA, Desterro JM, Botting CH, Naismith JH, Hay RT (2001) Polymeric chains of SUMO-2 and SUMO-3 are conjugated to protein substrates by SAE1/SAE2 and Ubc9. *J. Biol. Chem.* 276, 35368-35374.

Thompson JD, Higgins DG, Gibson TJ (1994) CLUSTAL W: improving the sensitivity of progressive multiple sequence alignment through sequence weighting, position-specific gap penalties and weight matrix choice. *Nucleic Acids Res.* 22, 4673-4680.

Ulrich HD (2008) The fast-growing business of SUMO chains. *Mol. Cell* 32, 301-305.

Vertegaal AC, Andersen JS, Ogg SC, Hay RT, Mann M, Lamond AI (2006) Distinct and overlapping sets of SUMO-1 and SUMO-2 target proteins revealed by quantitative proteomics. *Mol. Cell Proteomics* 5, 2298-2310.

Voinnet O, Lederer C, Baulcombe DC (2000) A viral movement protein prevents spread of the gene silencing signal in *Nicotiana benthamiana*. *Cell* 103, 157-167.

Voinnet O, Rivas S, Mestre P, Baulcombe D (2003) An enhanced transient expression system in plants based on suppression of gene silencing by the p19 protein of tomato bushy stunt virus. *Plant J.* 33, 949-956.

Vollbrecht E, Hake S (1995) Deficiency analysis of female gametogenesis in maize. *Dev. Genet.* 16, 44-63.

Watts FZ (2007) The role of SUMO in chromosome segregation. *Chromosoma* 116, 15-20.

Welchman RL, Gordon C, Mayer RJ (2005) Ubiquitin and ubiquitin-like proteins as multifunctional signals. *Nat. Rev. Mol. Cell Biol.* 6, 599-609.

Yang H, Kaur N, Kiriakopolos S, McCormick S (2006) EST generation and analyses towards identifying female gametophyte-specific genes in *Zea mays* L. *Planta* 224, 1004-1014.

Young B, Sherwood RT, Bashaw EC (1979) Cleared-pistil and thick-sectioning techniques for detecting aposporous apomixis in grasses. *Can. J. Bot.* 57, 1668-1672.

Zeng YX, Hu CY, Lu YG, Li JQ, Liu XD (2009) Abnormalities occurring during female gametophyte development result in the diversity of abnormal embryo sacs and leads to abnormal fertilization in indica/japonica hybrids in rice. *J. Integr. Plant Biol.* 51, 3-12.

Zhang FP, Mikkonen L, Toppari J, Palvimo JJ, Thesleff I, Janne OA (2008) Sumo-1 function is dispensable in normal mouse development. *Mol. Cell Biol.* 28, 5381-5390.

Zhao J (2007) Sumoylation regulates diverse biological processes. *Cell Mol. Life Sci.* 64, 3017-3033.

7   Supplemental data

Supplemental Table1. DSUL proteins are more closely related to SUMO than to ubiquitin proteins. Comparison of maize SUMO and DSUL with related ubiquitin and SUMO proteins. Homology of N- terminal (1st number) and C-terminal (2nd number) domains of ZmDSUL, HsISG15 and HsFAT10 are shown separately.

Proteins	Ubiquitin sequence homology (%)	SUMO sequence homology (%)
ZmSUMO1a	15[1]	42[4]
ZmSUMO1b	14[1]	41[4]
ZmDSUL	17, 15[1]	25, 22[3]
HsISG15	28, 36[2]	12, 18[4]
HsFAT10	27, 34[2]	15, 11[4]

n[1], n[2], n[3] and n[4] indicate protein sequence homology by using ZmUbi, sUbi, ZmSUMO1a and HsSUMO-1 proteins as references, respectively.
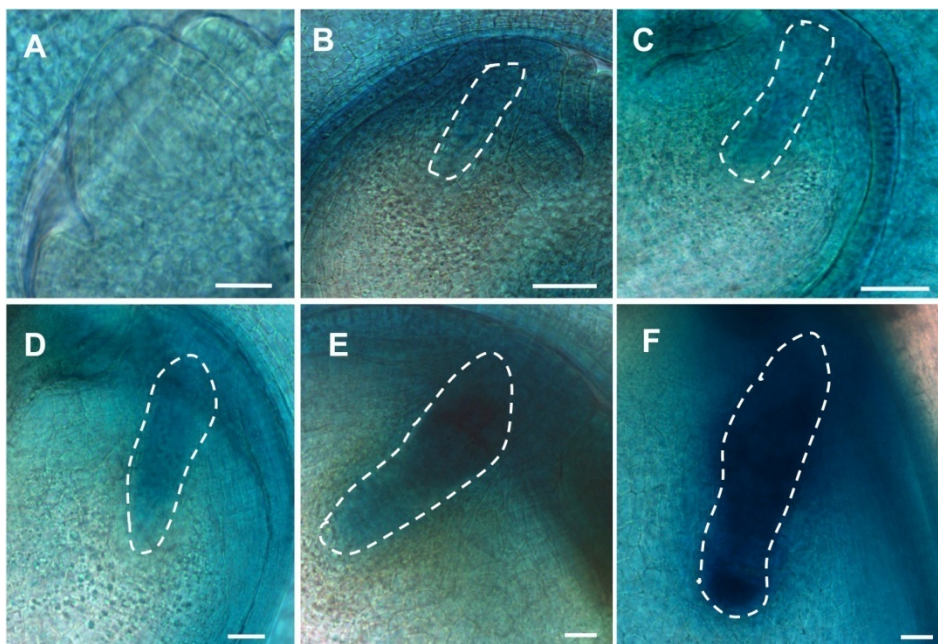
Supplemental Figure 1. Activity of the maize ubiquitin promoter during mega-gametogenesis. The maize ubiquitin promoter has been used to silence the *ZmDSUL* gene. In order to study its activity during female gametophyte development (megagametogenesis), transgenic maize plants carrying an *pUbi:GUS* reporter gene construct were analysed at various developmental stages after GUS staining. Female gametophytes (FG) are encircled in the individual images. (**A**) During megaspore mother cell (MMC) differentiation, GUS activity is detected at similar levels in maternal cell layers of the ovary, nucellus tissue, integument primordia and MMC. (**B-F**) At stages FG 2-7, GUS activitiy is detected in the whole ovule, but strongest activity is visible in the developing FGs. (**B**) stage FG 2, (**C**) stage FG4, (**D**) stage FG 5-6, (**E**) early stage FG7 and (**F**) late stage FG7. Scale bars are 50 µm.

Contribution to the paper:

Srilunchang K-o, **Krohn NG**, Dresselhaus T (2010) DiSUMO-like DSUL is required for nuclei positioning, cell specification and viability during female gametophyte maturation in maize. *Development* 137, 333-345.

Nadia G. Krohn regenerated transgenic maize plants carrying the *pZmDSUL:GFP* construct and performed genotypical and histological analyses of these plants. Moreover, she carried out part of the phenotypical analyses of *ZmDSUL*-RNAi ovules.

Herewith I confirm the accuracy of the statements.

Prof. Dr. Thomas Dresselhaus

Appendix

Vector maps

P_{UBI}:ZmEAL1-AS:iF2intron:ZmEAL1:OCSt
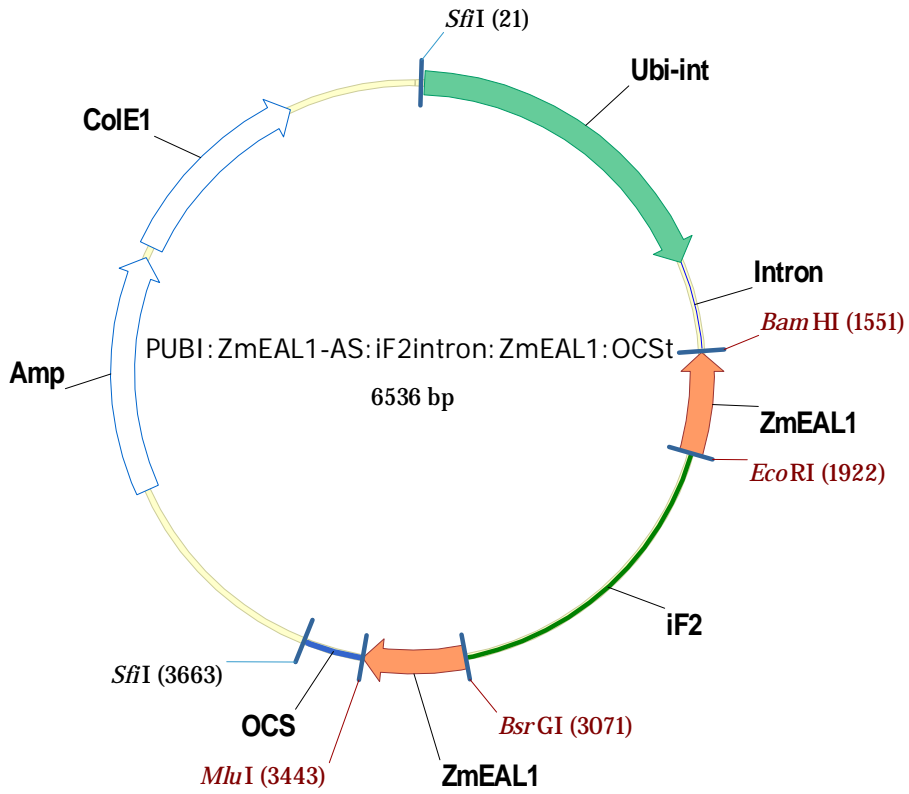
P_{ZmEAL1}:eGFP:NOSt
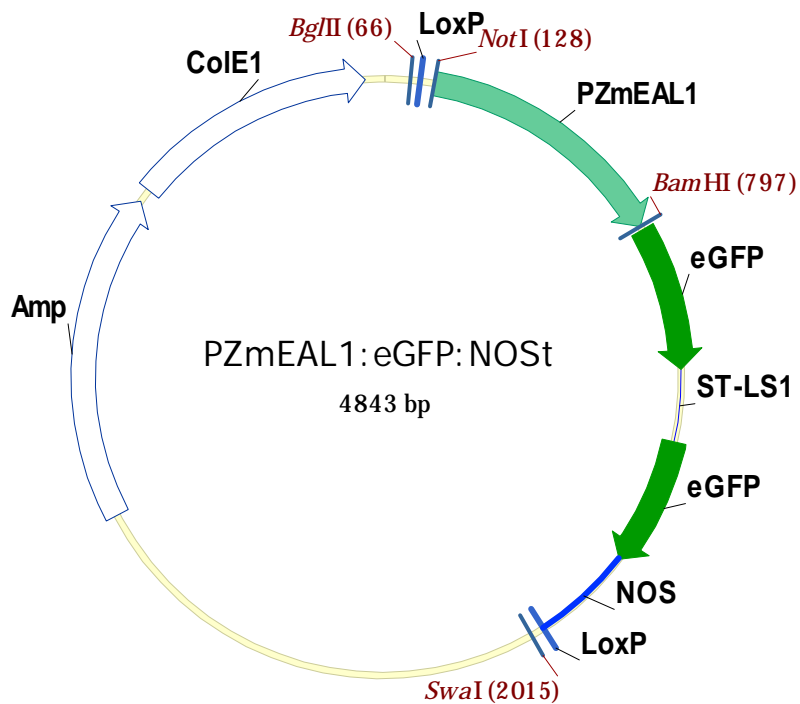
P~ZmEAL1~:ZmEAL1-eGFP:NOSt

Acknowledgements

Eidesstattliche Erklärung

Ich erkläre hiermit an Eides statt, dass ich die vorliegende Arbeit ohne unzulässige Hilfe Dritter und ohne Benutzung anderer als der angegebenen Hilfsmittel angefertigt habe; die aus anderen Quellen direkt oder indirekt übernommenen Daten und Konzepte sind unter Angabe des Literaturzitats gekennzeichnet.

Nadia Graciele Krohn

Regensburg, den 1 September 2010